Optimal Planning of Community Energy Storage Systems in Low-Voltage Distribution Networks

Jayaminda Anuradha Kariyawasam Bovithanthri

April 2025

A thesis submitted for the degree of

Doctor of Philosophy of

The Australian National University

School of Engineering

College of Systems and Society (CSS)

The Australian National University

Declaration

Except where otherwise indicated, this thesis is my own original work.

Jayaminda Anuradha Kariyawasam Bovithanthri
April 2025

Acknowledgements

First and foremost, I would like to express my sincere gratitude to my primary supervisor and panel chair, Dr. Chathurika Mediwaththe, for her invaluable support and guidance throughout my PhD journey, including during the challenging COVID period and her time away due to work commitments. Her unwavering mentorship and encouragement have played a key role in shaping my research. I am deeply thankful to my associate supervisor Dr. José Iria for his great support in writing research papers and for his insightful suggestions that helped to refine my work. I would also like to thank Prof. Lachlan Blackhall, my former panel chair, for his great support both academically and non-academically. I am grateful to Prof. Kylie Catchpole for being one of my associate supervisor and for her guidance. Also, a special thanks to the Australian National University for providing me with the resources, including the tuition fee and stipend scholarships that made this research possible.

I am deeply grateful to my wife, Sulakshi, who has been my everything and the constant source of strength, providing unwavering support throughout this journey. I would also like to thank my parents for raising me and providing the foundation that has allowed me to reach this stage in my life. I owe them everything for their love and sacrifices. My heartfelt thanks go to Dan and his parents, whose unwavering support and kindness were a great source of strength to me during difficult times. Finally, I would like to thank everyone, including my friends Masoume, Noah, Andrew, Anna, Shubhankar, Kevin, Ben, and Steve for their constant encouragement, and motivation in this journey.

Abstract

The increased adoption of renewable energy sources in modern power systems is mainly driven by their sustainable solutions for clean energy and potential to reduce energy costs. However, the intermittent and non-dispatchable nature of common renewable energy sources, such as photovoltaic energy systems, may restrict the ability to fully exploit their benefits. Energy storage systems are used to overcome these challenges efficiently. Community energy storage systems (CESSs) are an emerging type of energy storage system that can trade energy with multiple stakeholders, including prosumers, consumers, and the grid, thereby generating techno-economic benefits. The benefits of a CESS can be further enhanced by optimising its planning aspects, namely its location, size, and rated power.

In this thesis, we propose novel optimal CESS planning frameworks to benefit multiple stakeholders in low-voltage distribution networks. First, we develop a multi-objective CESS planning framework to deliver technical benefits to the network, and economic benefits to the CESS provider and prosumers. The results demonstrated that our model generates enhanced techno-economic benefits compared to models that do not utilise a CESS, and models that optimise only the CESS operation. Then, we present a multi-objective stochastic optimisation framework to optimally plan CESSs under different energy pricing schemes (EPSs) of the CESS provider, thereby producing economic benefits for a community of prosumers and the CESS provider equitably. The optimisation framework minimises the investment and expected operating cost of the CESS provider,

and the expected operating costs of prosumers. Our experiments show that under the EPS where the CESS provider trades energy with prosumers at the average grid energy price, and the objective of the CESS provider is traded-off moderately to improve the objective of prosumers, spreads the economic benefits for both beneficiaries most equitably. Next, we propose a multi-objective stochastic optimisation framework that can be used by governments to run auctions and select the best CESS project to financially support. So, CESS providers and energy community members can equitably benefit from the economic value generated by CESSs. Our experiments demonstrate that government financial support can accelerate the installation of CESSs and enhance their business viability. This can be achieved by boosting the economic benefits shared between CESS providers and communities, and ensuring these benefits are distributed equitably. Finally, we evaluate how the economic benefits for prosumers can be improved through optimal CESS planning under different energy trading schemes (ETSs). The results demonstrate that the ETS enabling prosumers to trade energy with both the grid and the CESS maximises their economic benefits.

Table of Contents

List of Abbreviations

AHP	Analytic Hierarchy Process
AUD	Australian Dollar
CESS	Community Energy Storage System
CPLEX	Complex Programming Linear Expressions
DNSP	Distribution Network Service Provider
EPS	Energy Pricing Scheme
ESS	Energy Storage System
ETS	Energy Trading Scheme
EV	Electric Vehicle
HV	High-Voltage
LV	Low-Voltage
MCS	Monte Carlo Simulation
MILP	Mixed-Integer Linear Programming
MV	Medium-Voltage
P2P	Peer-to-Peer

PDF	Probability Density Function
PhD	Doctor of Philosophy
PV	Photovoltaic
RESS	Residential Energy Storage System
RWM	Roulette Wheel Mechanism
UESS	Utility Energy Storage System
UK	United Kingdom
USA	United States of America

List of Figures

List of Tables

Chapter 1

Introduction

1.1 Motivation

1.1.1 Global Demand for Renewable Energy and Energy Storage Systems

Climate change is one of the most pressing challenges of our time, manifesting through a range of global environmental issues, including rising sea levels, increasing global temperatures, and the prevalence of extreme weather events. These challenges are primarily driven by greenhouse gas emissions resulting from the combustion of fossil fuels to meet energy demands. As the urgency to address climate change escalates, it is imperative to shift towards clean energy solutions that can mitigate its adverse effects.

In recent years, renewable energy sources such as solar photovoltaic (PV) and wind power systems have garnered significant attention from both the industry and the research community [Shang et al., 2024; Virah-Sawmy and Sturmberg, 2024]. These sources present cleaner and more sustainable alternatives to traditional fossil fuel-based energy generation, offering the potential to reduce greenhouse gas emissions and promote energy security. Moreover, the integration of renewable energy sources into the energy mix aligns with global efforts to combat climate change and meet international climate agreements.

However, despite their benefits, the intermittent and non-dispatchable nature of renewable energy sources presents challenges in fully leveraging their benefits. The variability in energy generation due to factors such as weather conditions and time of day complicates the reliability of renewable energy systems. Therefore, addressing these challenges is essential for optimising the utilisation of renewable energy sources and ensuring a stable and resilient energy supply.

Energy storage systems (ESSs) play a key role in overcoming the aforementioned challenges as they can store the surplus energy of renewable energy sources and release energy when it is required. ESSs have a wide range of power systems applications, and they are described in detail in Chapter 2.

1.1.2 Community Energy Storage Systems

Community energy storage systems (CESSs) also known as "Shared battery energy storage systems" and "Neighbourhood battery energy storage systems", are an emerging type of energy storage system, that can serve an energy community of multiple prosumers and consumers with in a low-voltage (LV) distribution network [Shaw et al., 2020; Dai et al., 2021; Mediwaththe et al., 2019; Mediwaththe and Blackhall, 2020b]. In other words, CESSs enable communities to collectively store surplus energy from their renewable energy sources, and use that stored energy when needed, thereby improving the flexibility and efficiency of local energy use. CESSs can also render benefits to its provider and the grid. Some of the CESS benefits gained by all these stakeholders can be mentioned as follows [Walker and Kwon, 2021a; Mohanty et al., 2024; Csereklyei et al., 2024; Yang et al., 2024b].

- Reduce or completely remove the need for individual prosumers to invest in their own batteries, making energy storage more accessible and cost-effective for an energy community.
- Help to reduce the peak energy demand from the grid by supplying stored energy during high consumption periods. This alleviates stress on the grid, leading to cost

savings and reducing the risk of grid overload conditions.

- Absorb excess PV generation during periods of low energy consumption and release the stored energy to prosumers and consumers when the energy consumption is high. This smoothens energy supply and demand fluctuations, enhancing grid stability.
- Increase the network hosting capacity without degrading the grid performance.
- Manage peak loads and help to defer the need for costly infrastructure upgrades, such as transmission line enhancements or grid expansion.
- Contribute to maintain stable voltage levels within the distribution network by absorbing excess energy during high generation periods, and supplying energy during high consumption periods.

1.1.2.1 Importance of Planning Community Energy Storage Systems

To fully leverage aforementioned benefits, it is essential to optimise the planning of CESSs together with their operation. Optimal CESS planning involves determining the best size, rated power, and the location. Optimised CESS planning ensures that the storage size matches the community's energy needs, minimises costs, and effectively integrates with renewable energy sources. Some of the possible CESS planning approaches are given below, highlighting their importance.

- **Multi-Objective CESS Planning:** In communities with CESSs, multiple stakeholders having competing objectives are often involved. Thus, a multi-objective CESS planning framework is essential as it can accommodate the diverse interests of stakeholders, enabling to evaluate trade-offs among various objectives. Nevertheless, planning of CESSs in a multi-objective setting is challenging as it is important to maximise the overall benefits of the CESS while ensuring a balanced distribution of benefits for all stakeholders.
- **Multi-Year CESS Planning:** Planning of CESSs in a multi-year period is impor-

tant for effective integration and sustainable energy management. However, this approach requires a thorough analysis of the long-term cost-benefits of CESSs, and understanding the business viability of CESS investments. Additionally, CESSs can be planned better in a multi-year setting, as it facilitates modelling the long-term changes of some factors such as energy demand, energy prices, and the growth of renewable energy resources installations. However, planning CESSs combining all of these uncertainties is challenging due to the high computational burden.

- **CESS Planning Under Uncertainty:** In the real-world, factors such as renewable energy generation, energy consumption (both real and reactive), energy prices, and the growth of renewable energy sources are subject to significant uncertainty. Incorporating uncertainty into the CESS planning enables decision-makers such as governments, community leaders and energy regulators to develop resilient CESS management strategies that can adapt to fluctuations of aforementioned factors.

- **CESS Planning Through Auctions:** Additionally, as the demand for renewable energy solutions rises, multiple CESS providers are competing to install and operate CESSs. Therefore, it is essential for decision-makers to have a proper approach, similar to that of auction mechanisms, to manage the installation of CESSs. In this thesis, we refer to the term "Auction" as the process where multiple CESS providers interested in installing and operating CESSs submit project offers to the auction, and a regulatory body selects the best project. Managing CESS installations through auctions is challenging as they require identifying the best CESS project among multiple project offers. However, selecting the best CESS project is further challenging, as project offers are subject to the uncertainties discussed earlier.

- **CESS Planning Under Different Energy Trading Schemes:** Typically, in CESS-integrated networks, prosumers trade energy with the grid and the CESS. Nevertheless, due to network infrastructure, regulatory, policy, technical, and geographical limitations, prosumers may not be able to trade energy both with the grid and the CESS. To address this issue, it is required to have flexible energy trading schemes. Moreover, prosumers with residential batteries may also want to benefit from CESSs. Hence, it is essential to investigate how the CESS planning can benefit a community of prosumers, both with and without residential batteries under different energy trading schemes.

In this context, CESS planning needs to be done balancing multiple objectives of different stakeholders, maximising the overall benefits of CESSs. Moreover, CESS planning needs to account for short-term and long-term uncertainties, enabling CESSs to adapt to changing conditions and ensuring their long-term sustainability. Another essential consideration is that how to manage the CESS installations of competing CESS providers, where auction mechanisms serve as a structured approach to identify the most beneficial projects. Furthermore, the diversity of prosumers and their energy trading schemes with the grid and/or the CESS needs to be accounted in CESS planning. Given these considerations, this thesis aims to address the following research questions:

- How can a CESS planning framework generate techno-economic benefits for multiple stakeholders?

- How to plan CESSs under a multi-objective setting and the uncertainty of multiple aspects including real and reactive energy consumption and PV generation, while valuing the energy trade through a CESS to generate a balanced distribution of economic benefits among multiple stakeholders?

- How to manage CESS installations through auctions to select the best CESS project that can economically benefit multiple stakeholders in balance?

- How does the CESS planning under different energy trading schemes impact the economic benefits for prosumers with and without residential batteries?

1.2 Thesis Objectives

The primary objective of this thesis is to develop CESS planning optimisation frameworks for benefiting different stakeholders in LV distribution networks. This primary objective is divided into the following sub-objectives:

- To formulate a multi-objective CESS planning framework that generates techno-economic benefits for multiple stakeholders.
- To develop a multi-objective CESS planning framework that incorporates the CESS provider's energy trade valuation, generating equitable economic benefits for multiple stakeholders under multiple aspects of uncertainty.
- To manage CESS installations through government-run auctions and select the best CESS project, ensuring a balanced distribution of economic benefits among multiple stakeholders
- To evaluate the impact of CESS planning under different energy trading schemes on the economic benefits for prosumers, both with and without residential batteries.

1.3 Thesis Contributions

The main contributions of this thesis can be summarised as follows:

1. In Chapter 3, we propose a multi-objective framework to plan CESSs for generating technical benefits for the network, and economic benefits for prosumers and the CESS provider. Through extensive simulations, we show that our optimisation framework outperforms models that optimise only the CESS operation, and generate improved benefits for all stakeholders.
2. In Chapter 4, we present a multi-objective stochastic optimisation framework to plan CESSs under different energy pricing schemes for the CESS provider. Our model can be adopted by decision-makers, including energy regulators, utilities, and community leaders to select the best CESS solution (i.e., the optimal CESS

planning aspects and the energy pricing scheme of the CESS provider) that delivers the most equitable outcome to the competing economic objectives of the CESS provider and prosumers.

3. In Chapter 5, we propose a multi-objective stochastic optimisation framework to manage government-run auctions and select the CESS projects that can generate an equitable distribution of economic benefits between CESS providers and communities of prosumers and consumers in a multi-year horizon. This model can be adopted by government agencies to select the best CESS projects to financially support, generating an equitable distribution of benefits among all stakeholders.

4. In Chapter 6, we propose a CESS planning framework to benefit a community of prosumers with and with residential batteries under different energy trading schemes. This framework enables to identify the best energy trading scheme that promotes community engagement in CESS energy management.

1.4 List of Publications

The list of publications produced by the research of this PhD thesis is given below:

[P1] **Anuradha, K. B. J.**; Mediwaththe, C. P.; and Mahmoodi, M., 2023. A multi-objective planning and scheduling framework for community energy storage systems in low-voltage distribution networks. In 2023 13th International Conference on Power, Energy and Electrical Engineering (CPEEE), 379–385. IEEE, Tokyo, Japan.

[P2] **Anuradha, K. B. J.**; Iria, J.; and Mediwaththe, C. P., 2024. Multi-objective planning of community energy storage systems under uncertainty. Electric Power Systems Research, 230 (2024), 110286.

[P3] **Anuradha, K. B. J.**; Iria, J.; and Mediwaththe, C. P., 2025. A Multi-objective stochastic optimization framework for government-run community energy storage systems auctions. Under minor revisions at Journal of Energy Storage, (2025).

[P4] **Anuradha, K. B. J.**; Iria, J.; and Mediwaththe, C. P., 2023. Evaluation of the economic benefits of community energy storage systems for prosumers. In 2023 IEEE Region 10 Symposium (TENSYMP), 1–6. IEEE, Canberra, Australia.

The chapters corresponding to these publications are mentioned in Table 1.1.

Table 1.1: Thesis chapters and their associated publications.

Thesis chapter	Publication
Chapter 3	[P1]
Chapter 4	[P2]
Chapter 5	[P3]
Chapter 6	[P4]

1.5 Thesis Structure

The thesis is structured as follows.

Chapter 2 presents a background study about energy storage systems followed by an extensive literature study on community energy storage systems. The chapter concludes outlining the potential research gaps of CESS energy management that need further investigation.

Chapter 3 proposes a CESS planning optimisation framework to enhance techno-economic benefits of multiple stakeholders. The proposed framework benefit the network by minimising network real energy loss, prosumers by minimising their energy trading costs with the grid, and the CESS provider by minimising their investment cost and energy trading costs with the grid. Simulations are carried out to test our model against the models that do not have a CESS, and models that optimise only the CESS operation.

Chapter 4 presents a multi-objective stochastic optimisation framework to select the best

CESS solution that delivers the most equitable outcome to the competing economic objectives of the CESS provider and prosumers. Our optimisation framework minimises the investment and operating cost of the CESS provider, and operating costs of prosumers. Simulation experiments are performed on a LV distribution network to optimally plan a CESS and identify the energy price from the CESS provider, so the economic benefits are distributed equitably among all stakeholders.

Chapter 5 demonstrates a multi-objective stochastic optimisation framework that can be used by governments to run auctions and select the best community CESS projects to support. This framework enables CESS providers and energy community to equitably benefit from the economic value generated by CESSs. Simulation experiments are conducted on an Australian LV network having a community of prosumers and consumers to evaluate our optimisation framework.

Chapter 6 evaluates the economic benefits for prosumers with and without residential batteries gained from CESS planning under different energy trading schemes. Simulations are carried out to identify the best energy trading scheme in a CESS planning framework that generates the highest economic benefits for all prosumers.

Chapter 7 concludes the thesis with a summary of key findings and possible future developments.

Chapter 2

Background and Literature Review

Optimal planning of CESSs has been generally regarded as a complex task as it involves interactions among multiple stakeholders such as its provider, prosumers, consumers, and the grid. In this thesis, we examine how different stakeholders can benefit from optimising CESS planning. This chapter presents the background and literature review conducted as a part of the thesis research. It is primarily divided into three sections. The first section is a background study of energy storage systems. The second section presents an extensive review of existing studies on optimal CESS operation, optimal CESS planning, and auction-based CESS energy management under several taxonomies. Finally, we conclude the chapter by highlighting the potential research gaps in CESS planning optimisation studies that were addressed by this PhD research.

2.1 Background

In this section, first, we provide a general overview of different types of ESSs. Then, we narrow down our discussion to electro-chemical ESSs, and describe about their different types based on their scale of use in power systems as utility, community and residential electro-chemical ESSs with real-world examples. Finally, we compare and contrast these electro-chemical ESSs considering their characteristics.

2.1.1 Energy Storage Systems

As mentioned in Chapter 1, ESSs can store the excess energy from renewable energy sources and release the energy back to the grid and/or prosumers when required. Table 2.1 provides a list of various energy storage system types and technologies, along with a brief description of their storage methods.

Table 2.1: Different types of energy storage systems [Arani et al., 2019; Rahman et al., 2020; Zhang et al., 2021; Hannan et al., 2021].

Type of energy storage	Technology	Description
Mechanical storage	Pumped-hydro storage	Stores gravitational potential energy by pumping water to higher elevations
	Compressed-air energy storage	Compresses air and stores it in underground caverns to generate power later
	Flywheels	Rotational energy stored in a high-speed rotor for rapid discharge
Electro-chemical storage	Li-ion batteries	Has a high energy density
	Lead-acid batteries	Low-cost but limited life cycle and energy density
	Flow batteries	Energy stored in liquid electrolytes and scalable for large energy storage
Thermal storage	Molten salt	Stores heat for electricity generation
	Phase change materials	Stores energy by changing the material state
Chemical storage	Hydrogen	Electricity converted to hydrogen through electrolysis
Electrical storage	Super capacitors	Stores energy electrostatically for immediate release
	Superconducting magnetic energy storage	Stores energy in magnetic fields in superconductors

These different types of ESSs are used in a wide range of power system applications. In this background study, we focus only on electro-chemical storage systems with battery technologies, classifying them into three categories based on their scale of use in power systems as follows: (i) utility energy storage systems (UESSs), (ii) community energy storage systems (CESSs), and (iii) residential energy storage systems (RESSs). Typically, large-scale and medium-scale UESSs used in generation and transmission level of power systems are batteries that operate at high-voltage (HV) levels, whereas medium-scale UESSs used in distribution level are the ones that operate at medium-voltage (MV) levels. CESSs are medium to small-scale batteries installed and operated in LV distribution networks, while RESSs are small-scale batteries used by prosumers in LV distribution networks. In the next section, we discuss about the aforementioned types of ESSs, along with their applications and real-world examples.

2.1.2 Utility Energy Storage Systems

These are are large-scale or medium-scale energy storage solutions, typically owned by utilities that operate at generation, transmission and distribution levels of power systems for many applications [Hameer and van Niekerk, 2015; Nguyen et al., 2020]. For instance, utilities in generation and transmission level exploit UESSs for energy arbitrage. Here, UESSs play a key role in energy arbitrage by storing energy when energy prices are low, and dispatching it back to the grid or using it internally when energy prices are high [Hameer and van Niekerk, 2015; Nguyen et al., 2020]. This strategy allows utilities to maximise their revenue, while enhancing grid stability and accommodating higher shares of renewable energy.

Generation and transmission utilities may use UESSs for network frequency regulation [RAO et al., 2020; Akram et al., 2020; Hosseini et al., 2022; Das et al., 2020]. Frequency regulation is essential for maintaining the stability and reliability of the power system, ensuring that the supply of electricity matches demand in real-time. Typically, UESSs with battery technologies are fast-responding, and hence, can respond almost instantaneously to changes in grid frequency. This rapid response is essential for stabilising the grid, following sudden changes in demand or generation. In the context of frequency regulation, UESSs can provide frequency control under two phases as primary and secondary [Rajan et al., 2021]. In primary control, UESSs can automatically respond to frequency deviations within a very short time, providing immediate support to maintain the grid stability. As the secondary control, they can be dispatched by utilities to fine-tune frequency adjustments after the initial response, ensuring long-term stability.

UESSs may also provide congestion management services within transmission networks [Tarashandeh and Karimi, 2021; Zhang et al., 2020]. Transmission network congestion occurs when the demand for electricity exceeds the capacity/limits of transmission lines, leading to potential overloads and reliability issues. Hence, transmission utilities may exploit UESSs to alleviate congestion by storing energy during low-demand periods and releasing it during high-demand periods, thus optimising the flow of electricity and enhancing grid reliability. Moreover, the use of UESSs for congestion management not only helps to defer costly transmission infrastructure upgrades, but also improves the operational flexibility of the grid, accommodating fluctuating demand more effectively.

The distribution network service providers (DNSPs) may also use UESSs for network applications. For instance, similar to that of transmission utilities, DNSPs may use UESSs for managing the distribution network congestion as described before [Iria et al., 2019; Oskouei and Gharehpetian, 2024; Pantoš, 2020]. Additionally, UESSs can support in network voltage regulation [Iria et al., 2019]. UESSs having the reactive power control capability can provide reactive power support, which is essential for voltage control in power systems. By injecting or absorbing reactive power as needed, UESSs can stabilise voltage levels. During low voltage situations at high energy consumption periods, UESSs can inject reactive power into the grid to raise voltage levels. Conversely, when the voltage levels are too high at low energy consumption periods, UESSs can absorb reactive power, helping to lower voltage levels. Moreover DNSPs are also benefited from UESSs, as UESSs can alleviate network energy losses and demand side management [Jokar et al., 2022]. In this context, UESSs support in levelling out the peak demand, leading to more efficient operation of the network and reducing energy losses.

2.1.2.1 Real-World Installations of Utility Energy Storage Systems

Table 2.2 summarises a list of real-world UESSs utilising battery technology used in HV and MV networks.

Table 2.2: Different utility energy storage systems projects in the world.

	Utility Energy Storage System	Technology
Large-scale UESSs	Hornsdale power reserve (Australia) [Reserve, 2023]	Li-ion battery
	Tesla Megapack at Moss Landing (USA) [Tesla, 2023]	Li-ion battery
	Fairbanks energy storage system (USA) [ABB, 2023]	Nickel-cadmium battery
	Dalian energy storage system (China) [DICP, 2022]	Vanadium redox flow battery
	Wiltshire energy storage system (UK) [SSE Renewables, 2024]	Li-ion battery
Medium-scale UESSs	Okinawa NaS battery energy storage system (Japan) [Data Center Dynamics, 2024]	Sodium-sulphur battery
	"RedoxWind project" battery energy storage system (Germany) [ICT, 2024]	Vanadium redox flow battery

2.1.3 Community Energy Storage Systems

As mentioned before, CESSs are medium to small-scale batteries (typically in the range of 100 kWh-5 MWh size) that can trade energy with different stakeholders such as multiple prosumers and consumers, and the grid to economically and/or technically benefit them including its provider [Shaw et al., 2020]. Usually, CESSs are available in LV distribution networks as in-front-of-the-meter energy storage systems. Recent research show a CESS of the equivalent size of multiple residential batteries may provide better benefits to the community and network [Walker and Kwon, 2021a; Zhang et al., 2022; Scheller et al., 2020].

As shown in Figure 2.1, a CESS charges by importing energy from multiple prosumers and the grid, and it discharges by exporting energy to the grid, prosumers and consumers. In the presence of a CESS, prosumers may import energy from the grid and/or the CESS if their PV generation is not enough to fulfil energy demand, and export energy back to them when the PV generation is high. Moreover, consumers satisfy their energy demand by importing energy from the grid and the CESS. Additionally, the grid may trade energy with the CESS and prosumers and consumers (see Figure 2.1). The flexibility gained by prosumers, consumers, the grid and the CESS to trade energy with multiple entities allow them to enhance their individual benefits compared with an energy trading setting in the presence of RESSs.

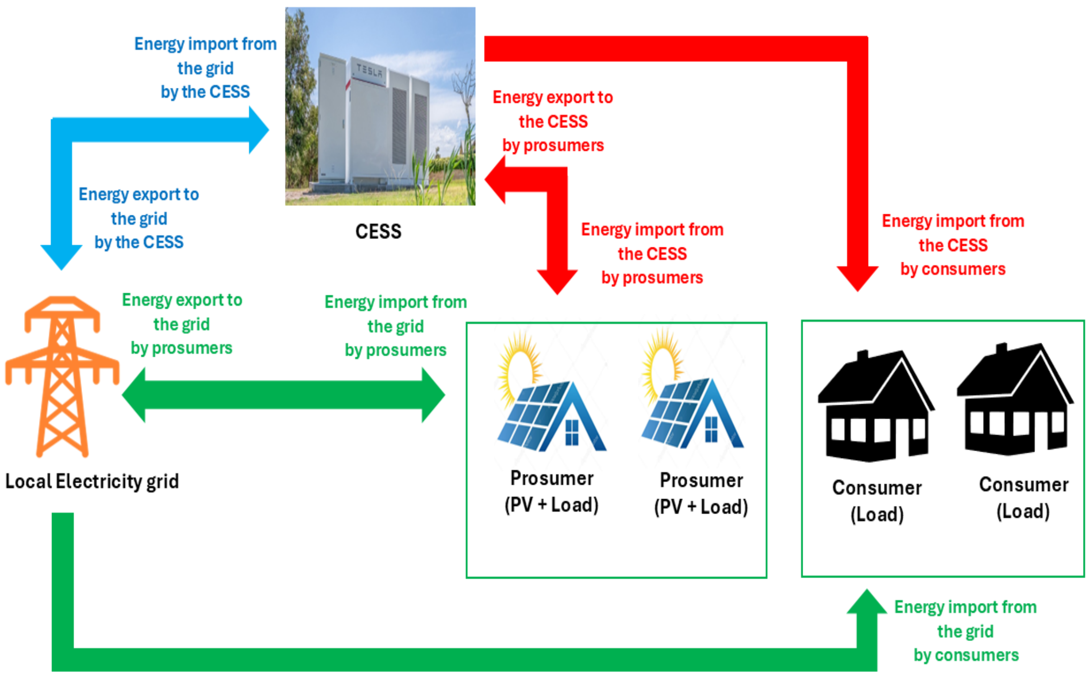

Figure 2.1: Operation of a CESS with energy imports and exports marked.

Similar to that of UESSs, CESSs also provide a wide range of benefits. For instance, CESSs increase the community's access to renewable energy sources as they can serve multiple prosumers and consumers [Shaw et al., 2020; Li et al., 2022b; Koirala et al., 2018]. Prosumers may store their excess energy from renewable sources such as PV systems during the day time, and use that energy when their energy consumption is high or PV generation is low. On the other hand, consumers who do not have individual renewable installations to benefit from shared renewable energy projects.

Investing in individual energy storage systems can be financially challenging for individual households. CESSs offer a solution to this by allowing those communities to share the costs of battery installations, maintenance, and operation among them. This collective approach reduces the financial burden on individuals, making energy storage more accessible [Chreim et al., 2024].

CESSs can help to accommodate the peak energy demand of the network, as they can discharge their stored energy during high energy consumption periods [Mediwaththe et al., 2019; Alam and Jang, 2023; Elio et al., 2021], thereby reducing strain on the network. By discharging energy to the network when needed, CESSs can reduce the necessity for utilities to rely on expensive peaking power plants, thereby lowering overall energy costs for community members.

CESSs can also enhance the network's hosting capacity by managing the variability of generation from renewables [Fatima et al., 2020]. By smoothing out the supply from these intermittently available resources, CESSs help to ensure that more renewable energy can be integrated into the network without causing system instability or congestion.

Additionally, upgrading network infrastructure to accommodate increased energy demand or to integrate more renewable energy sources can be costly [Zhao et al., 2023; Garg and Niazi, 2022]. CESSs can defer the need for such upgrades by effectively managing local demand and supply. Moreover, they can alleviate the stress on the existing infrastructure, allowing utilities to postpone expensive upgrades.

2.1.3.1 Real-World Installations of Community Energy Storage Systems

Several significant CESS installation projects have been undertaken globally, and a few key examples are described below.

- **Brooklyn-Queens Neighbourhood Program in USA.** This project, implemented by Con Edison, uses a battery system in Brooklyn and Queens to reduce demand on the local grid, improve reliability, and defer network upgrades. The CESS is a Li-ion battery of 12 MWh size [Strategies, 2023].

- **Yackandandah CESS in Australia.** A CESS with a size of 274 kWh installed in Victoria, Australia to enhance the local renewable energy usage and promote energy independence within the community [Yack, 2023].

- **Bondi CESS in Australia.** This is a CESS project in Bondi, New South Wales, Australia, aimed at improving local energy resilience and promoting the use of renewable energy. The CESS has a capacity of 412 kWh to accommodate the surplus PV generation of communities in Bondi. Figure 2.2 shows the CESS installed in Bondi [SolarQuarter, 2024].

Figure 2.2: The CESS in Bondi, Australia [SolarQuarter, 2024].

- **Tesla PowerBank CESS in Australia.** A CESS of a 474 kWh size is installed in Perth to serve residential communities across Maddington and Beechboro, Western Australia [Power, 2023b].
- **Stafford Hill Solar and Storage Project in USA.** The Stafford Hill project combines PV generation with battery storage capabilities, aiming to create a reliable and sustainable energy solution for the local community in Vermont, USA. This project features a CESS of 1.2 MWh size complemented with a solar array size of around 2.2 MW [Group, 2023].
- **CESS project in Rijsenhout, Netherlands.** This project features a storage capacity of 128 kWh, which serves a community of 35 households. The primary goal of the Rijsenhout project is to maximise the PV self-consumption of locally generated renewable energy [NL4WorldBank, 2017].

2.1.3.2 Current State of Community Energy Storage Systems Implementation and Regulatory Frameworks

In Australia, several pilot projects, such as the Flemington Community Battery in Victoria and the Solar Banks Program, highlight efforts to integrate CESSs into local energy markets. However, the regulatory landscape remains fragmented, as existing frameworks primarily focus on household and utility-scale energy storage systems. The Australian Energy Market Commission has introduced rule changes, such as the two-way electricity market reform, but barriers remain in defining the role of CESS providers, tariff structures, and revenue mechanisms.

In addition to Australia, several European countries, particularly Germany and the UK, have been at the forefront of CESS adoption. Germany's KfW battery storage program and the UK's Smart Local Energy Systems initiative support decentralised energy storage. Moreover, in the USA, CESS projects are emerging in states with ambitious renewable energy targets, such as California and New York. The California Energy Commission and the New York State Energy Research and Development Authority have funded pilot projects to explore community battery benefits. However, the Federal Energy Regulatory Commission is yet to establish clear guidelines on revenue stacking and market participation for community storage. Also, despite strong policy support from all these countries, the integration of CESSs in energy markets is still evolving.

2.1.4 Residential Energy Storage Systems

In practice, RESSs are also called as "Residential Batteries". These are small-scale batteries typically installed at residences in LV distribution networks. They are owned by prosumers who consume and produce energy (usually from rooftop PV). The excess PV generation during the daytime is stored in RESSs, enabling their owners to use that energy when the PV generation is low and during the times when the electricity demand is high.

Figure 2.3 illustrates the typical operation of a RESS. A RESS charges from the excess PV generation of the prosumer, and also from the grid (if grid connected). When the prosumer has a deficit of energy, the RESS discharges by exporting its energy back to the prosumer. Also, the RESS may discharge by exporting its stored energy back to the grid as shown in Figure 2.3.

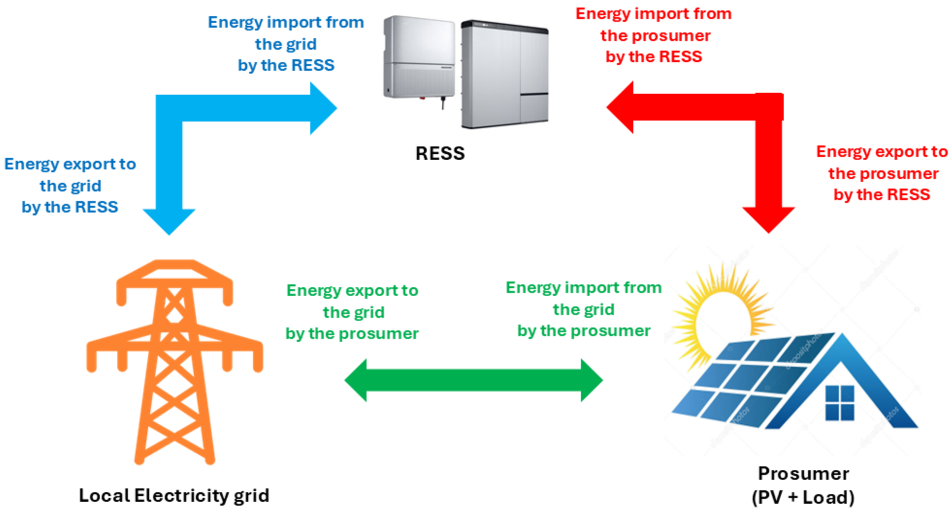

Figure 2.3: Operation of a RESS with energy imports and exports marked.

As mentioned before, prosumers with RESSs use the stored energy during peak energy consumption periods, reducing the reliance on grid electricity when prices are high, and thereby lowering their energy bills [Khezri et al., 2022; Tan et al., 2021; Shaqsi et al., 2020]. Additionally, RESSs are also useful in power outages, as they can partly or fully meet the energy requirements of their owners, thereby improving the energy reliability. Also, RESSs improve the PV self-consumption of prosumers lowering their electricity bills [Yu, 2021; Lu et al., 2020]. In this context, prosumers store the excess PV energy generated instead of exporting it to the grid. This self-consumption model allows prosumers with RESSs to draw less energy from the grid during times of high demand or low PV generation, further reducing their dependence on external electricity supply and decreasing overall energy costs. In turn, this increased utilisation of self-generated energy not only offers financial benefits, but also supports a more sustainable and balanced energy system by minimising grid demand.

RESSs can provide distribution network services through operating envelopes [Iria et al., 2021, 2023; Choudhury, 2022]. Operating envelopes are predefined limits set by the network operator for energy imports and exports at individual connection points, allowing RESSs to function within safe and optimal parameters. Some of the network services provided through operating envelopes include voltage and frequency regulation, local network congestion relief, and demand management. By controlling the export of stored solar energy, RESSs prevent excessive voltage rise, particularly in areas with high PV penetration. Controlled discharge of RESSs ensures that voltage remains within acceptable limits, enhancing the stability and efficiency of the network. Operating within defined envelopes, RESSs can quickly respond to grid frequency deviations by adjusting their charge/discharge rates, aiding in overall grid stability. In areas with network congestion, operating envelopes help to manage the export capacity of RESSs. By coordinating energy export across multiple RESSs, the distribution network can avoid overloads in constrained areas, optimising energy flow and preventing congestion-related issues. Moreover, by adhering to operating envelopes, RESSs can charge and discharge to reduce peak demand on the grid.

2.1.4.1 Real-World Installations of Residential Energy Storage Systems

This section presents real-world examples for RESSs utilised in LV distribution networks.

- Authors of [Iria and Soares, 2023] propose an energy-as-a-service business model to maximise the economic benefits for prosumers and the aggregator. In this study, a real-world community of prosumers with RESSs in Australia are used for simulations. Additionally, authors of [Iria et al., 2023] compare and contrast five bidding optimisation strategies, and authors of [Iria et al., 2021] propose a bidding optimisation strategy for an aggregator, enabling it to make network-secure, real-time bidding decisions in energy and reserve markets. In these studies also, the aforementioned community members with RESSs are used for simulation experiments.

- An energy management project is implemented in Netherlands by interconnecting RESSs to enhance the PV self-consumption of prosumers as mentioned in [Brouwer, 2018].

- The Vermont Green Mountain Power company provides subsidy schemes for prosumers to invest on RESSs, and enhance the energy reliability through a project called "Resilient Home" [Power, 2023a].

- The New York utility Con Edison uses RESSs for capacity reserves and defer network expansion. The utility provides subsidies for prosumers to install RESSs under the "Reforming the Energy Vision Initiative" [Coddington et al., 2017].

- The UK Power Networks in collaboration with Powervault aims to install RESSs at residential places in London to satisfy the network peak demand in Winter, to minimise the reliance on conventional fuel-based generation and reduce carbon emissions. The pilot project was implemented in 2018 [GOV.UK, 2023].

2.1.5 Comparison of Utility, Community, and Residential Energy Storage Systems

In this section, we compare and contrast utility, community, and residential energy storage systems. In addition to the operational difference, there are several key features that distinguish UESSs, RESSs, and CESSs. They are succinctly listed in Table 2.3.

Table 2.3: Comparison of UESSs, RESSs and CESSs [Hameer and van Niekerk, 2015; Shaw et al., 2020; Li et al., 2022a; Chatzigeorgiou et al., 2024].

Attribute	UESSs	CESSs	RESSs
Ownership	Utilities or energy companies	Third party or a community	Individual prosumers
Connection location	To the transmission or distribution network	To the distribution network in-front-of-the-meters of prosumers and consumers	To the behind the meter of a prosumer
Main Beneficiaries	Serve a transmission or a distribution network	Serve multiple prosumers and consumers	Serve individual prosumers
Size	Large scale and medium-scale	Medium scale to small-scale	Small-scale
Number of units	Typically, a single UESS in a network (But can be multiple at times)	Typically, a single CESS in a network (But can be multiple at times)	Typically, multiple RESSs in a network

2.2 Literature Review

There exists a vast literature on ESSs, including utility, community, and residential batteries discussed in the previous section. In this section, we specifically focus on the literature related to CESSs in LV distribution networks, as this thesis investigates how the optimal CESS planning can benefit LV stakeholders.

The benefits of CESSs can be further improved by optimising their operation (i.e., the charging and discharging schedule of the CESS) and planning (i.e., the CESS integration location, size, and its rated power including the charging and discharging schedule).

Therefore, the existing literature on optimal CESS energy management in LV distribution networks propose models to (i) optimise the CESS operation, and (ii) optimise the CESS planning. In this thesis, we synthesise the literature survey of those two under different categories namely; (a) the type of CESS optimisation model as deterministic models vs stochastic models, (b) the number of objective functions in the CESS optimisation model as single objective function vs multi-objective function, and (c) the analysis time of the CESS optimisation models as single-day vs multiple-days (for CESS operation) and single-year vs multi-year (for CESS planning). In addition to that, we explore the literature on auction-based models for CESS management. An extensive literature survey on optimal CESS energy management under the aforementioned categories are detailed in this section.

2.2.1 Optimal Operation of CESSs in Low-Voltage Networks

This section presents an extensive literature survey on studies that optimise the CESS operation based on the four different criteria mentioned above.

2.2.1.1 Deterministic versus Stochastic Optimisation Models

Although there are many well-established optimisation techniques, such as stochastic optimisation, robust optimisation, and chance-constrained optimisation, available to model uncertainties in CESS energy management problems, this literature survey focuses solely on stochastic optimisation due to its prevalent application in CESS management models. Additionally, while deterministic frameworks are also utilised in CESS operation studies, they often do not adequately address the uncertainties present in energy systems. In this section, we compare and contrast different studies on CESS operation that are proposed as deterministic and stochastic frameworks.

2.2.1.1.1 Deterministic Optimisation Models In deterministic optimisation models, it is assumed that all input data, including objective functions, constraints and parameters are known ahead from their forecasts [Boyd and Vandenberghe, 2004; Bazaraa et al., 2006; Bertsekas, 1999; Hillier and Lieberman, 2014]. Ease of implementation and reduced computational burden are some of the key advantages of deterministic optimisation models [Birge and Louveaux, 2011; Shapiro et al., 2009].

Several studies are proposed in the literature to deterministically optimise the CESS operation and maximise economic benefits for various stakeholders. For instance, a method built up on game theory concepts to maximise the revenue of the CESS provider and to minimise energy costs of prosumers and consumers is discussed in [Mediwaththe and Blackhall, 2020b]. In this study, the CESS operation is optimised in coordination with demand-side management to maximise the economic benefits for all stakeholders. In [Wang et al., 2018], a CESS operation optimisation model to accommodate the high PV generation by prosumers, and thereby, minimise the energy costs of prosumers is presented. Here, the optimal operation of the CESS contributes in maximising the PV self-consumption, reducing prosumers' reliance on grid energy and regulating voltage levels of the network. An optimisation model to optimise the CESS operation to maximise the economic benefits of prosumers and the energy service provider is proposed in [Oh and Son, 2019]. In this paper, both aforementioned beneficiaries are benefited from the CESS through peak shaving and energy arbitrage. A framework for optimising the charging and discharging schedule of a CESS based on real-time market prices is mentioned in [Arghandeh et al., 2014]. This work aims to minimise the operating costs of prosumers and consumers including the CESS provider.

A common feature of [Mediwaththe and Blackhall, 2020b; Wang et al., 2018; Oh and Son, 2019; Arghandeh et al., 2014] is that the PV generation by prosumers and real energy consumption by prosumers and consumers are assumed to be known ahead from their forecasts. In contrast to these works, some studies consider the reactive energy consumption by prosumers and consumers is also known, so the the CESS operation can be better optimised. For instance, authors of [Zhang et al., 2023] propose a method to optimise the CESS real and reactive power dispatch schedule to minimise the operating costs of the CESS provider and the distribution network service provider in the day-ahead electricity market. An energy cost sharing mechanism in a community of prosumers to promote the effective management of reactive power within a peer-to-peer energy sharing framework is explored in [Gu et al., 2023]. In this work, authors optimise the operation of a CESS to improve its reactive power support, and thereby economically benefit prosumers.

In addition to enhancing the economic benefits for CESS beneficiaries, several studies investigate ways to improve technical aspects, such as voltage regulation, load management, and overall system stability, through the optimisation of CESS operation. A study on the use of a CESS for load shifting in a residential community is mentioned in [Parra et al., 2020]. A similar study is presented by the same authors in [Parra et al., 2021] to perform load management in a community of energy users using a CESS. In [Yang et al., 2020], a transactive control strategy combined with an optimised CESS charging and discharging schedule is discussed. This proposed model is capable of adjusting network voltage levels based on real-time network conditions, enhancing the grid stability. Moreover, a comprehensive discussion on how the network power quality and the reliability of smart grids can be improved by optimal CESS operation is given in [Singh et al., 2018].

In the literature, certain studies including [Mediwaththe and Blackhall, 2020a; Nick et al., 2014] propose CESS energy management frameworks to improve techno-economic benefits of different stakeholders. In [Mediwaththe and Blackhall, 2020a], authors optimise the CESS operation to minimise the energy loss of the network and to minimise the energy costs of prosumers, consumers and the CESS provider. Moreover, authors of [Nick et al., 2014] suggest a CESS operation optimisation model to minimise voltage deviations of nodes, energy loss, and maximise the profits of the CESS provider. Additionally, authors of [van der Stelt et al., 2020; Dong et al., 2021] analyse how the optimal energy management of a CESS can economically benefit prosumers with smart appliances, and technically benefit the network through demand-side management. Additionally, certain studies propose frameworks to optimise the CESS operation and generate techno-economic-social benefits. For instance, the authors of [Hou et al., 2024a] propose a CESS management framework to minimise energy costs and maximise the operational safety of prosumers, while minimising carbon emissions.

2.2.1.1.2 Stochastic Optimisation Models All the aforementioned studies are built as deterministic models without modelling uncertainty. However, in reality, factors such real and reactive energy consumption, PV generation, energy prices are often subject to significant uncertainty. Neglecting the uncertainty of these factors may lead to inefficient CESS energy management, as the forecast errors can be high. According to [Boyd and Vandenberghe, 2004], there are several types of optimisation approaches to deal with uncertainty including stochastic optimisation, robust optimisation, and chance-constrained optimisation. In stochastic optimisation it is assumed the uncertain parameters follow a known distribution and the objective is to find the expected value of the objective function [Birge and Louveaux, 2011; Hillier and Lieberman, 2014; Shapiro et al., 2009]. In contrast to stochastic optimisation, robust optimisation works on the principle assuming the uncertainties lie within uncertainty sets and aims to find solutions that are feasible and perform well for any realisation of the uncertainties within those sets [Birge and Louveaux, 2011; Hillier and Lieberman, 2014; Shapiro et al., 2009; Ben-Tal et al., 2009]. In chance-constrained optimisation, constraints are only required to be satisfied with a certain probability. This allows some degree of risk or violation of constraints but ensures that violations occur infrequently [Birge and Louveaux, 2011; Hillier and Lieberman, 2014; Shapiro et al., 2009].

In the literature, there are several stochastic optimisation studies proposed to optimise the CESS operation under uncertainty. For instance, a method to minimise the energy costs of prosumers and maximise the profits of the CESS provider is mentioned in [Gu et al., 2023]. In this work, the uncertainties of real energy consumption and PV generation are modelled using a data-driven stochastic approach. Authors of [Walker and Kwon, 2021b] address the minimisation of energy costs for prosumers, taking into account the uncertainties of PV generation and real energy consumption. In [Li et al., 2022a], a CESS operation optimisation framework under the aforementioned uncertainties is proposed to minimise the energy costs of prosumers and the CESS provider based on an asymmetric Nash bargaining model. A machine-learning technique to model the uncertainty of real energy consumption is exploited in [Giraldo et al., 2021]. Here, the authors optimise the CESS operation to minimise the network real energy loss. All these studies discuss either economic or technical benefits gained by optimising the CESS operation under uncertainty.

In this branch of literature, some studies propose models to improve techno-economic benefits through optimal CESS operation. For instance, authors of [Pezeshki et al., 2014] investigate how to minimise the energy costs of prosumers and consumers, and the CESS provider, and to maximise the CESS lifetime by optimising the CESS operation under uncertainty. Here, a model-predictive control approach is exploited to optimise the CESS operation under the uncertainty of real energy consumption and PV generation. An energy sharing model in the presence of a CESS to minimise energy users (i.e., both prosumers and consumers) from optimal CESS operation is mentioned in [Dorahaki et al., 2023a]. In this article, the uncertainty of PV generation is stochastically modelled to reduce the energy bills and power interruptions for prosumers efficiently. In addition to that, a Markov- modulated rate process to model the uncertainties associated with wind energy production and optimise the CESS operation is suggested in [Wang et al., 2016]. These studies highlight the role of optimal CESS operation in enhancing techno-economic outcomes for different stakeholders under uncertainty.

2.2.1.2 Single-Objective versus Multi-Objective Optimisation Models

This section presents a comprehensive study of optimal CESS operation models categorised under single-objective and multi-objective frameworks.

2.2.1.2.1 Single-Objective Optimisation Models In this branch of literature, authors propose optimal CESS operation frameworks that aim to minimise a single objective. For instance, [Tucker and Alizadeh, 2022] the CESS operation is optimised to maximise the economic benefits of prosumers gained from the CESS. In this paper, the uncertainty of real energy consumption and weather conditions are also accounted. The same objective in [Tucker and Alizadeh, 2022] is considered by the authors of [Chang et al., 2022], and it is achieved by optimising the CESS energy allocation to all prosumers. Moreover, the authors of [Luo et al., 2020] investigates how the optimal CESS operation can minimise the overall operating cost of a microgrid. Here, the operation of a CESS in a microgrid is optimised under the uncertainty of energy consumption, and PV and wind energy generation. Also, an optimisation framework to maximise CESS provider's economic benefits through optimal CESS operation is mentioned in [Ma et al., 2022].

There are few studies in the literature that aim to optimise the CESS operation to generate technical benefits. For instance, a CESS management framework to minimise network congestion is discussed in [van Westering and Hellendoorn, 2020]. Furthermore, a CESS operation optimisation model to mitigate voltage excursions in unbalanced LV networks is proposed in [Alam et al., 2015]. In this study, a dynamic energy trading mechanism with the grid in all three phases by the CESS is proposed to minimise the neutral current and voltage deviations.

2.2.1.2.2 Multi-Objective Optimisation Models In multi-objective optimisation two or more conflicting objectives are aimed to be optimised simultaneously, enabling to value trade-offs of each objective. In this context, there are many ways to model multi-objective problems including the weighted-sum method, hierarchy method (epsilon-constraint method) [Grodzevich and Romanko, 2006], and multi-objective evolutionary algorithms [Zhou et al., 2011]. In the weighted-sum method, all objective functions are weighted according to their importance, and the weight factors are computed from the analytic hierarchy process [Grodzevich and Romanko, 2006]. In the hierarchy method, objective functions are first ranked according to their importance to the decision-makers. Then, each objective is minimised sequentially subject to a set of constraints of the optimisation problem, along with extra constraints defined by a trade-off threshold ϵ based on the optimal values achieved for the higher-priority objective functions. This process is repeated until the problem is solved for all objectives [Grodzevich and Romanko, 2006]. Multi-objective evolutionary algorithms rely on improving the quality of a population of solutions through iterations. Some of the widely used muli-objective evolutionary algorithms are NSGA-II (Non-dominated Sorting Genetic Algorithm II) and SPEA2 (Strength Pareto Evolutionary Algorithm 2) [Zhou et al., 2011]. These algorithms are particularly effective in exploring large, complex solution spaces and are often used to find a diverse set of Pareto-optimal solutions.

In the literature, a number of papers discuss optimal CESS operation to achieve multiple objectives of different stakeholders. For instance, authors of [Jo and Park, 2020] propose an optimal CESS operation scheme to maximise the revenue of the CESS provider and demand-side management. In [Houwing et al., 2023], the CESS operation is optimised to maximise the energy bill savings and fair access to CESS energy by prosumers. The economic benefits for peer-to-peer energy trading prosumers and the CESS provider are enhanced simultaneously through optimal CESS operation in [Gokcek et al., 2022]. An investigation on how the optimal CESS operation impacts the network voltage profile and the real energy loss is done in [Mahmoodi et al., 2020]. A multi-objective stochastic optimisation framework to optimise the CESS operation and thereby, minimise the expected energy imports from the grid by prosumers and maximise the use of renewable energy resources is presented in [Alam and Jang, 2023]. A case study on maximising the CESS provider's profits while minimising the curtailment of renewable energy resources in a German LV network is discussed in [Safarazi et al., 2020]. Moreover, a model that can minimise the energy costs and maximise the PV self-consumption of prosumers is suggested in [Hou et al., 2024b], by optimising the CESS operation. Also, an optimisation model capable of minimising the real energy loss, voltage deviations, and the ageing of the distribution transformer through a properly managed CESS is explored in [El-Batawy and Morsi, 2018]. Additionally, certain studies present multi-objective optimisation frameworks to generate environmental and economic benefits. For instance, the authors of [Schram et al., 2020; Wang et al., 2023] propose multi-objective optimisation frameworks to minimise carbon emissions and prosumers' energy costs through optimal CESS operation.

2.2.1.3 Single-Day versus Multiple-Days Optimisation Models

In general, operation problems are investigated as short-term problems, typically for a duration of one day or few weeks. In this section, we present a literature survey of optimal CESS operation models, focusing on both single-day and multiple-days analyses.

2.2.1.3.1 Single-Day Analyses In [Gerdroodbari et al., 2023], a study on benefiting both the distribution network service provider and prosumers by optimising the CESS operation is presented. Here, the authors have done the analysis for a period of one day, using the PV generation and energy consumption profiles of a community of prosumers obtained on a clear-sky day. Another study on optimal CESS operation to economically benefit a remote community of prosumers in Indonesia is mentioned in [Asri et al., 2023]. In this study, the operation of a CESS is optimised over a period of 24 hours to minimise the operating cost of prosumers in a microgrid. Moreover, authors of [Yang et al., 2024a; Abraham et al., 2022; Hou et al., 2024b] have also presented CESS operation optimisation frameworks to enhance the technical and economic benefits gained from a CESS considering an analysis period of one day. Also, the authors of [Wang et al., 2021a] propose an optimal CESS operation framework to minimise prosumers' operating costs. This study uses three energy consumption profiles namely, electricity consumption, cooling consumption, and heating consumption and PV generation profile of prosumers on a typical summer day for the analyses. In [Dorahaki et al., 2023b], the authors propose a CESS energy management mechanism to enhance economic benefits and comfort level of prosumers considering an analysis period of one day.

2.2.1.3.2 Multiple-Days Analyses In addition to the CESS works that are based on single-day analyses, there are some studies that have considered multiple-days in CESS modelling. For instance, authors of [Duque et al., 2022] aim to maximise the CESS provider' energy benefits while satisfying the technical limits of the network. In this paper, they optimise the CESS operation considering the real energy consumption and PV generation data for a period of one week. The authors of [Reddy and Padhy, 2024] propose a CESS operation optimisation method to enhance the network voltage profile while maximising the use of the CESS. Here, seasonal weather data of some selected days in a year are used for simulations. Additionally, authors of [Ho et al., 2016] propose daily and weekly optimal CESS operation modes, and selects the best mode that minimises the operation cost of the CESS provider.

2.2.2 Optimal Planning of CESSs in Low-Voltage Networks

This section presents a comprehensive study of literature on CESS planning. First, research works on deterministic and stochastic CESS planning optimisation models are presented. Next, CESS planning models classified as single-objective and multi-objective is given. Finally, the single-year and multi-year CESS planning models are compared and contrasted.

2.2.2.1 Deterministic versus Stochastic Optimisation Models

In the literature, there are significant number of studies on CESS planning that model uncertainties. However, in this thesis we focus only on the ones that use stochastic optimisation techniques due to its vast use in energy management problems. Additionally, there are some studies that utilise deterministic approaches to plan CESSs. Therefore, in this section, we review different studies on deterministic and stochastic CESS planning models.

2.2.2.1.1 Deterministic Optimisation Models This branch of literature is about CESS planning optimisation models that do not model uncertainties, including factors such as real and reactive energy consumption, PV generation, and energy prices. The authors of [Nazari et al., 2021] discuss a CESS planning model to joinlty invest on a CESS in a microgrid by the distribution network service provider and the microgrid operator. This framework allows to distribute the high CESS investment cost and increase the financial benefits for the investors. A similar work is mentioned in [Yang et al., 2021] to cooperatively invest on the installation of a CESS in a residential community by its community members, and thereby reduce their energy costs from sharing the CESS. A CESS planning scheme is suggested in [Xie et al., 2019] for load shifting by using a CESS to reduce the energy costs of prosumers.

There are few studies that aim to improve the technical benefits from a CESS by optimising its planning. A study on planning of CESSs is presented in [Alrashidi, 2022] to regulate the voltage levels of a LV network. A method to maximise the hosting capacity of a distribution network in the presence of a CESS is proposed in [Divshali and Söder, 2019]. In this study, a CESS that can store reactive energy in addition to real energy is considered. Additionally, studies in [Böhringer et al., 2021; Hung and Mithulananthan, 2011] explore analytical methods to plan CESSs and enhance techno-economic benefits of multiple stakeholders.

All these studies have proposed deterministic optimisation models to plan CESSs with no uncertainty. However, as mentioned before, these models may not provide best CESS outcomes as forecast errors of deterministic parameters such as PV generation, and real and reactive energy consumption can be significantly high.

2.2.2.1.2 Stochastic Optimisation Models In contrast to [Nazari et al., 2021; Yang et al., 2021; Xie et al., 2019; Alrashidi, 2022; Divshali and Söder, 2019; Böhringer et al., 2021], some papers have accounted for the uncertainties mentioned above in CESS planning. For instance, a multi-stage stochastic CESS planning model to economically benefit an energy using community is given in [Hafiz et al., 2019]. This study aims to minimise the energy costs of prosumers and consumers under the uncertainty of real energy consumption, PV generation, and grid energy prices over different seasons in a year. In this work, the authors utilise a multi-stage approach for CESS energy management, and the economic savings of prosumers and consumers are calculated using the net present value (NPV) approach. A research article on optimising the CESS planning under the uncertainty of PV and wind power generation, and real energy consumption of consumers and prosumers is discussed in [Wang et al., 2022]. In this paper, the uncertainties of aforementioned factors are accounted to better plan CESSs, and maximise the economic benefits for prosumers, consumers, and the CESS provider. Additionally, a game-theory approach for optimising the CESS planning considering the uncertainty of PV and wind power generation is discussed in [Liu et al., 2023]. In [Mahmoodi et al., 2020], authors have investigated how the CESS location impacts the voltage profile and energy losses in LV networks under the uncertainty of real energy consumption and PV generation. Here, the uncertainties are modelled using the monte-carlo simulation (MCS), which is one of the most adopted method to model uncertainties.

Optimisation models that model uncertainties in terms of scenarios are often computationally exhaustive. Therefore, it is imperative to reduce the number of scenarios by removing less probable outcomes and aggregating similar outcomes using scenario reduction techniques such as K-Means clustering method [Scarlatache et al., 2012]. Authors in [Pamshetti and Singh, 2022] have discussed a method to plan a CESS to exploit the high PV generation, and thereby, minimise prosumers' energy costs, CESS investment and operating cost, and carbon emissions concurrently. Here, the authors have exploited a normal distribution to model uncertainties of PV generation and real energy consumption, and then the roulette wheel mechanism to generate scenarios. Eventually, the K-means clustering method is used to keep the problem tractable while sustaining a fair approximation for uncertainties.

2.2.2.2 Single-Objective versus Multi-Objective Optimisation Models

This section presents a series of studies that optimise the CESS planning to achieve a single objective or multiple objectives together.

2.2.2.2.1 Single-Objective Optimisation Models In this context, the literature discusses optimal CESS planning models to achieve a single objective. A CESS planning approach to maximise the economic benefits of the retailer is explored in [Liu et al., 2021]. The research work in [Hossain et al., 2020] aims to achieve the same objective by accounting for the uncertainty of energy consumption and PV generation of prosumers. Moreover, a single-objective CESS planning model to reduce network real energy loss is suggested in [Ma et al., 2017]. In [Liu et al., 2024], a CESS is planned to minimise the carbon emissions. Also, the authors of [Hafiz et al., 2019] plan a CESS under uncertainty to maximise the energy savings of a community of prosumers. Additionally, a CESS is planned in [Glücker et al., 2024] to minimise the CESS provider's annual operating cost.

However, some studies on CESS planning have considered multi-objective frameworks as multiple objectives of different stakeholders can be achieved simultaneously. A detailed description of the existing literature on multi-objective CESS planning models is given below.

2.2.2.2.2 Multi-Objective Optimisation Models In [Terlouw et al., 2019], a multi-objective CESS planning optimisation framework is developed to benefit a community of energy users by reducing their energy costs, and the environment by alleviating the carbon emissions. The authors of [Wu et al., 2021] propose a CESS planning model to economically benefit prosumers and the CESS provider. In this paper, the benefits are shared using an asymmetric Nash bargaining model. Another study on CESS planning as mentioned in [Alam and Jang, 2023] is performed to benefit a community of prosumers by minimising their energy costs and maximising the PV self-consumption. Furthermore, an analytical approach to minimise the real energy loss of the network, energy costs of prosumers and the CESS provider, and the voltage deviations of the network is suggested in [Sardi et al., 2017]. The specialty of this model is that the three objectives are achieved in three stages using analytical approaches. Authors of [Morcilla and Jr., 2023] propose a method to increase the PV self-consumption and maximise the network reliability by optimising the CESS planning. Also, in [Ma et al., 2022], a CESS planning framework is proposed to minimise the solar and wind power generation curtailment, deferring network upgrades, peak shaving, frequency regulation in addition to maximising the economic benefits of the CESS provider. These studies demonstrate the diverse approaches to plan CESSs, highlighting the potential for optimising both technical and economic outcomes while addressing the unique needs of different stakeholders.

2.2.2.3 Single-Year versus Multi-Year Optimisation Models

Unlike operation problems, CESSs are typically planned over a long time period (at least for one year). However, CESSs are also planned in a multi-year setting, as the impact of interest rates can be factored in. This section presents different CESS planning studies categorised under single-year and multi-year frameworks.

2.2.2.3.1 Single-Year Optimisation Models In this branch of literature, there are studies that investigate how the CESS planning over a period of one year can benefit multiple stakeholders. For instance, an approach to optimally plan a CESS, and thereby, minimise the energy costs of an energy-using community is mentioned in [Nazari et al., 2021]. The authors of [Chen et al., 2022] propose a CESS planning framework under the uncertainty of PV generation to minimise the energy costs of prosumers. Furthermore, the authors of [Rodrigues et al., 2020] propose optimal CESS planning frameworks to economically benefit a community of prosumers and the CESS provider under three different CESS ownership models. In all of these studies, the CESSs are planned for a period of one year.

There are some studies that optimise the CESS planning to generate technical or environmental benefits in addition to the economic benefits. For instance, the authors of [van der Stelt et al., 2020] propose a CESS planning model to benefit multiple stakeholders by assessing the technical and economic feasibility of CESS installation. For this, they utilise energy consumption and PV generation data of a community of prosumers in Netherlands for a period of one year. A multi-objective CESS planning model to minimise carbon emissions and operating costs of prosumers is presented in [Khan et al., 2024]. Here, the authors test the developed CESS planning optimisation model using a one year data of energy consumption and PV generation. Also, a CESS planning framework aimed to maximise the economic benefits for the CESS provider while minimising the peak demand to benefit the network is given in [Kang et al., 2023].

2.2.2.3.2 Multi-Year Optimisation Models In this branch of literature, authors propose CESS planning models that account for the depreciation of asset values over a horizon with multiple years. For instance, authors of [Mahani et al., 2017] propose a multi-year optimisation model to plan CESSs primarily for maximising the economic benefits of the CESS provider. In [Ghaffari et al., 2022], a multi-year CESS planning scheme is presented to maintain the network power quality. A game-theory based CESS planning strategy to benefit a community of prosumers and the CESS provider in a multi-year period is explored in [Xie et al., 2022]. Authors of [Böhringer et al., 2021] propose an analytical method to plan a CESS to minimise the real energy loss in a multi-year horizon in LV networks. Also, the CESS provider's profit maximisation through optimal CESS planning is presented in [Sardi et al., 2016] in a multi-year period.

In contrast to [Mahani et al., 2017; Ghaffari et al., 2022; Xie et al., 2022; Böhringer et al., 2021; Sardi et al., 2016], authors of [To et al., 2022; Li et al., 2023] and [Saini et al., 2023] propose multi-year CESS planning models under uncertainty. In [To et al., 2022], the uncertainty of energy trading prices over a multi-year period is considered to plan a CESS, and thereby, maximise the economic benefits of the CESS provider. A game-theoretical approach to plan CESSs under the uncertainty of real energy consumption, PV and wind power generation is described in [Liu et al., 2023]. Furthermore, a multi-year CESS planning study to economically benefit its beneficiaries under the uncertainty of PV generation, real energy consumption and energy trading prices is proposed in [Saini et al., 2023].

2.2.3 Auction-Based Models in CESS Energy Management

In this branch of literature, researchers propose auction-based models to manage the CESS operation and/or planning to benefit different stakeholders. For instance, in [Thomas et al., 2020], an auction-based market mechanism is proposed to manage the operation of a CESS and help prosumers and consumers reduce their energy costs, and renewable energy providers increase their profits. In [Zhu et al., 2022], the authors propose a Lyapunov-based energy control and trading system to optimise the energy trade among prosumers having smart appliances in the presence of a CESS, enabling prosumers to reduce their energy costs. Here, a double-auction mechanism is exploited to determine the energy trading prices among prosumers. A combinatorial auction model integrated with a CESS operation optimisation framework is proposed in [Zaidi et al., 2018]. This study aims to minimise the energy costs of prosumers by allowing them to access the CESS energy through an auction. A similar work is presented in [Tushar et al., 2016] considering market dynamics, facilitating a community of energy users to access the CESS energy through competitive bids. Moreover, authors of [Wang et al., 2021b] propose to use auctions to decide how prosumers should share a CESS to economically benefit both the CESS provider and prosumers.

2.3 Concluding Remarks

In this chapter, first, we have explored how different types of energy storage systems are used in overcoming the challenges of renewable energy resources. Then, we have narrowed down our study to electro-chemical storage systems with battery technologies such as utility, community and residential energy storage systems. In this part, we have compared them against different attributes and discussed their power systems applications and real-world installations. Next, we have reviewed the literature on CESS energy management under different categories to understand the state-of-the-art of CESS utilisation in energy management problems.

The literature reveals a growing recognition of the importance of CESSs in enhancing renewable energy integration, yet significant gaps remain in the topic of optimising the CESS planning in LV networks. These are the identified gaps in this PhD research:

- Numerous studies on CESS planning optimisation have focused on generating technical or economic benefits, though these often cater to a single type of stakeholder. Additionally, techno-economic CESS planning frameworks in the literature are mainly built to maximise benefits for only one type of stakeholder, often disregarding the broader interests of other involved parties. Furthermore, while some studies aim to optimise CESS planning to benefit multiple stakeholders, they often do not take into account benefiting the network, the CESS provider, and community members together. To address these limitations, Chapter 3 of this research presents a multi-objective CESS planning framework aimed at generating technical benefits for the network, and economic benefits for the CESS provider and a community of prosumers.

- In the literature, many CESS planning studies aimed at benefiting multiple stakeholders are built as deterministic models. While some studies incorporate the uncertainties of PV generation and real energy consumption to enhance CESS planning accuracy, few works address the combined uncertainties of PV generation along with real and reactive energy consumption. Additionally, a common limitation across these studies is the inadequate valuation of energy trade through CESS, leading to a limited understanding of the overall economic benefits for stakeholders. Ensuring a balanced distribution of benefits among stakeholders is also crucial. Chapter 4 of this research builds on Chapter 3 to find an optimal CESS solution (i.e., the optimal CESS planning combined with selecting the most suitable energy pricing scheme for the CESS provider) for distributing the economic benefits among multiple stakeholders in balance.

- As discussed in the literature review section, many studies propose deterministic and stochastic optimisation models to plan CESSs considering single and multi-year frameworks. Stochastic models include the uncertainty of PV generation, real and reactive energy consumption, and energy trading prices. Additionally, the literature explores auction-based CESS-sharing models for operation purposes. Nevertheless, none of these works has investigated how decision-makers, such as governments, can use auctions to plan and select CESSs to financially support, combining both multi-year uncertainties and the objectives of multiple stakeholders. In Chapter 5, we address these research gaps and also extend the work in Chapter 4 by planning CESSs in a multi-year period to benefit multiple stakeholders in balance considering the competition among CESS providers, and multi-year uncertainties of the aforementioned factors.

- The existing research works on CESSs model the energy trade between prosumers, the CESS, and the grid in a way that there is no restriction for energy trade between each entity. However, due to policy, geographical, and network infrastructure limitations, the energy trade between each entity may not be possible, forcing to adopt different energy trading schemes. Moreover, the literature lacks discussion about how prosumers with RESSs can also benefit from CESSs. These research gaps are not addressed in Chapters 3, 4, and 5. In Chapter 6, we explore how the CESS planning under different energy trading schemes can generate economic benefits for prosumers, both with and without residential batteries.

This thesis seeks to bridge the identified research gaps by introducing innovative frameworks, offering valuable insights for policymakers and practitioners to effectively plan CESSs and optimise techno-economic benefits for diverse stakeholders.

Chapter 3

Multi-Objective Planning of Community Energy Storage Systems in a Deterministic Setting

In this chapter, we study the extent to which optimising the CESS planning generates network and economic benefits for multiple stakeholders. Our optimisation framework minimises real energy loss of the network, energy trading cost of prosumers and the CESS provider with the grid, and the CESS investment cost.

3.1 Introduction

As discussed in Chapter 2, CESSs can generate technical merits such as real energy loss minimisation, and economic benefits including the reduction of energy purchase cost of prosumers and consumers. Also, a CESS may be used in energy management problems to earn technical and monetary benefits together. Those merits can be fully exploited if the CESS planning is optimised simultaneously with its operation. In the literature, the problem of optimal planning of a CESS is typically addressed from the perspective of only one type of stakeholder. In this context, the result of this problem always maximises the benefits of only one type of stakeholder, leaving aside the other. A solution to address this issue is to solve the problem in a multi-objective setting. Thus, a multi-objective CESS planning optimisation formulation that can generate techno-economic benefits for multiple stakeholders would be an effective alternative to overcome the challenges in the literature.

This chapter presents a multi-objective optimisation framework to plan CESSs, and thereby, minimise the real energy loss of the network, investment cost of the CESS provider, and energy trading cost with the grid by prosumers and the CESS provider. The optimisation framework is built as a mixed-integer quadratic model while taking into account the distribution network limits. The analytic hierarchy process (AHP) is used for fairly weighting the objective functions. Simulations are carried out to test our framework against the models that do not have a CESS, and models that optimise only the CESS operation.

The rest of this chapter is structured as follows. Section 3.2 presents the system models. The proposed CESS planning optimisation framework is described in Section 3.3. Section 3.4 presents the numerical and graphical results. We conclude this chapter in Section 3.5.

3.2 System Models

In this section, we first describe the notations used in this chapter, followed by the network power flow model, energy trade model and the CESS model, respectively.

3.2.1 Notations and Preliminaries

We consider a radial distribution network which is described by the graph $\mathcal{G} = (\mathcal{V}, \mathcal{E})$, where $\mathcal{V} = \{0, 1, ..., N\}$ is the set of all nodes, and $\mathcal{E} = \{(\alpha, \beta)\} \subset \mathcal{V} \times \mathcal{V}$ is the set of all lines in the network. $\mathcal{Z}_\alpha$ represents the set of all nodes downstream of node α including itself. Node 0 is the slack node which represents the secondary side of the distribution transformer. The resistance and reactance of the line connecting α and β nodes are denoted by $r_{\alpha,\beta}$ (in Ω) and $x_{\alpha,\beta}$ (in Ω), respectively. The squared value of the voltage magnitude of node α at time $t \in \mathcal{T}$ is given by $U_\alpha(t)$ (in V^2). Here, $\mathcal{T}$ is the set of all time intervals in the analysis period, and Δt (in hours) is the difference between two consecutive time intervals.

In this thesis, we consider the positive power absorption convention for all nodes. Real power, reactive power and current flow from node α to β at time t are denoted by $P_{\alpha,\beta}(t)$ (in kW), $Q_{\alpha,\beta}(t)$ (in kVAR) and $I_{\alpha,\beta}(t)$ (in A), respectively. For node $\alpha \in \mathcal{V} \setminus \{0\}$, $V_\alpha(t)$ (in V), $p_\alpha(t)$ (in kW) and $q_\alpha(t)$ (in kVAR) represent the voltage magnitude, real power absorption and reactive power absorption, respectively. Moreover, we assume V_0 is fixed and known. Also, $e_\alpha^{B,ch}(t)$ (in kWh) and $e_\alpha^{B,dis}(t)$ (in kWh) are the charging and discharging energy of the CESS connected at node α at time t, respectively. In this chapter, we consider that there are multiple prosumers at each node. Therefore, $p \in \mathcal{P}_\alpha$ and $\mathcal{P}_\alpha \subset \mathcal{P}$, where p is a prosumer, $\mathcal{P}_\alpha$ is the set of prosumers at node α, and $\mathcal{P}$ is the set of all prosumers in the network. Additionally, we assume that the real energy consumption $e_p^D(t)$ (in kWh), reactive energy consumption $e_p^Q(t)$ (in kVARh) and PV generation $e_p^{PV}(t)$ (in kWh) of each prosumer are known ahead from their forecasts.

The typical energy transactions that may ensue between prosumers, the grid and the CESS provider in the presence of a CESS is shown in Figure 3.1. In this chapter, we use the notation $e_p^B(t)$ (in kWh) to denote the energy trade with the CESS by the p^{th} prosumer at node α at time t. When a prosumer imports energy from the CESS, $e_p^B(t) > 0$, and when a prosumer exports energy to the CESS, $e_p^B(t) < 0$. The energy trade by a prosumer with the grid, and the energy trade by the CESS with the grid at time t are given by $e_p^G(t)$ (in kWh) and $e^{B,G}(t)$ (in kWh), respectively. The same sign convention used for $e_p^B(t)$ is valid for $e_p^G(t)$ and $e^{B,G}(t)$. The mathematical relationships between energy trades shown in Figure 3.1 are described in Section 3.2.3.

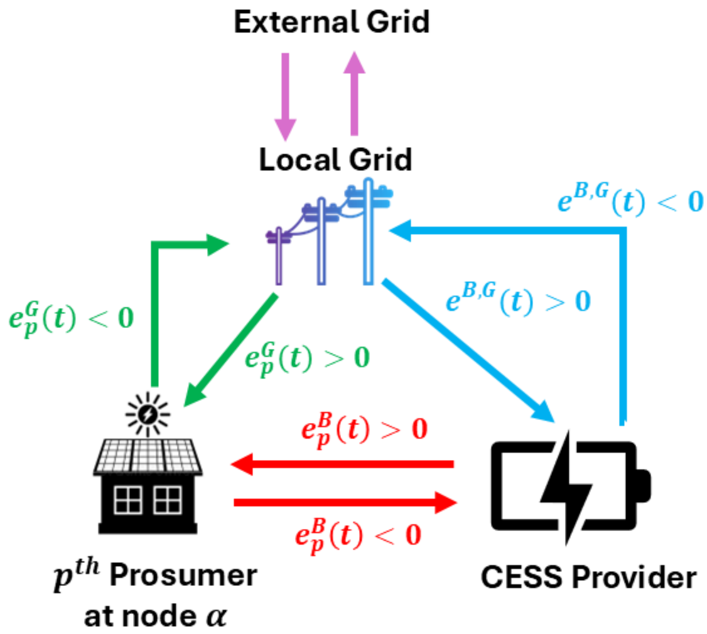

Figure 3.1: Energy trade between a prosumer, the CESS provider and the grid.

3.2.2 Network Power Flow Model

The relationship between the line power flows and node absorptions, as described by the linearised Distflow model in [Baran and Wu, 1989; Lin and Bitar, 2018], is given by (3.1) and(3.2).

$$P_{\alpha,\beta}(t) = p_\alpha(t) + \sum_{\theta:\beta\rightarrow\theta} P_{\beta,\theta}(t) \tag{3.1}$$

$$Q_{\alpha,\beta}(t) = q_\alpha(t) + \sum_{\theta:\beta\rightarrow\theta} Q_{\beta,\theta}(t) \tag{3.2}$$

The nodal real and reactive power absorptions are illustrated by the equations (3.3) and (3.4). Additionally, we assume prosumers' PV systems and the CESS operate at unity power factor.

$$p_\alpha(t) = \frac{1}{\Delta t}\left\{\sum_{p\in P_\alpha} e_p^D(t) - \sum_{p\in P_\alpha} e_p^{PV}(t) + e_\alpha^{B,ch}(t) - e_\alpha^{B,dis}(t)\right\} \quad \forall\alpha \in \mathcal{V}\setminus\{0\}\,, \quad t\in \mathcal{T} \tag{3.3}$$

$$q_\alpha(t) = \frac{1}{\Delta t}\left\{\sum_{p\in P_\alpha} e_p^Q(t)\right\} \qquad \forall\alpha \in \mathcal{V}\setminus\{0\}\,, \quad t\in \mathcal{T} \tag{3.4}$$

The linearised Distflow equations given in (3.1) and (3.2) can be written in matrix format as (3.5),

$$\mathbf{U} = U_0\mathbf{1} - 2\tilde{\mathbf{R}}\mathbf{p} - 2\tilde{\mathbf{X}}\mathbf{q} \qquad \forall t\in \mathcal{T} \tag{3.5}$$

where $\mathbf{U}=|\mathbf{V}(t)|^2$ is the vector of squared voltage magnitudes of nodes, $\mathbf{1}$ is a vector of all ones and $U_0 = |V_0|^2$ is the squared voltage magnitude of the slack node. Also, $\mathbf{p}$ and $\mathbf{q}$ are the vectors of nodal real and reactive power absorption. The matrices $\tilde{\mathbf{R}}$ and $\tilde{\mathbf{X}} \in \mathbb{R}^{N\times N}$ have the elements $R_{\alpha,\beta} = \sum(a,b) \in L_\alpha \cap L_\beta r_{a,b}$ and $X_{\alpha,\beta} = \sum(a,b) \in L_\alpha \cap L_\beta x_{a,b}$, respectively where L_α is the set of lines on the path connecting node 0 and α [Baran and Wu, 1989; Lin and Bitar, 2018].

The squared voltage magnitudes at each node needs to be maintained within its allowable voltage magnitude limits. This is guaranteed by the inequality given in (3.6). Here, $\underline{\mathbf{U}} = \underline{U}\mathbf{1}$ and $\overline{\mathbf{U}} = \overline{U}\mathbf{1}$, where $\underline{U}$ (in V^2) and $\overline{U}$ (in V^2) are the minimum and maximum squared voltage magnitude limits.

$$\underline{\mathbf{U}} \leq \mathbf{U} \leq \overline{\mathbf{U}} \qquad \forall t\in \mathcal{T} \tag{3.6}$$

3.2.3 Energy Trade Model

The equations (3.7) and (3.8) demonstrate how prosumers trade energy with the CESS and the grid. When a prosumer experiences a deficit of its PV generation to balance its real energy consumption, that deficit is fulfilled by importing energy from the CESS and the grid as described by (3.7). On the other hand, if a prosumer has a surplus PV generation, that prosumer exports the excess PV energy to the CESS and the grid as given by (3.8). The mathematical relationship between $e^{B,G}(t)$, $e_p^B(t)$, $e_\alpha^{B,ch}(t)$ and $e_\alpha^{B,dis}(t)$ can be written as (3.9).

If $e_p^D(t) \geq e_p^{PV}(t)$:

$$0 \leq e_p^G(t) + e_p^B(t) = e_p^D(t) - e_p^{PV}(t) \quad \forall \alpha \in \mathcal{V} \setminus \{0\}, \ p \in P_\alpha, \ t \in \mathcal{T} \tag{3.7a}$$

$$0 \leq e_p^G(t) \leq e_p^D(t) - e_p^{PV}(t) \quad \forall \alpha \in \mathcal{V} \setminus \{0\}, \ p \in P_\alpha, \ t \in \mathcal{T} \tag{3.7b}$$

Otherwise:

$$e_p^G(t) + e_p^B(t) = e_p^D(t) - e_p^{PV}(t) \leq 0 \quad \forall \alpha \in \mathcal{V} \setminus \{0\}, \ p \in P_\alpha, \ t \in \mathcal{T} \tag{3.8a}$$

$$e_p^D(t) - e_p^{PV}(t) \leq e_p^G(t) \leq 0 \quad \forall \alpha \in \mathcal{V} \setminus \{0\}, \ p \in P_\alpha, \ t \in \mathcal{T} \tag{3.8b}$$

$$e^{B,G}(t) = \sum_{\alpha=1}^{N} \left\{ \sum_{p \in P_\alpha} e_p^B(t) + e_\alpha^{B,ch}(t) - e_\alpha^{B,dis}(t) \right\} \quad \forall \alpha \in \mathcal{V} \setminus \{0\}, \ p \in P_\alpha, \ t \in \mathcal{T} \tag{3.9}$$

3.2.4 Community Energy Storage System Model

The set of constraints (3.10)-(3.12) model the CESS planning aspects, and (3.13)-(3.17) model the CESS operation, respectively. The equation (3.10) finds the optimal CESS location, where A_α is a binary variable. Also, (3.10) ensures that only one CESS is installed in the network. If $A_\alpha = 0$, it implies that there is no CESS at node α. If $A_\alpha = 1$, then the CESS is connected to node α. To determine the optimal CESS size $E_\alpha^{B,C}$ (in kWh), the inequality given in (3.11) is utilised. For a case $A_\alpha = 0$, (3.11) makes $E_\alpha^{B,C}$ also to be zero. When $E_\alpha^{B,C} = 0$, the values $E_\alpha^B(t)$, $p_\alpha^{B,ch}(t)$ and $p_\alpha^{B,dis}(t)$ in (3.15) and (3.16) also turn out to be zero, where $E_\alpha^B(t)$ (in kWh) is the energy level of the CESS at node α at time t. Also, $\underline{E}^B$ and $\overline{E}^B$ are the minimum and maximum allowable CESS size, respectively. The inequality in (3.12) guarantees the rated power of the CESS $P_\alpha^{B,P}$ (in kW) is bounded by its minimum $\underline{P}^B$ (in kW) and maximum $\overline{P}^B$ (in kW) allowable values.

$$\sum_{\alpha=1}^{N} A_\alpha = 1 \quad \forall \alpha \in \mathcal{V} \setminus \{0\}, A_\alpha \in \{0,1\} \tag{3.10}$$

$$A_\alpha \underline{E}^B \leq E_\alpha^{B,C} \leq A_\alpha \overline{E}^B \quad \forall \alpha \in \mathcal{V} \setminus \{0\}, A_\alpha \in \{0,1\} \tag{3.11}$$

$$A_\alpha \underline{P}^B \leq P_\alpha^{B,P} \leq A_\alpha \overline{P}^B \quad \forall \alpha \in \mathcal{V} \setminus \{0\}, A_\alpha \in \{0,1\} \tag{3.12}$$

The equations (3.13) and (3.14) imply that the CESS charging and discharging energy should not exceed the rated power $P_\alpha^{B,P}$ of the CESS. The temporal variation of the energy level of the CESS is expressed by (3.15), where μ^{ch} and μ^{dis} are the charging and discharging efficiencies of the CESS. Also, the CESS energy level at any time in a day should be within its upper and lower state of charge limits. This is governed by (3.16), and $\underline{\sigma}$ and $\overline{\sigma}$ are two percentage coefficients of the CESS size. The continuity of the CESS operation over the next day is guaranteed by the inequality given by (3.17) which is bounded by a small positive number ξ [Mediwaththe and Blackhall, 2020b,a]. Note that t_c in (3.17) represents the day number of the year. Here $t_c \in \mathcal{T}_C$, where $\mathcal{T}_C = \{1, 2, ..., N_T/24\}$ and N_T is the cardinality of set $\mathcal{T}$.

$$0 \leq e_\alpha^{B,ch}(t) \leq P_\alpha^{B,P} \Delta t \quad \forall \alpha \in \mathcal{V} \setminus \{0\}, \ t \in \mathcal{T} \tag{3.13}$$

$$0 \leq e_\alpha^{B,dis}(t) \leq P_\alpha^{B,P} \Delta t \quad \forall \alpha \in \mathcal{V} \setminus \{0\}, \ t \in \mathcal{T} \tag{3.14}$$

$$E_\alpha^B(t) = E_\alpha^B(t-1) + \mu^{ch} e_\alpha^{B,ch}(t) - \frac{1}{\mu^{dis}} e_\alpha^{B,dis}(t) \quad \forall \alpha \in \mathcal{V} \setminus \{0\}, \ t \in \mathcal{T} \tag{3.15}$$

$$\underline{\sigma} E_\alpha^{B,C} \leq E_\alpha^B(t) \leq \overline{\sigma} E_\alpha^{B,C} \quad \forall \alpha \in \mathcal{V} \setminus \{0\}, \ t \in \mathcal{T} \tag{3.16}$$

$$\left| E_\alpha^B(24t_c) - E_\alpha^B(0) \right| \leq \xi \quad \forall \alpha \in \mathcal{V} \setminus \{0\}, \ t_c \in \mathcal{T}_C \tag{3.17}$$

3.3 Optimisation Framework and Problem Formulation

In this study, we aim to minimise the real energy loss of the network, energy trading costs of prosumers and the CESS provider with the grid, and to minimise the CESS investment cost. Therefore, we formulate a multi-objective function by combining those objectives, and its formulation is described in this section.

3.3.1 Objective Functions

In this section, we present the three objective functions and their corresponding mathematical equations.

3.3.1.1 Minimising the Real Energy Loss of the Network

The real energy loss in a network can be written as (3.19), in terms of (3.18), and by taking $U_\alpha(t) \approx U_0(t)\ \ \forall \alpha \in \mathcal{V} \setminus \{0\}$ [Baran and Wu, 1989; Lin and Bitar, 2018].

$$|I_{\alpha,\beta}(t)|^2 = \frac{P^2_{\alpha,\beta}(t) + Q^2_{\alpha,\beta}(t)}{U_\alpha(t)} \quad \forall (\alpha,\beta) \in \mathcal{E},\ \ t \in \mathcal{T} \tag{3.18}$$

$$f_{Eloss} = \sum_{t\in\mathcal{T}} \sum_{(\alpha,\beta)\in\mathcal{E}} r_{\alpha,\beta}\, |I_{\alpha,\beta}(t)|^2\, \Delta t \tag{3.19}$$

3.3.1.2 Minimising the Energy Trading Cost of Prosumers and the CESS Provider with the Grid

The first term of the objective function given in (3.20) relates to the energy trading cost with the grid by prosumers, and latter for the CESS provider. In (3.20), $\lambda^G(t)$ (in AUD/kWh) is the grid energy price at time t. In this study, the cost of energy trading between prosumers and the CESS is excluded, since the focus is solely on evaluating the energy trading cost with the grid by prosumers and the CESS provider.

$$f_{En,cost} = \sum_{t\in\mathcal{T}} \lambda^G(t) \left\{ \sum_{\alpha=1}^{N} \sum_{p\in P_\alpha} e^G_p(t) + e^{B,G}(t) \right\} \tag{3.20}$$

For $\lambda^G(t)$, we consider a one-for-one non-dispatchable energy buyback scheme such that the same energy price for both imports and exports of energy from the grid by prosumers and the CESS provider is used [Martin, 2012]. This kind of an energy pricing scheme can effectively value the PV energy as being same as the energy imported from the grid, which is usually generated by a conventional generation method.

3.3.1.3 Minimising the Investment Cost of the CESS Provider

The third objective is to minimise the investment cost of the CESS which is given by (3.21) [Zheng et al., 2020]. The fixed CESS investment cost and the cost of the CESS for a unit size are given by γ_{CES} (in AUD) and δ_{CES} (in AUD/kWh), respectively. Note that, in this chapter we do not value the cost of CESS rated power, and this limitation is addressed in Chapter 4 and 5.

$$f_{Inv,cost} = \gamma_B + \delta_B E_{\alpha}^{B,C} \tag{3.21}$$

3.3.2 Problem Formulation

The three objective functions are normalised and weighted to form the multi-objective function in (3.22), according to the techniques described in [Grodzevich and Romanko, 2006]. The normalisation guarantees the objective functions are converted into a form that they can be added together (since f_{Eloss} is measured in kWh, and $f_{En,cost}$, $f_{Inv,cost}$ are measured in AUD).

$$\begin{aligned}\mathbf{x}^* = \underset{\mathbf{x}\in X}{argmin} \quad w_1 \left\{ \frac{f_{Eloss} - f_{Eloss}^{utopia}}{f_{Eloss}^{Nadir} - f_{Eloss}^{utopia}} \right\} + w_2 \left\{ \frac{f_{En,cost} - f_{En,cost}^{utopia}}{f_{En,cost}^{Nadir} - f_{En,cost}^{utopia}} \right\} \\ + w_3 \left\{ \frac{f_{Inv,cost} - f_{Inv,cost}^{utopia}}{f_{Inv,cost}^{Nadir} - f_{Inv,cost}^{utopia}} \right\}\end{aligned} \tag{3.22}$$

In (3.22), $x \in X$ is the decision variable vector of the optimisation framework, and X is the feasible set which is constrained by (3.1)-(3.17), and w_i is the weight coefficient of the i^{th} objective function. The decision variable vector constitute the vector of optimal

CESS location, rated power, size, charging and discharging energy, CESS energy trade with the grid, and prosumers' energy trade with the grid, respectively.

$$f_{Eloss}^{utopia} = f_{Eloss}(\mathbf{x}^*_{\mathbf{Eloss}}) \tag{3.23a}$$

$$f_{En,cost}^{utopia} = f_{En,cost}(\mathbf{x}^*_{\mathbf{En,cost}}) \tag{3.23b}$$

$$f_{Inv,cost}^{utopia} = f_{Inv,cost}(\mathbf{x}^*_{\mathbf{Inv,cost}}) \tag{3.23c}$$

$$\mathbf{x}^*_{\mathbf{Eloss}} = \underset{\mathbf{x}\in X}{argmin} \quad f_{Eloss} \tag{3.24a}$$

$$\mathbf{x}^*_{\mathbf{En,cost}} = \underset{\mathbf{x}\in X}{argmin} \quad f_{En,cost} \tag{3.24b}$$

$$\mathbf{x}^*_{\mathbf{Inv,cost}} = \underset{\mathbf{x}\in X}{argmin} \quad f_{Inv,cost} \tag{3.24c}$$

$$f_{Eloss}^{Nadir} = Max\left\{f_{Eloss}(\mathbf{x}^*_{\mathbf{Eloss}}), f_{Eloss}(\mathbf{x}^*_{\mathbf{En,cost}}), f_{Eloss}(\mathbf{x}^*_{\mathbf{Inv,cost}})\right\} \tag{3.25a}$$

$$f_{En,cost}^{Nadir} = Max\left\{f_{En,cost}(\mathbf{x}^*_{\mathbf{Eloss}}), f_{En,cost}(\mathbf{x}^*_{\mathbf{En,cost}}), f_{En,cost}(\mathbf{x}^*_{\mathbf{Inv,cost}})\right\} \tag{3.25b}$$

$$f_{Inv,cost}^{Nadir} = Max\left\{f_{Inv,cost}(\mathbf{x}^*_{\mathbf{Eloss}}), f_{Inv,cost}(\mathbf{x}^*_{\mathbf{En,cost}}), f_{Inv,cost}(\mathbf{x}^*_{\mathbf{Inv,cost}})\right\} \tag{3.25c}$$

$$\mathbf{x} = (\mathbf{A}_\alpha, \mathbf{P}_\alpha^{\mathbf{B,P}}, \mathbf{E}_\alpha^{\mathbf{B,C}}, \mathbf{e}_\alpha^{\mathbf{B,ch}}, \mathbf{e}_\alpha^{\mathbf{B,dis}}, \mathbf{e}^{\mathbf{B,G}}, \mathbf{e}_{\mathbf{p}}^{\mathbf{G}}) \tag{3.26}$$

In summary, the optimisation framework is solved for the multi-objective function in (3.22), subject to the constraints given by (3.1)–(3.17). Since (3.22) being a quadratically constrained convex multi-objective function, the problem is solved from the mixed-integer quadratic program optimiser of the CPLEX Python-Pyomo.

3.4 Simulations and Results

In this section, first, we mention the details of data used for simulations, followed by the results.

3.4.1 Test Data

For simulations, a 7-node LV radial distribution network given in Figure 3.2 is used and its line data can be found in [Zeraati et al., 2018]. Also, real energy consumption and PV generation data of 30 prosumers in an Australian residential community were used for simulations [sol]. Also, we randomly allocated multiple prosumers to each node. Hence, $\sum_{\alpha=1}^{N} |P_\alpha| = 30$, and the number of prosumers at each node are marked in Figure 3.2. In this study, reactive energy consumption of prosumers is not considered due to the lack of sufficient real data. As the optimisation involves not only a scheduling problem but also a planning problem, the optimisation is performed over a long time period. Thus, we consider one year time period split in one hour time intervals (i.e.$|\mathcal{T}| = 8760$) for simulations.

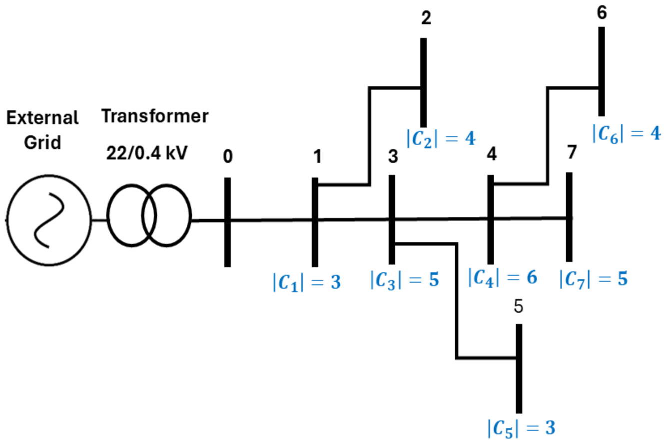

Figure 3.2: 7-Node LV radial distribution network.

In this study, the voltage and power base are taken as 400 V and 100 kVA, respectively. In addition to that, $V_0 = 1\,p.u.$, $\underline{U} = 0.9025\,p.u.$, $\overline{U} = 1.1025\,p.u.$, $\underline{\sigma} = 0.05$, $\overline{\sigma} = 1$, $\mu^{ch} = \mu^{dis} = 0.98$, $\underline{E}^B = 200\ kWh$, $\overline{E}^B = 2000\ kWh$, $\underline{P}^B = 20\ kW$, $\overline{P}^B = 200\ kW$, $\xi = 0.0001\ kWh$ and $\Delta t = 1\ h$ are used as the model parameters. The values of γ_B and δ_B are taken as 24000 AUD and 300 AUD/kWh as specified in [Zheng et al., 2020]. Additionally, the weighting factors w_1, w_2 and w_3 were calculated according to the principles of analytic hierarchy process (AHP) described in [Saaty, 2004]. We considered a moderate plus importance for both $f_{En,cost}$ and $f_{Inv,cost}$ compared to f_{Eloss}, and an equal importance for $f_{En,cost}$ and $f_{Inv,cost}$. Hence, based on the AHP method, the values of w_1, w_2 and w_3 were calculated as 1/9, 4/9 and 4/9, respectively. Figure 3.3 depicts how the grid energy price varies with the time of the day that follows a time-of-use tariff scheme. As seen in Figure 3.3, the grid energy price is 0.24871 AUD/kWh during T_1(from 12am-7am) & T_5(from 10pm-12am), 0.31207 AUD/kWh during T_2(from 7am-3pm) & T_4 (from 9pm-10pm) and 0.52602 AUD/kWh during T_3(from 3pm-9pm) [Origin, 2018].

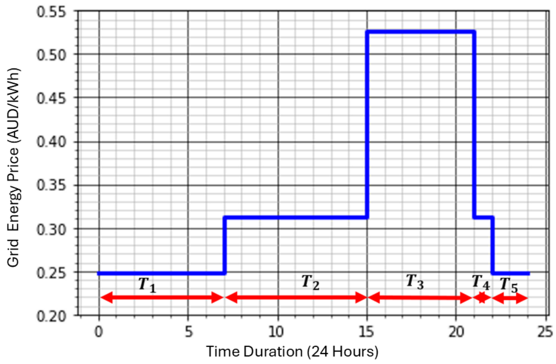

Figure 3.3: Variation of the grid energy price $\lambda^G(t)$ for a period of 24 hours.

3.4.2 Results

The first part of this section presents the results of our model, comparing it with models that do not include a CESS and those that optimise only the CESS operation. In the second part, we analyse the energy trade between different stakeholders, and the temporal variation of the CESS energy in a typical day.

3.4.2.1 CESS Planning Results and Techno-Economic Benefits of Stakeholders

We conducted a case study to understand how the network and economic benefits vary with and without optimal CESS planning. For this, we compare the results of our model with five cases, where in four cases, we arbitrarily chose the CESS locations (i.e. without optimal CESS planning), and the other case without a CESS.

In this study, we considered the case without a CESS as Base Case, our optimisation framework as Case I, while the rest as Case II-V. The same optimisation framework (except the constraint that finds the optimal CESS location), and the model parameters as for Case I were used for Case II-V. A synopsis of the results for the six cases are tabulated in Table 3.1.

According to Table 3.1, Case III, IV and V produce different optimal sizes for the CESS, as different nodes produce unique optimal CESS sizes. Moreover, the results indicate that the benefits are higher in Cases I-V, that incorporate CESSs, compared to the Base Case with no CESS. This implies that the use of CESSs contributes to generate higher techno-economic benefits for all stakeholders compared to models that do not utilise a CESS. Moreover, Case I, that optimises all the CESS planning aspects, generates the highest benefits, while Cases II-V, where the CESS locations are arbitrarily chosen, result in lower benefits. In other words, our model in Case I, that optimises all the CESS planning aspects, has produced the highest real energy loss and cost reduction percentages, compared to all the other cases. Hence, it is clear that Case I yields the minimum values for all the three objective functions, and this justifies the effectiveness of our optimisation framework compared to the models that optimise only the CESS operation.

3.4.2.2 Energy Transactions of Stakeholders

To understand the operation of the CESS and the energy trade of different entities, we arbitrarily select a single day from Case I for our discussion. Figure 3.4 shows the variation of cumulative energy trade of prosumers with the grid. Since $\sum_{\alpha=1}^{N} \sum_{p \in P_\alpha} e_p^G(t)$ being a positive value approximately during T_1, T_3, T_4, T_5 time intervals, it implies that prosumers tend to import energy from the grid to satisfy their real energy consumption requirement during those time periods. On the other hand, during T_2 (time period of the day typically the PV generation is high), prosumers export some of their surplus PV energy to the grid. This is evident as $\sum_{\alpha=1}^{N} \sum_{p \in P_\alpha} e_p^G(t) < 0$ during T_2. This behaviour guarantees a profit for prosumers for their exported energy.

Table 3.1: Summary of case study results.

	CESS Location A_α (Node)	Optimal CESS Size $E_\alpha^{B,C}$ (kWh)	Real Energy Loss f_{Eloss} (kWh)	Energy Trading Cost With the Grid $f_{En,cost}$ (AUD)	CESS Investment Cost $f_{Inv,cost}$ (AUD)
Base Case (Without the CESS)	Not applicable	Not applicable	110117	45585	Not applicable
Case I (Proposed Model)	4 (optimal)	482	78201 (29%)[1]	38520 (15%)[1]	168645
Case II	3 (chosen)	601	80250 (27%)[1]	43362 (5%)[1]	204396
Case III	5 (chosen)	601	81961 (26%)[1]	43840 (4%)[1]	204396
Case IV	6 (chosen)	482	80761 (27%)[1]	44154 (3%)[1]	168645
Case V	7 (chosen)	548	86083 (22%)[1]	43625 (4%)[1]	188307

[1] Percentage loss or cost reduction with respect to their corresponding values without a CESS.

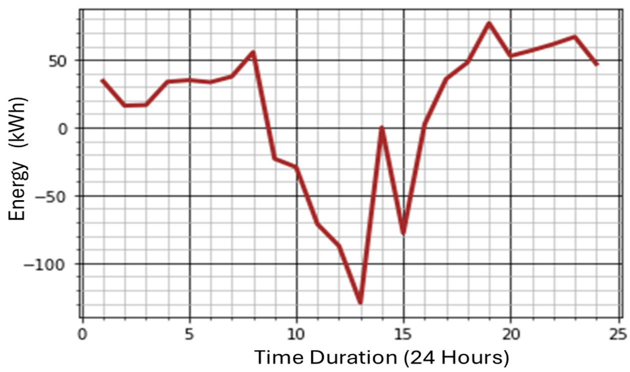

Figure 3.4: Cumulative energy trade by prosumers with the grid.

Figure 3.5 depicts prosumers trade energy with the CESS provider in a day. During T_2, prosumers export a part of their surplus PV energy to the CESS. On the contrary, during other time periods, prosumers import energy from the CESS for their real energy consumption. This action results in reducing costs for prosumers as the amount of energy imported from the grid is minimised.

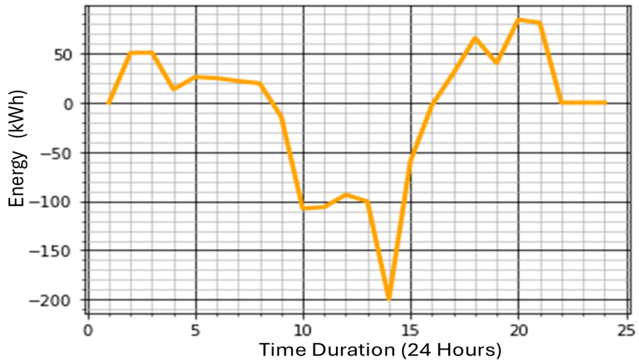

Figure 3.5: Cumulative energy trade by prosumers with the CESS.

Figure 3.6 illustrates how the CESS trades energy with the grid. As the grid energy price during T_1 being the lowest, the CESS tends to import energy from the grid (i.e. $e^{B,G}(t) > 0$) during T_1. This guarantees that the CESS is charged with low-priced energy from the grid. However, during T_2, T_3 and T_4, it is seen that the CESS exports its energy back to the grid (i.e. $e^{B,G}(t) < 0$). This happens as the CESS provider maximises its revenue by exporting energy back to the grid.

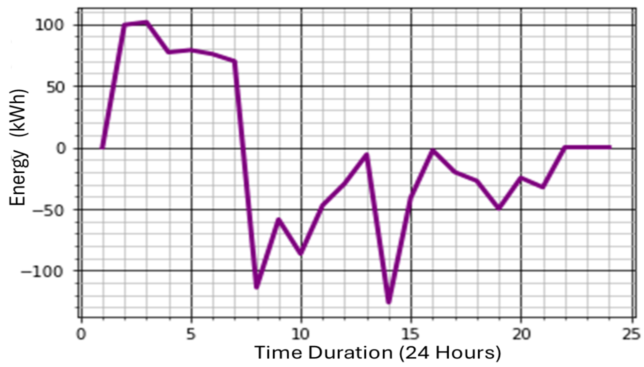

Figure 3.6: Energy trade with the grid by the CESS.

In Figure 3.7, it is observed that during T_1, the CESS charges (from the low-priced grid energy) and partially discharges by the end of T_1. During T_2, the CESS continues to charge and by the end of this time period, it reaches its maximum energy level. The stored energy in the CESS is fully utilised during T_3 and T_4 for partially supplying the real energy requirement of prosumers. This facilitates economic benefits for prosumers as the amount of expensive energy imported by them from the grid is lowered. Additionally, observing the temporal variation of the CESS energy level reveals that the peak value of the CESS energy level corresponds to the optimal CESS size, which was determined to be 482.15 kWh.

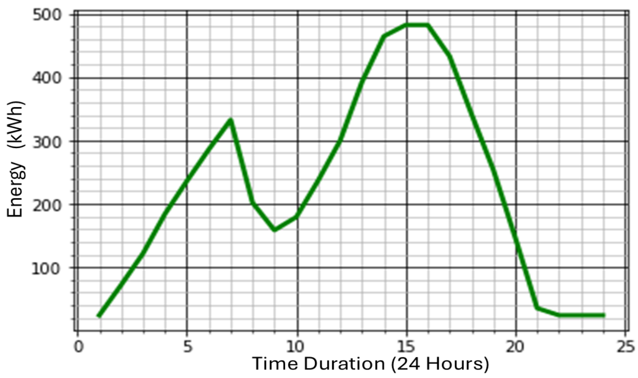

Figure 3.7: Temporal variation of the CESS energy level.

3.5 Concluding Remarks

In this chapter, we have explored how the multi-objective CESS planning can generate enhanced network and economic benefits for multiple stakeholders. To this end, we developed a multi-objective mixed-integer quadratic optimisation framework to minimise three objectives: (i) network real energy loss, (ii) energy trading cost of prosumers and the CESS provider with the grid, and (iii) the CESS investment cost. Simulation results highlighted our multi-objective optimisation framework is competent in generating improved techno-economic benefits compared with the case without a CESS, and optimisation models that optimise only the operation of a CESS.

This study has certain limitations that need to be addressed. For instance, the energy trade of prosumers with the CESS was not valued as our focus was solely on valuing the energy trade with the grid by prosumers and the CESS provider. However, this can lead to limited understanding about the overall financial benefits gained by prosumers and the CESS provider from a CESS. Therefore, it is important to value the energy trade through a CESS from a properly selected CESS provider's energy price. Additionally, we built our optimisation framework assuming parameters such as real energy consumption and PV generation of prosumers are known ahead from their forecasts. In reality, these parameters are often subject to uncertainty, so their forecast errors can be high, making the CESS planning decisions ineffective. Hence, it is essential to account for the uncertainty of energy consumption (both real and reactive) and PV generation to better plan CESSs. Moreover, it is also important to distribute the CESS benefits in balance, so all stakeholders are benefited equitably. In the next chapter, we address all these limitations and extend our optimisation framework to plan CESSs with a properly selected CESS provider's energy pricing scheme to benefit all stakeholders equitably under uncertainty.

Chapter 4

Multi-Objective Planning of Community Energy Storage Systems Under Uncertainty

In this chapter, we evaluate how the planning of a CESS under different energy pricing schemes (EPSs) of the CESS provider can economically benefit prosumers and the CESS provider equitably. By saying equitably, we mean a balanced distribution of economic benefits between prosumers and the CESS provider. This chapter extends the work in Chapter 3 to plan CESSs under the uncertainties of real and reactive energy consumption and PV generation, and select the most suitable CESS provider's energy price to generate a balanced distribution of benefits among all stakeholders.

4.1 Introduction

As discussed in Chapter 3, it is imperative to optimise the planning aspects of a CESS concurrently with its operation. Additionally, energy management problems involving a CESS may have competing objectives among different stakeholders such as minimising the investment and operating costs of the CESS for the CESS provider and minimising the operating costs for prosumers. Also, it is essential to value the energy trade by a CESS to economically benefit its provider and/or prosumers suitably. Thus, a multi-objective optimisation framework with a properly selected CESS provider's EPS can help decision makers such as utilities, energy regulators, and community leaders to identify the trade-offs between those objectives, and thereby benefit both prosumers and the CESS provider equitably.

In this chapter, we examine the extent to which the planning of a CESS can benefit prosumers and the CESS provider equitably. To this end, we present a multi-objective stochastic optimisation framework to size and place a CESS under three EPSs with different energy pricing schemes for the CESS provider. This multi-objective stochastic framework helps decision-makers to select the solution that delivers the most equitable economic benefits to prosumers by minimising their operating costs, and the CESS provider by minimising the investment and operating costs of the CESS under three EPSs. We exploit the hierarchical (ϵ- constraint) method to rank the objectives of the CESS provider and prosumers based on their importance for decision-makers under three EPSs. Furthermore, the uncertainties are modelled using the normal probability distribution. Then, the roulette wheel mechanism (RWM) is exploited to formulate a scenario-based stochastic program. The initial scenarios obtained from the RWM, are then reduced using the K-Means clustering algorithm, to make the problem tractable. We do simulation experiments on an LV distribution network with 30 real-world prosumers from an energy community, to optimally plan a CESS and select the most suitable CESS provider's energy price that spreads the economic benefits among all stakeholders equitably.

This chapter is structured as follows. The system models of this chapter are presented in Section 4.2. The stochastic modelling is described in Section 4.3. The formulation of the multi-objective stochastic optimisation framework is described in Section 4.4. Section 4.5 presents the numerical and graphical results, and Section 4.6 concludes the chapter.

4.2 System Models

In this chapter, each entity namely, prosumers, the CESS provider, and the grid can trade energy between them, as illustrated in Figure 4.1. This section details models of energy trading of each entity, network power flow, the CESS, and the energy pricing.

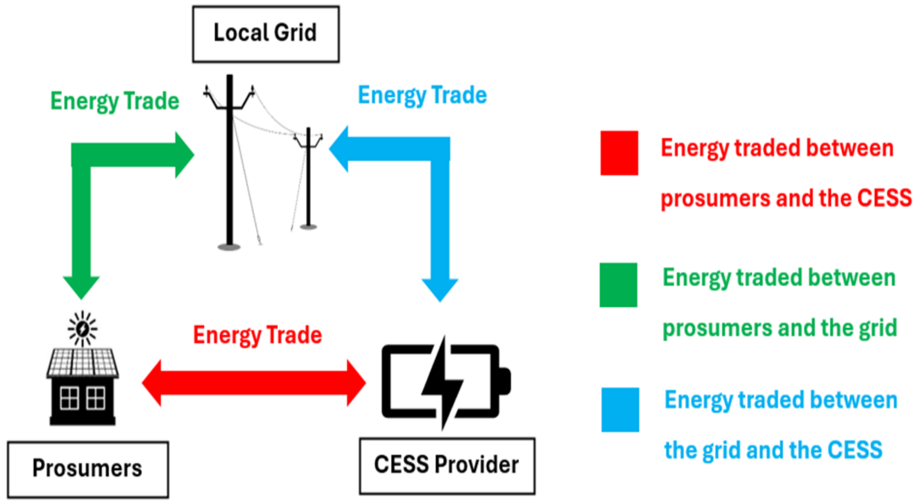

Figure 4.1: Energy trade between prosumers, the grid, and the CESS provider.

4.2.1 Preliminaries

In this chapter also, we assume prosumers $\mathcal{P}$ have rooftop PV systems, and the CESS is owned by a third party. All the analyses in this chapter are done at time $t \in \mathcal{T}$, where $\mathcal{T}$ is the set of time instances, and Δt is the difference between two consecutive time instances. Moreover, we consider the uncertainty of PV generation and the energy consumption (real and reactive) of prosumers. To model uncertainties, we use two normal probability density functions (PDFs) each for real energy consumption and PV generation of prosumers, which are then discretised to formulate a scenario-based stochastic program. The uncertainty of reactive energy consumption is modelled assuming the real and reactive energy consumption of prosumers are correlated. Due to the computational complexity of such a stochastic program, it is imperative to use a scenario reduction approach to reduce the number of scenarios to keep the problem tractable. For this, we use the K-Means clustering algorithm. In this study, the initial set of scenarios is denoted by $\mathcal{W}$, and the set of scenarios obtained after applying the K-Means algorithm is given by $\mathcal{S}$. Further explanation of the uncertainty modelling is given in Section 4.3.

4.2.2 Energy Trade Model

This section models how prosumers, the CESS provider and the grid trade energy. As seen in Figure 4.1, $\forall p \in \mathcal{P},\ t\in \mathcal{T},\ s\in \mathcal{S}$, prosumers trade energy $e^{G}_{p,s}(t)$ with the grid, and $e^{B}_{p,s}(t)$ the CESS to balance the mismatch of their PV energy generation $e^{PV}_{p,s}(t)$ and real energy consumption $e^{D}_{p,s}(t)$. For prosumers' energy imports from the grid, $e^{G}_{p,s}(t) > 0$, and $e^{G}_{p,s}(t) < 0$ for their energy exports to the grid. The same sign convention is used for energy trades between the CESS and prosumers.

When $e^{D}_{p,s}(t) \geq e^{PV}_{p,s}(t)$, prosumers import energy from the grid and/or the CESS, as described by (4.1).

$$\begin{aligned} &If \quad e^{D}_{p,s}(t) \geq e^{PV}_{p,s}(t) \\ &\qquad\qquad 0 \leq e^{G}_{p,s}(t) + e^{B}_{p,s}(t) = e^{D}_{p,s}(t) - e^{PV}_{p,s}(t) \end{aligned} \tag{4.1a}$$

$$0 \leq e^{G}_{p,s}(t) \leq e^{D}_{p,s}(t) - e^{PV}_{p,s}(t) \quad \forall p \in \mathcal{P},\ t\in \mathcal{T},\ s\in \mathcal{S} \tag{4.1b}$$

When $e^{D}_{p,s}(t) < e^{PV}_{p,s}(t)$, prosumers export their excess PV energy to the grid and/or the CESS, as is described by (4.2).

$$\begin{aligned} &If \quad e^{D}_{p,s}(t) < e^{PV}_{p,s}(t) \\ &\qquad\qquad e^{G}_{p,s}(t) + e^{B}_{p,s}(t) = e^{D}_{p,s}(t) - e^{PV}_{p,s}(t) \leq 0 \end{aligned} \tag{4.2a}$$

$$e^{D}_{p,s}(t) - e^{PV}_{p,s}(t) \leq e^{G}_{p,s}(t) \leq 0 \quad \forall p \in \mathcal{P},\ t\in \mathcal{T},\ s\in \mathcal{S} \tag{4.2b}$$

Note that, when $e^{D}_{p,s}(t) \geq e^{PV}_{p,s}(t)$, energy trade between prosumers, the grid and the CESS provider happen according to (4.1), and when $e^{D}_{p,s}(t) < e^{PV}_{p,s}(t)$, it is (4.2) that governs the energy trade of them.

The energy trade by the CESS with the grid is given by (4.3), where $e_s^{B,G}(t)$, $e_{\alpha,s}^{B,ch}(t)$ and $e_{\alpha,s}^{B,dis}(t)$ are the energy trade by the CESS with the grid, the CESS charging energy and the CESS discharging energy, respectively.

$$e_s^{B,G}(t) = \sum_{\alpha=1}^{N} \left\{ \sum_{p\in\mathcal{P}} e_{p,s}^{B}(t) + e_{\alpha,s}^{B,ch}(t) - e_{\alpha,s}^{B,dis}(t) \right\} \quad \forall p \in \mathcal{P},\ t\in \mathcal{T},\ s\in \mathcal{S} \tag{4.3}$$

4.2.3 Network Power Flow Model

In this study also, we consider a radial distribution network described by the graph $\mathcal{G} = (\mathcal{V}, \mathcal{E})$, where $\mathcal{V} = \{0, 1, ..., N\}$ is the set of all nodes, and $\mathcal{E} = \{(\alpha, \beta)\} \subset \mathcal{V} \times \mathcal{V}$ is the set of all lines. The slack node represents the secondary side of the distribution transformer. The resistance and the reactance of the line (α, β) are $r_{\alpha,\beta}$ and $x_{\alpha,\beta}$, respectively. For scenario s at time t, real and reactive power flows from α to β node are represented by $P_{\alpha,\beta,s}(t)$ and $Q_{\alpha,\beta,s}(t)$, respectively. Furthermore, $\forall\alpha \in \mathcal{V}\backslash \{0\}$, $t\in \mathcal{T}$, $s\in \mathcal{S}$, real power absorption, reactive power absorption, voltage magnitude are given by $p_{\alpha,s}(t)$, $q_{\alpha,s}(t)$, and $V_{\alpha,s}(t)$, respectively. The linearised Distflow equations (4.4)-(4.6) are used to model power flows in the radial network [Baran and Wu, 1989]. These linearised Distflow equations compute good results in small LV networks since the relaxed losses are small. Let $U_{\alpha,s}(t) = V^2_{\alpha,s}(t)$.

$$P_{\alpha,\beta,s}(t) = p_{\alpha,s}(t) + \sum_{\theta:\beta\to\theta} P_{\beta,\theta,s}(t) \quad \forall(\alpha, \beta) \in \mathcal{E},\ t\in \mathcal{T},\ s\in \mathcal{S} \tag{4.4}$$

$$Q_{\alpha,\beta,s}(t) = q_{\alpha,s}(t) + \sum_{\theta:\beta\to\theta} Q_{\beta,\theta,s}(t) \quad \forall(\alpha, \beta) \in \mathcal{E},\ t\in \mathcal{T},\ s\in \mathcal{S} \tag{4.5}$$

$$U_{\beta,s}(t) = U_{\alpha,s}(t) - 2(r_{\alpha,\beta}P_{\alpha,\beta,s}(t) + x_{\alpha,\beta}Q_{\alpha,\beta,s}(t)) \quad \forall(\alpha, \beta) \in \mathcal{E},\ t\in \mathcal{T},\ s\in \mathcal{S} \tag{4.6}$$

The real and reactive power absorbed by the node α at time t in scenario s can be expressed by (4.7) and (4.8). Here, we assume there are multiple prosumers at each node, and the CESS operates at a unity power factor. We denote prosumers at node α by $\mathcal{P}_\alpha \subset \mathcal{P}$. Let $e^{Q}_{p,s}(t)$ be the reactive energy consumption per prosumer.

$$p_{\alpha,s}(t) = \frac{1}{\Delta t}\Big(\sum_{p\in\mathcal{P}_\alpha} e^{D}_{p,s}(t) - \sum_{p\in\mathcal{P}_\alpha} e^{PV}_{p,s}(t) + e^{B,ch}_{\alpha,s}(t) - e^{B,dis}_{\alpha,s}(t)\Big) \qquad \forall\alpha \in \mathcal{V}\setminus\{0\},\ t\in \mathcal{T},\ s\in \mathcal{S} \tag{4.7}$$

$$q_{\alpha,s}(t) = \frac{1}{\Delta t}\Big(\sum_{p\in\mathcal{P}_\alpha} e^{Q}_{p,s}(t)\Big) \quad \forall\alpha \in \mathcal{V}\setminus\{0\},\ t\in \mathcal{T},\ s\in \mathcal{S} \tag{4.8}$$

We use (4.9) to guarantee the voltage magnitude of nodes are within lower ($\underline{V}$) and upper ($\overline{V}$) bounds, where $\underline{U} = \underline{V}^2$ and $\overline{U} = \overline{V}^2$. The line thermal limits are not explicitly modelled, as they do not constrain the optimisation problems in our case study. However, they can be easily added if required.

$$\underline{U} \leq U_{\alpha,s}(t) \leq \overline{U} \qquad \forall\alpha \in \mathcal{V}\setminus\{0\},\ t\in \mathcal{T},\ s\in \mathcal{S} \tag{4.9}$$

4.2.4 Community Energy Storage System Model

The CESS planning and operational aspects are modelled by (4.10)-(4.12) and (4.13)-(4.16), respectively. The optimal CESS at node α is characterised by its size $E^{B,C}_{\alpha}$ and rated power $P^{B,P}_{\alpha}$. The binary variable A_α is 1 when α is the optimal CESS node. The minimum and maximum CESS size limits and the maximum CESS power are denoted by $\underline{E}^B$, $\overline{E}^B$ and $\overline{P}^B$, respectively. The charging and discharging of the CESS are modelled by (4.13a)-(4.13f). We use the binary variable $B_{\alpha,s}(t)$ and two continuous variables $x_s(t) \in \mathbb{R}^+$ and $y_s(t) \in \mathbb{R}^+$ to make sure charging and discharging of the CESS do not occur simultaneously. When the CESS charges, $B_{\alpha,s}(t) = 1$, and thus, $0 \leq e^{B,ch}_{\alpha,s}(t) \leq x_s(t) = P^{B,P}_{\alpha}\Delta t \leq \overline{P}^B\Delta t$. When the CESS discharges, $B_{\alpha,s}(t) = 0$, and hence, $0 \leq e^{B,dis}_{\alpha,s}(t) \leq y_s(t) = P^{B,P}_{\alpha}\Delta t \leq \overline{P}^B\Delta t$. The variation of the CESS energy level with time is modelled by (4.14), the CESS energy level is maintained within the minimum and maximum allowable energy levels by (4.15), and the CESS continuous operation over the next day is facilitated by (4.16). In (4.14) and (4.15), $E^{B}_{\alpha,s}(t)$ is the CESS energy level at time t in scenario s. The parameters μ^{ch}, μ^{dis} and $\underline{\sigma}, \overline{\sigma}$ are the charging and discharging efficiencies of the CESS, and the minimum and maximum percentage coefficients of the CESS size, respectively. Also, ξ is a small positive number, and $t_c \in \mathcal{T}_C$ where $\mathcal{T}_C = \{1, 2, ..., |\mathcal{T}|/24\}$.

$$\sum_{\alpha=1}^{N} A_\alpha = 1 \quad \forall \alpha \in \mathcal{V} \setminus \{0\}, A_\alpha \in \{0, 1\} \tag{4.10}$$

$$A_\alpha \underline{E}^B \leq E^{B,C}_\alpha \leq A_\alpha \overline{E}^B \quad \forall \alpha \in \mathcal{V} \setminus \{0\}, A_\alpha \in \{0, 1\} \tag{4.11}$$

$$0 \leq P^{B,P}_\alpha \leq A_\alpha \overline{P}^B \quad \forall \alpha \in \mathcal{V} \setminus \{0\}, A_\alpha \in \{0, 1\} \tag{4.12}$$

$$0 \leq e^{B,ch}_{\alpha,s}(t) \leq x_s(t) \tag{4.13a}$$

$$e^{B,ch}_{\alpha,s}(t) \leq x_s(t) \leq \overline{P}^B \Delta t B_{\alpha,s}(t) \tag{4.13b}$$

$$-\overline{P}^B \Delta t (1 - B_{\alpha,s}(t)) \leq x_s(t) - P^{B,P}_\alpha \Delta t \leq 0 \tag{4.13c}$$

$$0 \leq e^{B,dis}_{\alpha,s}(t) \leq y_s(t) \tag{4.13d}$$

$$e^{B,dis}_{\alpha,s}(t) \leq y_s(t) \leq \overline{P}^B \Delta t (1 - B_{\alpha,s}(t)) \tag{4.13e}$$

$$-\overline{P}^B \Delta t B_{\alpha,s}(t) \leq y_s(t) - P^{B,P}_\alpha \Delta t \leq 0 \quad \forall \alpha \in \mathcal{V} \setminus \{0\}, \ t \in \mathcal{T}, \ s \in \mathcal{S} \tag{4.13f}$$

$$E^B_{\alpha,s}(t) = E^B_{\alpha,s}(t-1) + \mu^{ch} e^{B,ch}_{\alpha,s}(t) - \frac{1}{\mu^{dis}} e^{B,dis}_{\alpha,s}(t) \quad \forall \alpha \in \mathcal{V} \setminus \{0\}, \ t \in \mathcal{T}, \ s \in \mathcal{S} \tag{4.14}$$

$$\underline{\sigma} E_{\alpha}^{B,C} \leq E_{\alpha,s}^{B}(t) \leq \overline{\sigma} E_{\alpha}^{B,C} \quad \forall \alpha \in \mathcal{V} \setminus \{0\}, \ t \in \mathcal{T}, \ s \in \mathcal{S} \tag{4.15}$$

$$\left| E_{\alpha,s}^{B}(24t_c) - E_{\alpha,s}^{B}(0) \right| \leq \xi \quad \forall \alpha \in \mathcal{V} \setminus \{0\}, \ t_c \in \mathcal{T}_C, \ s \in \mathcal{S} \tag{4.16}$$

4.2.5 Energy Pricing Schemes

The CESS provider trades energy with prosumers at a price $\lambda^B(t)$, and the grid trades energy with prosumers and the CESS at a price $\lambda^G(t)$. We adopt a one-for-one non-dispatchable energy buyback method for both energy trading prices, to value the energy imports and exports equally, from the CESS provider and the grid by prosumers [Martin, 2012]. Also, we assume there is no competition among prosumers to access the CESS.

Due to the limited availability of real data about EPSs for CESS providers, we exploit three different EPSs for the CESS provider in terms of the grid energy price, and select the EPS that delivers the most equitable economic benefits for prosumers and the CESS provider. The relationship between $\lambda^G(t)$ and $\lambda^B(t)$ in each EPS is given by (4.17).

$$\lambda^B(t) = \begin{cases} \lambda^{G,\text{avg}} = \frac{\sum_{t=1}^{24} \lambda^G(t)}{24} & \text{in EPS 1} \\ \delta \lambda^G(t) \quad \text{for } \delta > 1 & \text{in EPS 2} \\ \delta \lambda^G(t) \quad \text{for } 0 < \delta < 1 & \text{in EPS 3} \end{cases} \tag{4.17}$$

4.3 Stochastic Modelling

In this section, we model the uncertainty of energy consumption and PV generation of prosumers using the normal PDF. Also, we describe how we generate scenarios using the RWM and how the K-Means clustering method is used to reduce the number of scenarios and decrease the computational complexity of our optimisation problems.

4.3.1 Uncertainty of Energy Consumption and PV Generation of Prosumers

We model the uncertainty of real and reactive energy consumption and PV generation using the normal distribution $f^{N}_{D,PV,t}(.)$ described by (4.18)[1]. Its mean, standard deviation, and sample values as functions of prosumers and time are denoted by μ^t_p, Ψ^t_p and X^t_p, respectively. For real energy consumption, $\mu^t_p = \mu^{D,t}_p$, $\Psi^t_p = \Psi^{D,t}_p$ and $X^t_p = X^{D,t}_p$, and for PV generation, $\mu^t_p = \mu^{PV,t}_p$, $\Psi^t_p = \sigma^{PV,t}_p$ and $X^t_p = X^{PV,t}_p$. As mentioned previously, the uncertainty of reactive energy consumption is obtained assuming a correlation with the real energy consumption, which is described in the next subsection.

$$f^{N}_{D,PV,t}(X) = \frac{1}{\Psi^t_p\sqrt{2\pi}}e^{-0.5\left(\frac{X^t_p-\mu^t_p}{\Psi^t_p}\right)^2} \quad \forall p \in \mathcal{P},\ t \in \mathcal{T} \tag{4.18}$$

4.3.2 Scenario-Based Stochastic Program

Since the normal distribution is a continuous PDF, it represents an infinite number of realisations of the random variables. Here, a realisation refers to a sample energy consumption or PV generation of a prosumer at a given time. A large number of realisations can model the uncertainty better at the expense of a large computational burden. Hence, we approximate the normal PDF from a set of discrete functions to have a finite number of realisations for reducing the complexity of uncertainty modelling. Thus, we use the RWM proposed in [Aghaei et al., 2015; Amjady et al., 2009] to approximate the normal PDF by a set of discrete functions which are represented by seven intervals, each with a width of a standard deviation σ, and centred around each realisation. Note that, we specifically use seven intervals, as this enables us to approximate the normal PDF about 87% of its area. When the historical real energy consumption is μ, and its standard deviation is Ψ, intervals 1-7 of the normal PDF are centred around the seven realisations μ, $\mu+\Psi$, $\mu-\Psi$, $\mu+2\Psi$, $\mu-2\Psi$, $\mu+3\Psi$ and $\mu-3\Psi$ as shown in Figure 4.2(a).

[1] In this study, we used normal distributions to derive stochastic features of PV generation and energy consumption of prosumers as this approach has been extensively justified and used in the literature. However, modelling the uncertainty of energy consumption and PV generation using non-parametric distributions can be a good alternative solution to the use of normal distributions.

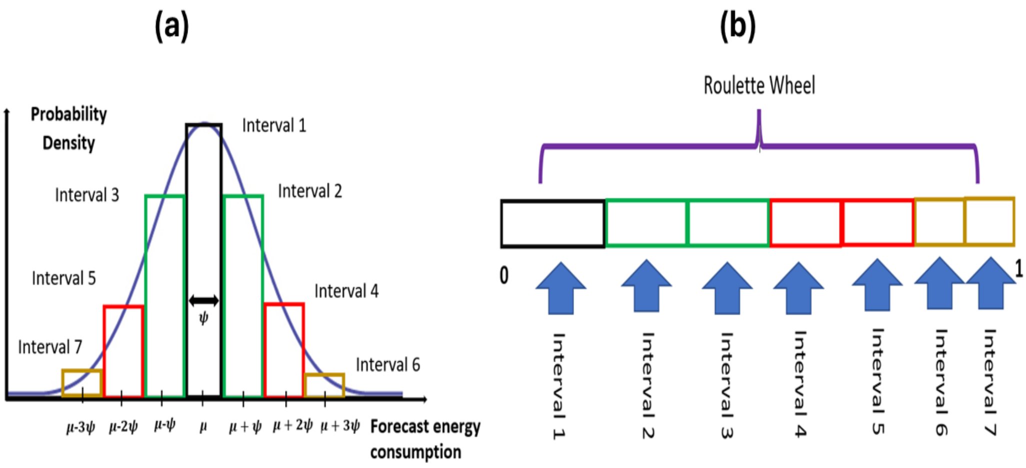

Figure 4.2: (a) Discretisation of normal PDF into seven intervals, (b) Roulette wheel partitioned into seven intervals, each with a width of the normalised probability of the corresponding energy consumption.

The same approach is used to model the uncertainty of PV generation by discretising normal PDF. Additionally, we assume real and reactive energy consumption of prosumers are correlated by a power factor of 0.9. Hence, the probabilities of the realisations of reactive energy consumption are deduced from the probabilities of real energy consumption. For these realisations of PV generation and energy consumption, we obtain their corresponding probabilities and generate scenarios as follows.

- Do Step 1 to Step 4 $\quad \forall p \in \mathcal{P}, t \in \mathcal{T}$

Step 1: Calculate the seven realisations for each real energy consumption and PV energy generation. In this study, we assume $\Psi = 0.02\mu$. The computed realisations are taken as the midpoints of the seven σ-wide intervals in the normal distributions. In this way, the continuous normal PDFs are discretised and approximated as discrete functions. Then, the probability density for each realisation is calculated by (4.18). Once the probability densities are available, the probability for the occurrence of each PV generation, real, and reactive energy consumption are found by taking the product of probability density and the width Ψ of each interval.

Step 2: Since the continuous PDFs are approximated by discretising them, the sum of probabilities obtained after the discretisation will only be close to unity but not exactly equal to one. To have the sum of the probabilities equal to unity, we normalise the calculated probabilities one by one, by taking the sum of probabilities and dividing each probability by the sum. This is done for the seven realisations obtained from each PDF separately.

Step 3: We exploit the RWM explained in [Aghaei et al., 2015] to construct three roulette wheels in the range [0,1], each having seven intervals. Then, we assign the normalised seven probabilities obtained from each PDF to the [0,1] range. Hence, each interval has a width of the normalised probability of the corresponding real and reactive energy consumption and PV generation. The construction of a roulette wheel corresponds to the discretisation of the normal PDF in Figure 4.2(a), and a sample roulette wheel obtained like that is shown in Figure 4.2(b).

Step 4: Generate $N_w = |\mathcal{W}|$ number of random numbers between 0 and 1, which follow the uniform distribution, to guarantee the random numbers are generated without any bias.

- Do Step 5 $\quad \forall p \in \mathcal{P},\, t \in \mathcal{T},\, m \in \mathcal{M}$

Step 5: Assign each random number to the two roulette wheels according to their magnitudes. Select $\phi^{D,t}_{p,w}, \phi^{PV,t}_{p,w}$, $e^{D}_{p,w}(t)$, and $e^{PV}_{p,w}(t)$ from the roulette wheels corresponding to the value of the random number. Here, $\phi^{D,t}_{p,w} = \phi^{Q,t}_{p,w}$, $e^{Q}_{p,w}(t) = 0.48 e^{D}_{p,w}(t)$ (since power factor is assumed to be 0.9), where $\phi^{D,t}_{p,w}, \phi^{Q,t}_{p,w}$ and $\phi^{PV,t}_{p,w}$ are the normalised probabilities of $e^{D}_{p,w}(t)$, $e^{Q}_{p,w}(t)$ and $e^{PV}_{p,w}(t)$, respectively. In this way, the set of initial scenarios is obtained.

- Do Step 6 $\quad \forall t \in \mathcal{T},\, w \in \mathcal{W}$

Step 6: Using the values found in Step 5, calculate the overall probability $\Omega_{w,t}$ in (4.19), which gives the probability for the occurrence of scenario m at time t.

$$\Omega_{w,t} = \frac{\left(\prod_{\alpha=1}^{N}\left(\prod_{p \in P_\alpha} \phi^{D,t}_{p,w}\phi^{Q,t}_{p,w}\phi^{PV,t}_{p,w}\right)\right)}{\sum_{w=1}^{N_w}\left(\prod_{\alpha=1}^{N}\left(\prod_{p \in P_\alpha} \phi^{D,t}_{p,w}\phi^{Q,t}_{p,w}\phi^{PV,t}_{p,w}\right)\right)} \tag{4.19}$$

- Do Step 7 $\forall p \in \mathcal{P},\ t \in \mathcal{T},\ s \in \mathcal{S}$

Step 7: A scenario reduction approach is essential in scenario-based stochastic programs to keep the problem tractable while sustaining a fair approximation for the uncertainty. Thus, the initially generated scenarios $\mathcal{W}$, are then reduced to $\mathcal{S}$ ($N_s = |\mathcal{S}|$) using the K-Means clustering algorithm mentioned in [Scarlatache et al., 2012]. For this, the K-Means algorithm is applied to the sample values of real energy consumption and PV generation of prosumers separately and obtains a new set of values for $e^{D}_{p,s}(t)$, $e^{Q}_{p,s}(t)$ and $e^{PV}_{p,s}(t)$. Then, the new overall probability $\omega_{s,t}$ for the occurrence of scenario s at time t is computed by (4.20). The numerical values found for $\omega_{s,t}$, $e^{D}_{p,s}(t)$, $e^{Q}_{p,s}(t)$, and $e^{PV}_{p,s}(t)$ $\forall p \in \mathcal{P},\ t \in \mathcal{T}, s \in \mathcal{S}$ are then fed into the system models and optimisation framework discussed in Section 4.2 and 4.4.

$$\omega_{s,t} = \frac{\Omega_{s,t}}{\sum_{s=1}^{N_s} \Omega_{s,t}} \tag{4.20}$$

4.4 Multi-Objective Optimisation Framework

In this chapter, we aim to minimise the investment and the operating cost of the CESS provider, and the operating costs of prosumers to benefit both stakeholders together. This section describes the objective functions and presents a summary of the algorithm of our optimisation framework.

4.4.1 Objective Functions

This section presents the objective functions of the CESS provider and prosumers, along with their corresponding mathematical equations.

4.4.1.1 Objective of the CESS Provider

The objective of the CESS provider is given by (4.21). It aims to minimise the investment cost of the CESS (first term of (4.21)), and the expected annual operating cost (second term of (4.21)).

$$f_C = G(C_P^B P_\alpha^{B,P} + C_C^B E_\alpha^{B,C}) + \sum_{t \in \mathcal{T}} \sum_{s=1}^{N_s} \omega_{s,t} \left\{ -\lambda^B(t) \sum_{\alpha=1}^{N} \sum_{p \in \mathcal{P}_\alpha} e_{p,s}^B(t) + \lambda^G(t) e_s^{B,G}(t) \right\} \tag{4.21}$$

In (4.21), $G = \frac{d(1+d)^T}{(1+d)^T-1}$, where G, d and T are the equivalent annualised cost of the CESS, discount rate and the CESS lifetime, respectively. Also, C_P^B and C_C^B are the CESS investment cost per kW (in AUD/kW) and per kWh (in AUD/kWh), respectively.

The expected annual cost of operating the CESS is a combination of the cost of trading energy with prosumers and the grid. The negative sign associated with the cost of trading energy with prosumers is due to the sign convention described in Section 4.2.2. Also, we impose the condition $f_C \leq 0$ in our optimisation program, such that a CESS is only installed when it is profitable for the CESS provider.

4.4.1.2 Objective of Prosumers

The objective of prosumers is to minimise their expected annual operating costs given by (4.22). The first term of (4.22) is the energy trading cost with the grid, and the latter is the energy trading cost with the CESS.

$$f_P = \sum_{t \in \mathcal{T}} \sum_{s=1}^{N_s} \omega_{s,t} \left\{ \lambda^G(t) \sum_{\alpha=1}^{N} \sum_{p \in \mathcal{P}_\alpha} e_{p,s}^G(t) + \lambda^B(t) \sum_{\alpha=1}^{N} \sum_{p \in \mathcal{P}_\alpha} e_{p,s}^B(t) \right\} \tag{4.22}$$

4.4.2 Optimisation Framework and Solution Method

The optimisation problems involving multi-objectives can be solved using methods, such as the weighted sum method and the hierarchical (ϵ-constraint) method. In this chapter, we use the hierarchical method as it is the recommended method for optimisation problems with linear objective functions [Grodzevich and Romanko, 2006]. In this method, first, each competing objective function is ranked according to its importance. Then each objective is minimised one by one subject to a set of constraints and additional constraints formed by a trade-off threshold ϵ of the optimal value obtained for the higher-ranked objective functions. For instance, in case of a problem with two objective functions written in descending order according to their importance as f_1 and f_2, we first minimise f_1 such that $x \in X$, where X is the feasible region. If the optimal value of f_1 is f_1^*, we then minimise f_2 such that $x \in X$ and $f_1(x) \leq f_1^*(1+\epsilon)$. Here, ϵ is the trade-off threshold of f_1^*, which is the maximum that is allowed to be traded-off f_1^* to improve f_2. Note that, the trade-off threshold ϵ is usually set by the decision-makers to distribute benefits among stakeholders. This method overcomes the deficiency of the weighted sum method which tends to give corner solutions of the Pareto-frontier, which are not the practically desirable outcomes. Further explanation about the hierarchical method can be found in [Grodzevich and Romanko, 2006].

In this study, we rank the objective f_C as important than the objective f_P. Let $\mathbf{x} = (\mathbf{A}_\alpha, \mathbf{P}_\alpha^{\mathbf{B,P}}, \mathbf{E}_\alpha^{\mathbf{B,C}}, \mathbf{e}_\alpha^{\mathbf{B,ch}}, \mathbf{e}_\alpha^{\mathbf{B,dis}}, \mathbf{e}_\mathbf{p}^{\mathbf{B}}, \mathbf{e}_\mathbf{p}^{\mathbf{G}})$ be the decision variable vector with its elements being the vector of optimal CESS node, rated power, size, charging energy, discharging energy, prosumers' energy trade with the CESS and the grid, respectively. The feasible set is given by X. For EPS 1, we solve (4.23) subject to (4.1)-(4.16), (4.17a), and (4.24). Here, f_C^* is the optimal value of f_C obtained by solving (4.21) subject to (4.1)-(4.16), and (4.17a). Similarly, we solve (4.23) subject to (4.1)-(4.16), (4.17b), and (4.24) for EPS 2, and (4.23) subject to (4.1)-(4.16), (4.17c), and (4.24) for EPS 3. The optimisation problems for each EPS are solved as separate mixed-integer linear programs (MILPs) using the hierarchical method. Algorithm 1 summarises the solution method for our optimisation problems.

$$\underset{\mathbf{x}\in X}{min} \quad f_P \tag{4.23}$$

$$s.t. \quad f_C \leq f_C^*(1+\epsilon), \tag{4.24}$$

Algorithm 1: Algorithm to Run the Multi-Objective Stochastic Optimisation Framework.

1: Input $\mu_p^{D,t}, \mu_p^{PV,t} \quad \forall p \in \mathcal{P}, t \in \mathcal{T}$

2: Execute Steps 1 to 7 detailed in Section 4.3.2 to model the uncertainty of energy consumption (both real and reactive) and PV generation of prosumers.

3: Return $\omega_{s,t}$, $e^D_{p,s}(t)$, $e^Q_{p,s}(t)$, and $e^{PV}_{p,s}(t) \quad \forall p \in \mathcal{P}, t \in \mathcal{T}, s \in \mathcal{S}$.

4: Individually solve the optimisation problems under EPS 1-3, as MILPs.

4.5 Simulations and Results

This section begins with a detailed overview of the test data, followed by a comprehensive analysis of the results.

4.5.1 Test Data

For simulations, a radial distribution network with 7 nodes given in Figure 4.3 was considered, and its data can be found in [Zeraati et al., 2018]. The historical PV generation and real energy consumption data of 30 residential prosumers from an Australian community, for 1 year, measured in 1-hour time intervals were used for simulations [sol]. Also, we randomly assigned the 30 prosumers to each node except for the slack node (see Figure 4.3). Therefore, $\sum_{\alpha=1}^{N} |P_\alpha| = 30$. As model parameters, we assumed $V_0 = 1\, p.u.$, $\underline{V} = 0.95\, p.u.$, $\overline{V} = 1.05\, p.u.$, $\overline{P}^B = 200\, kW$, $\underline{E}^B = 50\, kWh$, $\overline{E}^B = 1000\, kWh$, $\mu^{ch} = \mu^{dis} = 0.98$, $\underline{\sigma} = 0.05$, $\overline{\sigma} = 1$, $\xi = 0.0001\, kWh$, $\Delta t = 1\, h$, $d = 0.1$, and $T = 12.5$ years. We took $C^B_P = 463\, AUD/kW$, and $C^B_C = 795\, AUD/kWh$ assuming Li-ion as the CESS technology [Zakeri and Syri, 2015]. Also, the time-of-use grid energy price $\lambda^G(t)$ used in Chapter 3 was used to value energy trade with the grid by prosumers and the CESS provider [Origin, 2018]. The energy prices of the grid and the CESS provider in each EPS are shown in Figure 4.4. In EPS 1, $\lambda^B(t) = \lambda^{G,avg} = 0.34180\, AUD/kWh$, in EPS 2 we took $\delta = 1.5$ since $\lambda^B(t) > \lambda^G(t)$, and in EPS 3 we used $\delta = 0.5$ as

$\lambda^B(t) < \lambda^G(t)$. Moreover, we considered 50 initial scenarios (i.e. $N_w = 50$), which were then reduced to 10 (i.e. $N_s = 10$) by using the K-Means clustering algorithm to solve the optimisation problem in each EPS. Simulations for the three EPSs were implemented in Python-Pyomo and solved using the mixed-integer linear solver from CPLEX.

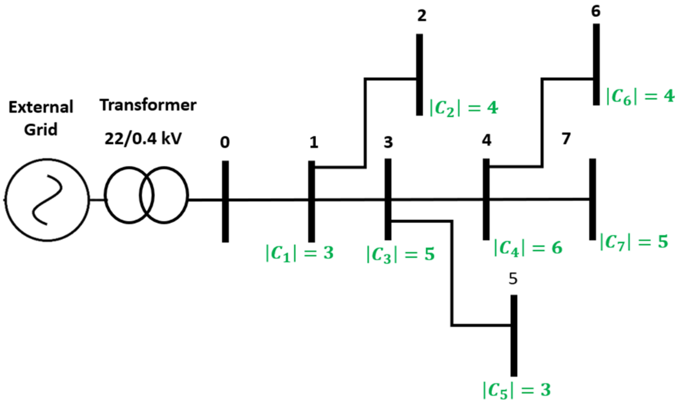

Figure 4.3: 7-Node LV radial feeder with the number of prosumers marked at each node.

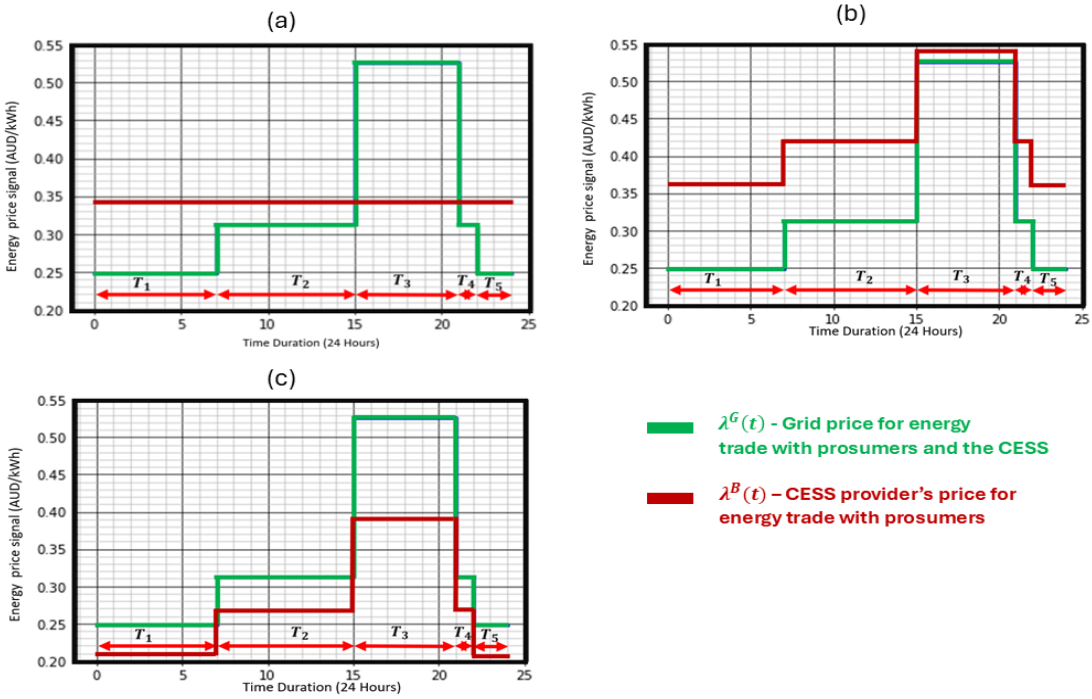

Figure 4.4: Grid and the CESS provider's energy prices in (a) EPS 1, (b) EPS 2, and (c) EPS 3.

4.5.2 Results

This section presents a detailed analysis of the results obtained from our model. We first conduct a case study to understand the impact of EPS and the trade-off threshold on planing and operational decisions. Then, we analyse the energy trade between stakeholders for each EPS. Finally, we evaluate the quality of our stochastic solutions.

4.5.2.1 Identifying the Impact of Trade-off Threshold ϵ and EPS on Planning and Operational Decisions

We conducted experiments to understand how the value of the trade-off threshold ϵ impacts planning and operational decisions, and thereby select the CESS solution that provides the most equitable economic benefits for the CESS provider and prosumers. For this, we considered Cases I, II and III. In Case I, we set $\epsilon = 25\%$ to make a slight trade-off of f_C, in Case II, we enforce $\epsilon = 50\%$ to make a moderate trade-off of f_C, and in Case III, we trade-off f_C significantly by setting $\epsilon = 75\%$ to improve f_P. Table 4.1 summarises the planning and operational results obtained for each EPS in Cases I-III.

Table 4.1: Planning and operational results for each case under the three EPSs. Positive monetary values are costs and negative ones are revenues.

		A_α	$E_\alpha^{B,C}$ (kWh)	$P_\alpha^{B,P}$ (kW)	f_C (AUD)	f_P (AUD)
Case I	EPS 1	3	831	189	-162427 (74%)[1]	109287 (34%)[2]
	EPS 2	3	831	189	-219496	166705
	EPS 3	3	831	189	-169011 (77%)[1]	110224 (34%)[2]
Case II	EPS 1	3	819	183	-111492 (51%)[1]	68825 (59%)[2]
	EPS 2	4	686	175	-146331 (67%)[1]	114224 (31%)[2]
	EPS 3	3	810	181	-105619 (48%)[1]	58624 (65%)[2]
Case III	EPS 1	3	745	182	-50344 (23%)[1]	67216 (60%)[2]
	EPS 2	7	543	184	-73165 (33%)[1]	85789 (49%)[2]
	EPS 3	4	790	178	-52810 (24%)[1]	51036 (69%)[2]

[1] Revenue percentage concerning the max. revenue. [2] Cost reduction percentage concerning the max. cost.

In Case I, the optimal planning decisions (i.e., the CESS location, and size) are the same for all EPSs. This happens because planning decisions are prevalent over the operating decisions for the three EPSs in this case. This implies that a lower trade-off threshold, such as 25% of f_C, is not significant enough to change the planning decisions even under different EPSs. Nevertheless, in Case II, when ϵ is increased to a moderate value of 50%, it is observed that the planning decisions have changed, and also they are different for each EPS. In Case III, we further increased the trade-off threshold ϵ to 75%, meaning that the objective of the CESS provider is further traded-off to improve the objective of prosumers. In this case also, the planning decisions are different for each EPS. In Case II and III, it is observed that EPS 2 has produced the smallest CESS sizes, and EPS 1 and 3 have produced the largest CESS sizes. This implies that a higher value for ϵ produces different planning decisions for each EPS.

In Case II, it is observed a decrease in the revenue of the CESS provider, and the operating costs of prosumers compared to Case I. In Case III, the same trend as in Case II is observed as the revenue of the CESS provider has further reduced, while the costs of prosumers have further decreased under the three EPSs. The decrease in the revenue of the CESS provider and the costs of prosumers in Case II and III is a result of higher trading-off the objective of the CESS provider to increase the economic benefits for prosumers. Additionally, in Case II and III, it is the EPS 2 that produces the highest revenue for the CESS provider, while EPS 1 and 3 produce the least costs for prosumers. In summary, the results show that for higher trade-off threshold values of ϵ, both planning and operational decisions change based on the EPS.

To select the most equitable CESS solution for both stakeholders, we computed the revenue percentage for the CESS provider concerning its maximum revenue, and the cost reduction percentage of prosumers concerning their maximum operating costs. From the results in Table 4.1, we select EPS 1 in Case II (i.e., when $\lambda^B(t) = \lambda^{G,avg}$ and $\epsilon = 50\%$) as the most suitable CESS solution to equitably spread the economic benefits of the CESS provider and prosumers.

4.5.2.2 Comparison of the Economic Benefits of Prosumers and the CESS Provider for Different EPSs

In this section, we discuss how the economic benefits for prosumers and the CESS provider change with the EPS. Also, we analyse how energy transactions between prosumers, the grid, and the CESS occur under each EPS, considering Case II. For this, we analyse a selected day with a duration of 24 hours.

EPS 1: When: $\boldsymbol{\lambda^{B}(t)=\lambda^{G,avg}}$**,** $\forall t \in \mathcal{T}$;

Figure 4.5 depicts how prosumers trade energy with the grid (blue plot) and the CESS (orange plot), and the CESS energy level variation with time (red plot). In Figure 4.5, the energy imports and exports by prosumers are seen as positive and negative values, respectively. During T_3, $\lambda^B(t) < \lambda^G(t)$, and during T_1, T_2 T_4, T_5, $\lambda^B(t) > \lambda^G(t)$. According to Figure 4.5, prosumers import energy only from the grid during T_1. Since $\lambda^B(t) > \lambda^G(t)$ during this period, it is not economically beneficial for prosumers to import expensive energy from the CESS. During T_2, in the period with high PV generation, prosumers export the excess PV energy to the CESS, as $\lambda^B(t) > \lambda^G(t)$, resulting in higher revenue from the CESS provider. Since $\lambda^B(t) < \lambda^G(t)$ during T_3, prosumers import energy from the CESS, so they have to pay less for the imported energy. During T_4 and T_5, prosumers import energy only from the grid as $\lambda^B(t) > \lambda^G(t)$. Considering the temporal variation of the CESS energy level, it is observed that the CESS charges during T_1 from the low-priced grid energy, and it discharges partially by the end of T_1. The CESS continues to charge during T_2 until it reaches its full capacity using the excess PV generation of prosumers. This is evident as the CESS energy level has reached its full capacity of 819 kWh during T_2. During T_3, the CESS exports its energy back to prosumers, and at the end of the day, the CESS reaches its initial energy level.

EPS 2: When: $\boldsymbol{\lambda^{B}(t)=1.5\lambda^{G}(t)}$**,** $\forall t \in \mathcal{T}$;

In EPS 2, as illustrated in Figure 4.6, prosumers import energy only from the grid during T_1, T_3 T_4, and T_5, the times of the day in which the PV generation is insufficient

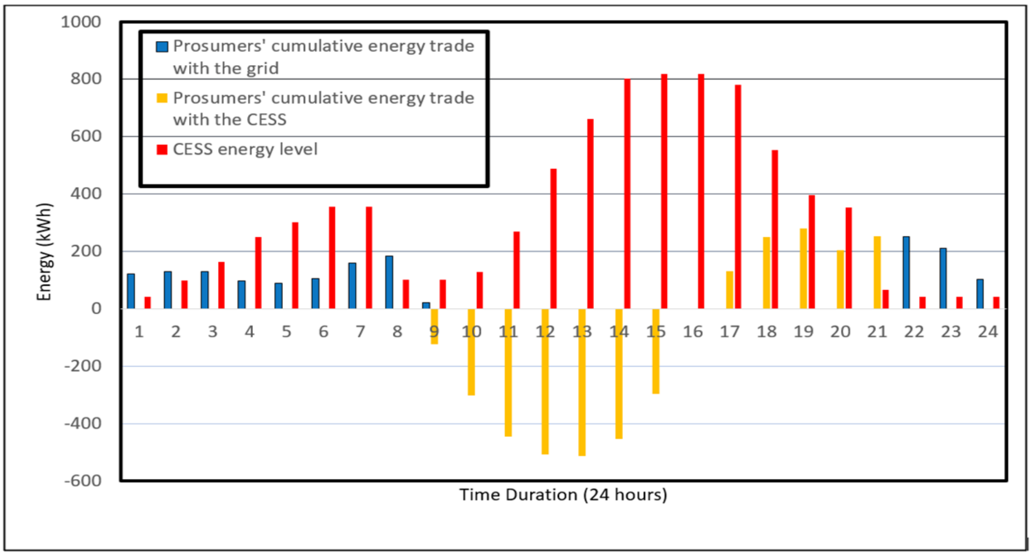

Figure 4.5: Energy trade by prosumers with the grid and the CESS, and the temporal variation of the CESS energy under EPS 1 in Case II when $\lambda^B(t) = \lambda^{G,avg}$.

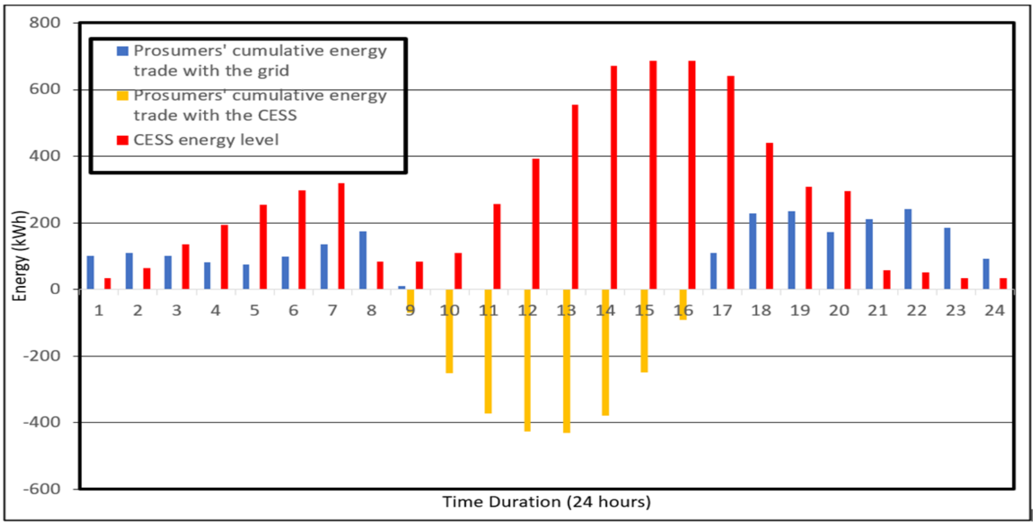

Figure 4.6: Energy trade by prosumers with the grid and the CESS, and the temporal variation of the CESS energy under EPS 2 in Case II when $\lambda^B(t) = 1.5\lambda^G(t)$.

to fulfil the energy demand of prosumers and during T_2, prosumers export their excess PV generation to the CESS. Since $\lambda^B(t) > \lambda^G(t)$, importing energy from the grid gives lesser costs, and exporting energy to the CESS generates higher earnings for prosumers. In this EPS, the CESS charges from the grid energy and partially discharges by the end of T_1, and again charges from the excess PV energy of prosumers during T_2, and continues to discharge during T_3, T_4 and T_5 until it reaches its initial energy level at the start of the day.

EPS 3: When: $\boldsymbol{\lambda^B(t)=0.5\lambda^G(t)}$, $\forall t \in \mathcal{T}$;

In contrast to EPS 2, prosumers import energy only from the CESS during $T_1, T_3\ T_4, T_5$, and during T_2, prosumers export their excess PV generation to the grid. This is observed in Figure 4.7. Since $\lambda^B(t) < \lambda^G(t)$, importing energy from the CESS generates lesser costs, and exporting energy to the grid provides higher earnings for prosumers. The temporal variation of the CESS energy level is also shown in Figure 4.7.

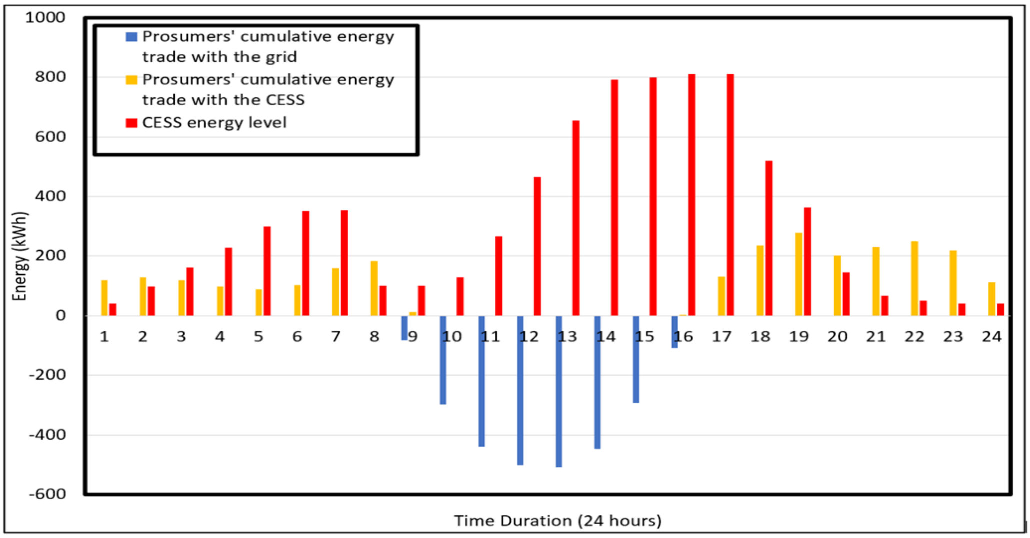

Figure 4.7: Energy trade by prosumers with the grid and the CESS, and the temporal variation of the CESS energy under EPS 3 in Case II when $\lambda^B(t) = 0.5\lambda^G(t)$.

4.5.2.3 Evaluation of the Quality of the Stochastic Solution

To assess the accuracy of the solutions obtained from our stochastic programs, we used the out-of-sample simulation method discussed in [Roald and et al., 2023]. For simplicity, we considered only the results obtained under EPS 1 in Case II. Then, we generated another 20 scenarios and formed a new scenario set $\mathcal{D}$ such that $\mathcal{W} \cap \mathcal{D} = \emptyset$, $\mathcal{S} \cap \mathcal{D} = \emptyset$, and $|\mathcal{S}| < |\mathcal{D}|$. In the out-of-sample simulation method, we fixed the values of the planning decision variables in (4.21) and deterministically solved for f_C and f_P for 20 times excluding the scenario dependency of (4.1)-(4.16), (4.21), and (4.22), and calculated the average of the objectives. The average investment and operating cost of the CESS provider, and the operating costs of prosumers were found as AUD -115370 and AUD 73169, respectively. To measure the quality of the stochastic solution, we used the Value of Stochastic Solution (VSS) metric, which gives the difference between the deterministic and the stochastic solution of the objective function [Roald and et al., 2023]. The calculated value of VSS is 5.94%, and lower VSS values imply a higher quality stochastic solution.

4.5.2.4 Comparison of MCS and RWM for Scenario Generation

In this section, we compare the Monte Carlo simulation (MCS) method to our method (RWM), considering EPS 1 in Case II. To compare these two methods, we generated 50 scenarios using the MCS and RWM methods, and afterwards, we used K-Means clustering to reduce the number of scenarios to 10, in order to maintain stochastic optimisation problems tractable.

The results of Table 4.2 show that our method (RWM + K-Means clustering) performed slightly better than the MCS + K-Means clustering method. We used VSS to evaluate the quality of the stochastic solutions obtained from the two scenario generation and reduction methods.

Table 4.2: Value of the Stochastic Solution considering two scenario generation and reduction methods under EPS 1 in Case II.

Scenario generation and reduction method	Value of the Stochastic Solution (VSS)
MCS + K-Means Clustering	6.78 %
RWM + K-Means Clustering	5.94 %

4.5.2.5 Pareto-Frontier

In this work, we optimise the CESS planning and its operation to minimise prosumers' operating costs while minimising the investment and operating costs of the CESS provider. Hence, our work considers multi-objective optimisation, which generates a set of optimal solutions instead of a single unique solution. The set of solutions obtained forms the Pareto-frontier, and Figure 4.8 shows the Pareto-frontier under EPS 1 in Case II.

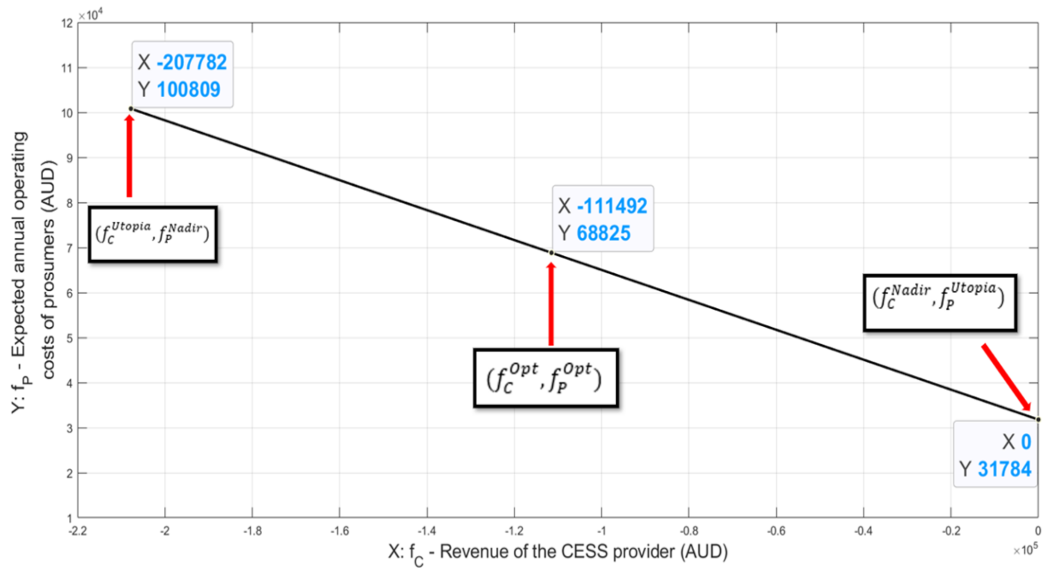

Figure 4.8: Pareto-frontier of the multi-objective stochastic optimisation model under EPS 1 in Case II.

The corner points of the Pareto-frontier are the utopia (i.e., lower bounds of the Pareto-frontier) and the nadir (i.e., upper bounds of the Pareto-frontier) values, which are marked in Figure 4.8 [Grodzevich and Romanko, 2006]. We name the utopia and nadir values of f_C and f_P as f_C^{Utopia} and f_P^{Utopia}, and f_C^{Nadir} and f_P^{Nadir}. Since we exploited the hierarchical method to find the optimal solution of our multi-objective optimisation framework, it gives a solution point on the Pareto-frontier avoiding the corner points as the solution. In this work, we name this solution by the coordinates (f_C^{Opt},f_P^{Opt}) on the Pareto-frontier (see Figure 4.8). The obtained solution under EPS 1 in Case II for the CESS provider's investment cost and operating revenue and prosumers' operating costs are AUD -111492 and AUD 68825, which balances benefits between prosumers and the CESS provider.

4.6 Concluding Remarks

In this chapter, we have evaluated how the planning of CESSs under uncertainty impacts the economic benefits for prosumers and the CESS provider. For this, we have proposed a multi-objective stochastic optimisation framework to select the best EPS of the CESS provider and optimise the CESS planning aspects, and thereby, deliver the most equitable outcome to the competing economic objectives of the CESS provider and prosumers. We model uncertainties of PV generation, and real and reactive energy consumption using stochastic scenarios generated initially by a roulette wheel mechanism (RWM) and then aggregated by the K-Means clustering algorithm to reduce the computational complexity of our optimisation problems.

Simulation results indicated that optimal equity in benefits for both the CESS provider and prosumers is achieved when energy trading occurs at the average grid energy price. In this scenario, a moderate trade-off ($\epsilon = 50\%$) of the planning and operating objectives of the CESS provider enhances economic benefits for prosumers, resulting in the most equitable outcome for both stakeholders.

In the next chapter, we extend this work to run CESS auctions and select the best CESS project that generates a balanced distribution of benefits among multiple stakeholders under multi-year uncertainties.

Chapter 5

A Multi-Objective Stochastic Optimisation Framework for Government-Run Community Energy Storage Systems Auctions

This chapter proposes a multi-objective stochastic optimisation framework that can be used by governments to run auctions and select the best CESS projects to support. From this, CESS providers and energy community members can equitably benefit from the economic value generated by CESSs. In this chapter, we extend the work from Chapter 4 by planning CESSs considering the competition among multiple CESS providers to install and operate CESSs, and accounting for the combined uncertainty of real and reactive energy consumption, PV generation, energy prices, and the number of PV installations in a multi-year period.

5.1 Introduction

Australia aims to install more than 400 CESSs [Department of Climate Change and Water, 2024]. To foster the installation of CESSs in LV networks, the Australian government has been running auctions to provide support to the best CESS initiatives [Power, 2024; Synergy, 2024]. Managing CESS installation auctions is challenging as they require identifying the best CESS project offers (i.e., the CESS provider, investment cost, energy trading price, technology, location, size, and time to install). Additionally, these decisions are subjected to the multi-year uncertainty of energy trading prices, the number of PV installations, and the net load of prosumers and consumers in the community. It is also important to distribute the economic benefits of CESSs between CESS providers and the community equitably.

In this chapter, we propose a multi-objective stochastic optimisation model to help governments run auctions to select the best CESS projects to support. The auction accepts offers from competing CESS providers that constitute the data of the CESS location, size, install time, technology, provider, investment cost, and energy trading price. The auction is run by a government agency which selects CESS projects that maximise the economic benefits and distribute them equitably among CESS providers and community members. The multi-objective stochastic optimisation accounts for the multi-year uncertainties of PV generation, real and reactive energy consumption, energy trading prices, and PV installations. The uncertainties are modelled from Monte Carlo simulations (MCSs) by generating multi-year scenarios, and the K-Means clustering method is also used to reduce the number of scenarios to maintain the optimisation tractable. We carry out experiments on an Australian LV network with a community of prosumers and consumers to evaluate our optimisation framework.

The structure of this chapter is as follows. Section 5.2 describes the CESS auction used to select the best CESS project. The multi-objective stochastic optimisation framework is detailed in Section 5.3, and Section 5.4 presents the models of the network power flow, the CESS, and the energy trade. The uncertainty modelling is explained in Section 5.5.

Sections 5.6 presents the case study results and the discussion. Section 5.7 provides the concluding remarks of the chapter.

5.2 Government-Run Auctions to Support Community Energy Storage Systems Installation

In this chapter, we explore the use of auctions by governments to select the best CESS projects to support. Through this framework, a government agency provides financial assistance to ensure the economic viability of CESS installations, promoting a equitable distribution of benefits between CESS providers and communities through its support. We define equitable as a balanced distribution of economic benefits between all parties that benefit from the CESS.

Figure 5.1 illustrates the CESS auction. CESS providers, who are interested in installing and operating CESSs, submit project offers to the auction. These offers include details such as the investment cost, energy trading price, location, size, technology, and installation timeline of the CESS. For simplicity, we assume that the project offers remain fixed once they are submitted to the auction. A government agency oversees the auction, utilising our multi-objective stochastic optimisation framework to identify the most suitable CESS projects to support. The goal of the government agency is to support CESS projects that maximise benefits for both communities and CESS providers, ensuring an equitable distribution of these benefits. It is noteworthy that the auction described here is inspired by a framework currently being used by the Australian government to decide which CESS projects should receive financial support [Agency, 2023].

5.3 Multi-Objective Stochastic Optimisation Framework

In this section, we present the formulation of the multi-objective function, and the hierarchy method (ϵ-constraint method) used to solve the multi-objective optimisation problem. The constraints are described in the following section.

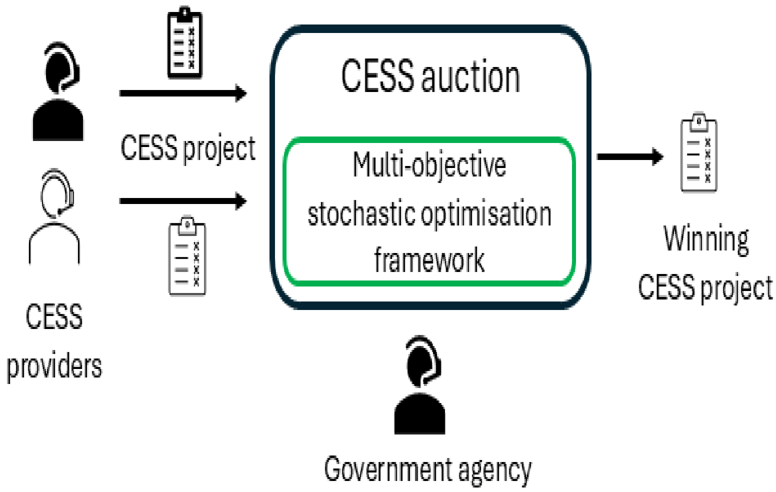

Figure 5.1: CESS auction.

5.3.1 Objective Functions

In this section, we detail the objectives of prosumers and consumers, and the CESS provider with their corresponding mathematical equations.

5.3.1.1 Objective of Prosumers and Consumers

Prosumers and consumers aim to minimise their expected energy costs, and this is expressed by (5.1), where its first and second terms are the expected energy trading cost of prosumers with the grid and the CESS, and the last term is the expected energy trading cost of consumers with the grid and the CESS, respectively. We denote the set of prosumers, consumers, and the CESS providers who join the auction by $\mathcal{P}$, $\mathcal{C}$, and $\mathcal{K}$, respectively. Also, $\mathcal{M}$ is the set of planning years, with $\mathcal{T}_m \in \mathcal{M}$ and $t \in \mathcal{T}_m$, where $\mathcal{T}_m$ is the set of time instances in the m^{th} planning year. The set of multi-year scenarios obtained from the scenario trees for modelling the uncertainties is denoted by $\mathcal{W}$. The set of multi-year scenarios obtained after applying the K-means clustering method to keep the optimisation tractability is given by $\mathcal{S}$. Section 5.5 describes this in detail.

$$
\begin{aligned}
f^{E,U}_{m,k} &= \sum_{p\in\mathcal{P}}\sum_{t\in\mathcal{T}_m}\sum_{s\in\mathcal{S}}\omega_{m,k,s}(t)\left\{\left(\lambda^{G,Im}_{m,s}(t)+\lambda^{G,Ex}_{m,s}(t)\right)e^{G}_{p,k,s}(t)\right\}\\
&\quad+\sum_{p\in\mathcal{P}}\sum_{t\in\mathcal{T}_m}\sum_{s\in\mathcal{S}}\omega_{m,k,s}(t)\left\{\left(\lambda^{B,Im}_{m,s}(t)+\lambda^{B,Ex}_{m,s}(t)\right)e^{B}_{p,k,s}(t)\right\}\\
&\quad+\sum_{c\in\mathcal{C}}\sum_{t\in\mathcal{T}_m}\sum_{s\in\mathcal{S}}\omega_{m,k,s}(t)\left\{\lambda^{G,Im}_{m,s}(t)e^{G}_{c,k,s}(t)+\lambda^{B,Im}_{m,s}(t)e^{B}_{c,k,s}(t)\right\}
\end{aligned}
\tag{5.1}
$$

In (5.1), $e^{G}_{p,k,s}(t)$ and $e^{B}_{p,k,s}(t)$, $e^{G}_{c,k,s}(t)$ and $e^{B}_{c,k,s}(t)$ are the energy trade with the grid and the CESS per prosumer, energy trade with grid and the CESS per consumer, respectively. We model the energy imports as positive, and energy exports as negative. For instance, when a prosumer imports energy from the grid, it is $e^{G}_{p,k,s}(t) > 0$, and when a prosumer exports energy to the grid, it is $e^{G}_{p,k,s}(t) < 0$. Also, $\lambda^{G,Im}_{m,s}(t)$ and $\lambda^{B,Im}_{m,s}(t)$, $\lambda^{G,Ex}_{m,s}(t)$ and $\lambda^{B,Ex}_{m,s}(t)$ are the prices of the energy imported from the grid and the CESS, and prices of the energy exported to the grid and the CESS, respectively. The probability of scenario s at time t in the m^{th} planning year for the k^{th} CESS provider is given by $\omega_{m,k,s}(t)$.

We then express (5.1) to find its net present value (NPV) (given in (5.2), as our optimisation framework evaluates the benefits of the best CESS project in a multi-year horizon. In (5.2), $\mathbf{x}$ is the decision variable vector, X is the feasible set, and d_k is the CESS discount rate. We mention the elements of the decision variable vector in Section 3.2.

$$
\min_{\mathbf{x}\in X}\ f^{E,U} = \sum_{k\in\mathcal{K}}\sum_{m\in\mathcal{M}}\frac{f^{E,U}_{m,k}}{(1+d_k)^m}
\tag{5.2}
$$

5.3.1.2 Objective of the CESS Provider

The CESS provider aims to minimise its investment and expected energy costs, and its overall objective is given by (5.3). The CESS investment cost is the first term of (5.3), and the second term is the government subsidy given to invest on the CESS in the m^{th}

planning year. The following terms of (5.3) are the expected energy trading cost with the grid, and prosumers and consumers, respectively, where $e^{B,G}_{k,s}(t)$ is the energy trade by the CESS with the grid. The set of possible CESS installation nodes is given by $\mathcal{J}$. The equivalent annualised cost of the CESS G_k is expressed in terms of the CESS expected lifetime T_k, and the CESS discount rate d_k. Therefore, $G_k = \frac{d_k(1+d_k)^{T_k}}{(1+d_k)^{T_k}-1}$. The investment cost for the CESS size $E^{B,C}_{m,k,i}$ is given by $B_{m,k}$ (in AUD/kWh), and its values for a multi-year period were obtained from [Cole and Karmakar, 2023]. Also, S_m (in AUD/kWh) is the government financial support given to the CESS provider to invest on the CESS in the m^{th} planning year.

$$
\begin{aligned}
f^{E,B}_{m,k} = &\sum_{i\in\mathcal{J}} G_k B_{m,k} E^{B,C}_{m,k,i} - \sum_{i\in\mathcal{J}} G_k S_m E^{B,C}_{m,k,i} \\
&+ \sum_{t\in\mathcal{T}_m}\sum_{s\in\mathcal{S}} \omega_{m,k,s}(t) \left\{ \left(\lambda^{G,Im}_{m,s}(t) + \lambda^{G,Ex}_{m,s}(t)\right) e^{B,G}_{k,s}(t) \right\} \\
&+ \sum_{t\in\mathcal{T}_m}\sum_{s\in\mathcal{S}} \omega_{m,k,s}(t) \left\{ -\left(\lambda^{B,Im}_{m,s}(t) + \lambda^{B,Ex}_{m,s}(t)\right) \sum_{p\in\mathcal{P}} e^{B}_{p,k,s}(t) - \lambda^{B,Im}_{m,s}(t) \sum_{c\in\mathcal{C}} e^{B}_{c,k,s}(t) \right\}
\end{aligned}
\tag{5.3}
$$

Similar to (5.2), we express (5.3) to find its NPV as described by (5.4). We impose the constraint (5.5) to make sure the CESS provider earns revenue. Moreover, we introduce the budget constraint (5.6) to our optimisation problem, such that the financial support is capped by the grant ϑ (in AUD) given by the government for the best CESS project.

$$
\min_{\mathbf{x}\in X} \quad f^{E,B} = \sum_{k\in\mathcal{K}}\sum_{m\in\mathcal{M}} \frac{f^{E,B}_{m,k}}{(1+d_k)^m} \tag{5.4}
$$

$$
f^{E,B} \le 0 \tag{5.5}
$$

$$S_m E^{B,C}_{m,k,i} \leq \vartheta \quad \forall k \in \mathcal{K},\ m \in \mathcal{M},\ i \in \mathcal{J} \tag{5.6}$$

5.3.2 Use of Hierarchy Method to Solve the Optimisation Framework

In our study, we use the hierarchy method to solve our multi-objective optimisation problem. In this method, the objective functions are ranked according to their importance for decision makers, depending on their interest in which beneficiary they want to benefit more. Due to the competing nature of objectives, one of the objective can be improved only at the cost of degrading the other. In hierarchy method, the more important objective is allowed to be traded-off up to a threshold percentage (say ϵ) of its optimal value to improve the less important objective. Therefore, by adjusting the value of the trade-off threshold percentage ϵ suitably, it is possible to spread the benefits from a multi-objective optimisation framework among beneficiaries. A detailed description about the hierarchy method can be found in [Grodzevich and Romanko, 2006].

In this study, the decision variable vector $\mathbf{x}$ constitutes the elements $\mathbf{A_{m,k,i}}$, $\mathbf{E^{B,C}_{m,k,i}}$, $\mathbf{P^{B,P}_{m,k,i}}$, $\mathbf{e^{B,ch}_{i,k}}$, $\mathbf{e^{B,dis}_{i,k}}$, $\mathbf{e^{B}_{p,k}}$, $\mathbf{e^{G}_{p,k}}$, $\mathbf{e^{B}_{c,k}}$, $\mathbf{e^{G}_{c,k}}$, $\mathbf{e^{B,G}_{k}}$, which are the vectors of optimal CESS location with its install year and the provider, size, rated power, charging energy, discharging energy, energy trade with the CESS by prosumers, energy trade with the grid by prosumers, energy trade with the CESS by consumers, energy trade with the grid by consumers, and the energy trade with the grid by the CESS, respectively. In this work, we rank $f^{E,B}$ as more important than $f^{E,U}$. We then solve (5.4) subject to constraints (5.5)-(5.6), and (5.8)-(5.25) as a mixed-integer linear program (MILP). From that, we obtain the optimal value of $f^{E,B}$ as f^{E,B^*}. Here, we use a trade-off threshold percentage ϵ for f^{E,B^*} to improve $f^{E,U}$. Finally, we solve (5.2) subject to constraints (5.5)-(5.7), and (5.8)-(5.25) also as a MILP.

$$f^{E,B} \leq f^{E,B^*}(1+\epsilon) \tag{5.7}$$

5.4 System Models

This section describes the system models and constraints of the multi-objective stochastic optimisation framework. We begin by describing the power flow model, followed by the energy trading model, CESS planning and operation model.

5.4.1 Network Power Flow Model

We model the power flows in a radial network using the linearised Distflow equations listed in (5.8)-(5.10). For this, we consider a radial network represented by the graph $\mathcal{G} = (\mathcal{V}, \mathcal{E})$, such that $\mathcal{V} = \{0, 1, ..., N\}$ is the set of nodes, and $\mathcal{E} = \{(\alpha, \beta)\} \subset \mathcal{V} \times \mathcal{V}$ is the set of lines in the network. The slack node 0 is connected to the secondary side of the LV distribution transformer. The resistance and reactance of the line $(\alpha, \beta) \in \mathcal{E}$ are given by $r_{\alpha,\beta}$ and $x_{\alpha,\beta}$, respectively. Moreover, $\forall$ $(\alpha, \beta) \in \mathcal{E}$, $k \in \mathcal{K}$, $t \in \mathcal{T}_m$, $m \in \mathcal{M}$, $s \in \mathcal{S}$, the real power and reactive power flow from α to β are denoted by $P_{\alpha,\beta,k,s}(t)$ and $Q_{\alpha,\beta,k,s}(t)$, respectively. Additionally, the voltage magnitude, real power absorption, and reactive power absorption at node α are represented by $V_{\alpha,k,s}(t)$, $p_{\alpha,s}(t)$, and $q_{\alpha,k,s}(t)$, respectively. Also, $U_{\alpha,k,s}(t) = V^2_{\alpha,k,s}(t)$, as given in (5.10).

$$P_{\alpha,\beta,k,s}(t) = p_{\alpha,k,s}(t) + \sum_{\theta:\beta\to\theta} P_{\beta,\theta,k,s}(t) \qquad \forall(\alpha, \beta) \in \mathcal{E},\ k \in \mathcal{K},\ t \in \mathcal{T}_m\ ,\ m \in \mathcal{M},\ s \in \mathcal{S} \tag{5.8}$$

$$Q_{\alpha,\beta,k,s}(t) = q_{\alpha,k,s}(t) + \sum_{\theta:\beta\to\theta} Q_{\beta,\theta,k,s}(t) \qquad \forall(\alpha, \beta) \in \mathcal{E},\ k \in \mathcal{K},\ t \in \mathcal{T}_m\ ,\ m \in \mathcal{M},\ s \in \mathcal{S} \tag{5.9}$$

$$U_{\beta,k,s}(t) = U_{\alpha,k,s}(t) - 2(r_{\alpha,\beta}P_{\alpha,\beta,k,s}(t) + x_{\alpha,\beta}Q_{\alpha,\beta,k,s}(t)) \qquad \forall(\alpha, \beta) \in \mathcal{E},\ k \in \mathcal{K},\ t \in \mathcal{T}_m\ ,\ m \in \mathcal{M},\ s \in \mathcal{S} \tag{5.10}$$

In this chapter also, we assume all the rooftop PV and the CESS operate at unity power factor. The $p_{\alpha,k,s}(t)$ and $q_{\alpha,k,s}(t)$ in (5.8) and (5.9) are further expanded in (5.11) and (5.12), respectively. The charging and discharging energy of the CESS are given by $e^{B,ch}_{\alpha,k,s}(t)$ and $e^{B,dis}_{\alpha,k,s}(t)$. Also, we assume that only a single prosumer or consumer is present at a given node, with none of them at potential CESS nodes. The real and reactive energy consumption of prosumers and consumers are given by $e^{D}_{p,k,s}(t)$, $e^{Q}_{p,k,s}(t)$, $e^{D}_{c,k,s}(t)$, and $e^{Q}_{c,k,s}(t)$, respectively. Let $e^{PV}_{p,k,s}(t)$ and Δt denote PV generation of prosumers, and the difference between two successive time instances of t, respectively.

$$p_{\alpha,k,s}(t) = \frac{1}{\Delta t}(e^{D}_{p,k,s}(t) - e^{PV}_{p,k,s}(t) + e^{D}_{c,k,s}(t) + e^{B,ch}_{\alpha,k,s}(t) - e^{B,dis}_{\alpha,k,s}(t)) \quad \forall \alpha \in \mathcal{V} \setminus \{0\}\,,\ k \in \mathcal{K},\ t \in \mathcal{T}_m\,,\ m \in \mathcal{M},\ s \in \mathcal{S} \tag{5.11}$$

$$q_{\alpha,k,s}(t) = \frac{1}{\Delta t}(e^{Q}_{p,k,s}(t) + e^{Q}_{c,k,s}(t)) \quad \forall \alpha \in \mathcal{V} \setminus \{0\}\,,\ k \in \mathcal{K},\ t \in \mathcal{T}_m\,,\ m \in \mathcal{M},\ s \in \mathcal{S} \tag{5.12}$$

We also constrain the voltage magnitude of all nodes within lower ($\underline{V}$) and upper ($\overline{V}$) bounds, such that $\underline{U} = \underline{V}^2$ and $\overline{U} = \overline{V}^2$. This is described by the constraint (5.13). Here, the line thermal limits are not explicitly modelled, as they do not constrain the optimisation problem in our case study.

$$\underline{U} \leq U_{\alpha,k,s}(t) \leq \overline{U} \quad \forall \alpha \in \mathcal{V} \setminus \{0\}\,,\ k \in \mathcal{K},\ t \in \mathcal{T}_m\,,\ m \in \mathcal{M},\ s \in \mathcal{S} \tag{5.13}$$

5.4.2 Energy Trade Model

In this section, we model the energy trade of different entities as shown in Figure 5.2. Here, the CESS imports energy from prosumers and the grid, and exports energy to consumers, prosumers and the grid. Similarly, the grid imports energy from prosumers and the CESS, and exports energy to consumers, prosumers and the CESS. Prosumers import/export energy from/to the CESS and the grid. However, consumers can only import energy from the grid and the CESS. In this study, we do not consider peer-to-peer energy trade by prosumers and consumers.

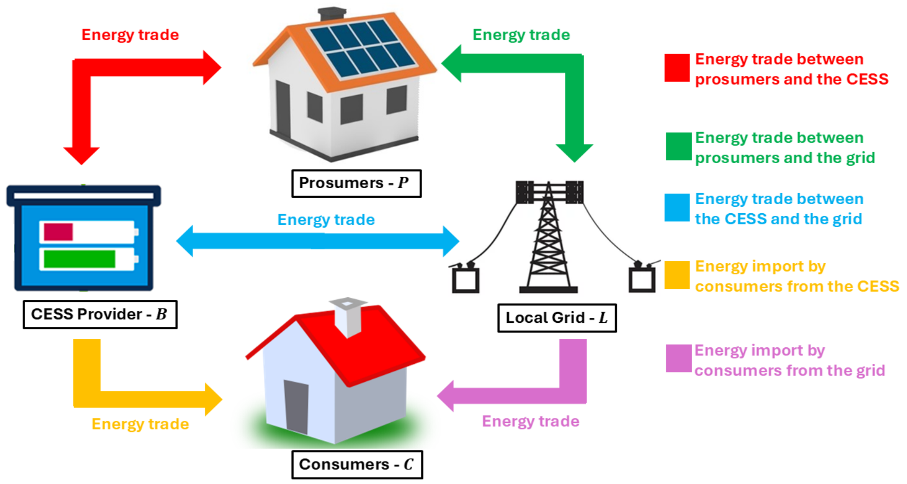

Figure 5.2: Energy trade of consumers, prosumers, the CESS and the grid.

As described by (5.14), prosumers trade energy $e^{G}_{p,k,s}(t)$ with the grid, and $e^{B}_{p,k,s}(t)$ with the CESS to balance the difference of their PV generation $e^{PV}_{p,k,s}(t)$, and real energy consumption $e^{D}_{p,k,s}(t)$, $\forall p \in \mathcal{P},\ k \in \mathcal{K}\ , t \in \mathcal{T}_m,\ m \in \mathcal{M},\ s \in \mathcal{S}$. The energy imports and exports of prosumers are modelled by (5.14) and (5.15).

$$\begin{aligned} &If \quad e^{D}_{p,k,s}(t) \geq e^{PV}_{p,k,s}(t) \\ &\qquad 0 \leq e^{G}_{p,k,s}(t) + e^{B}_{p,k,s}(t) = e^{D}_{p,k,s}(t) - e^{PV}_{p,k,s}(t) \end{aligned} \tag{5.14a}$$

$$0 \leq e^{B}_{p,k,s}(t) \leq e^{D}_{p,k,s}(t) - e^{PV}_{p,k,s}(t) \quad \forall p \in \mathcal{P},\ k \in \mathcal{K},\ t \in \mathcal{T}_m,\ m \in \mathcal{M},\ s \in \mathcal{S} \tag{5.14b}$$

$$\begin{aligned} &If \quad e^{D}_{p,k,s}(t) < e^{PV}_{p,k,s}(t) \\ &\qquad e^{G}_{p,k,s}(t) + e^{B}_{p,k,s}(t) = e^{D}_{p,k,s}(t) - e^{PV}_{p,k,s}(t) \leq 0 \end{aligned} \tag{5.15a}$$

$$e^{D}_{p,k,s}(t) - e^{PV}_{p,k,s}(t) \leq e^{B}_{p,k,s}(t) \leq 0 \quad \forall p \in \mathcal{P},\ k \in \mathcal{K},\ t \in \mathcal{T}_m,\ m \in \mathcal{M},\ s \in \mathcal{S} \tag{5.15b}$$

Since consumers do not have PV systems, they can only import energy from the grid and the CESS, as described by (5.16).

$$0 \leq e^{G}_{c,k,s}(t) + e^{B}_{c,k,s}(t) = e^{D}_{c,k,s}(t) \tag{5.16a}$$

$$0 \leq e^{B}_{c,k,s}(t) \leq e^{D}_{c,k,s}(t) \quad \forall c \in \mathcal{C},\ k \in \mathcal{K},\ t \in \mathcal{T}_m,\ m \in \mathcal{M},\ s \in \mathcal{S} \tag{5.16b}$$

As shown in Figure 5.2, the CESS provider trades energy $e^{B,G}_{k,s}(t)$ with the grid as well. This is expressed by constraint (5.17).

$$\begin{gathered} e^{B,G}_{k,s}(t) = \sum_{p \in \mathcal{P}} e^{B}_{p,k,s}(t) + \sum_{c \in \mathcal{C}} e^{B}_{c,k,s}(t) + \sum_{i \in \mathcal{J}} \left\{ e^{B,ch}_{i,k,s}(t) - e^{B,dis}_{i,k,s}(t) \right\} \\ \forall p \in \mathcal{P},\ c \in \mathcal{C},\ k \in \mathcal{K},\ t \in \mathcal{T}_m,\ m \in \mathcal{M},\ s \in \mathcal{S} \end{gathered} \tag{5.17}$$

The CESS, prosumers and consumers import energy from the grid at a price $\lambda^{G,Im}_{m,s}(t)$, and prosumers and the CESS export energy to the grid at a price $\lambda^{G,Ex}_{m,s}(t)$. Similarly, prosumers and consumers import energy from the CESS at a price $\lambda^{B,Im}_{m,s}(t)$, and prosumers export energy to the CESS at a price $\lambda^{B,Ex}_{m,s}(t)$. Here, $\lambda^{B,Im}_{m,s}(t) = \delta_k \lambda^{G,Im}_{m,s}(t)$ and $\lambda^{B,Ex}_{m,s}(t) = \delta_k \lambda^{G,Ex}_{m,s}(t)$, where δ_k is the CESS provider's energy trading price coefficient submitted in the auction. Note that, we let $\lambda^{B,Im}_{m,s}(t)$ and $\lambda^{B,Ex}_{m,s}(t)$ to be known parameters to preserve the linearity of the optimisation framework. Additionally, we use $\lambda^{G,Ex}_{m,s}(t) = a\lambda^{G,Im}_{m,s}(t)$ and $\lambda^{B,Ex}_{m,s}(t) = a\lambda^{B,Im}_{m,s}(t)$ relationships with $a < 1$ to replicate a net billing scheme. This pricing scheme favours prosumers' PV self-consumption [To et al., 2022].

5.4.3 Community Energy Storage System Model

This section presents the constraints that model the planning (i.e., CESS size, location, and time to install) and operation of the CESS. The binary variable $A_{m,k,i}$ in constraint (5.18) selects the best node to install the CESS, and constraint (5.19) ensures that the

CESS is only installed in one year. The size of the CESS $E^{B,C}_{m,k,i}$ is defined by constraint (5.20). Constraint (5.21) defines the relationship between the CESS rated power $P^{B,P}_{m,k,i}$ and the CESS size $E^{B,C}_{m,k,i}$ using the coefficient D_k (in h). In (5.20), the lower and upper limits of the allowable CESS size are given by $\underline{E}^{B}_{k}$ and $\overline{E}^{B}_{k}$, respectively. Constraint (5.22) regulates the charging and discharging of the CESS. The auxiliary variables $x_{i,k,s}(t)$, $y_{i,k,s}(t) \in \mathbb{R}^{+}$, and the binary variable $B_{i,k,s}(t)$, avoid the simultaneous charging and discharging of the CESS. The maximum limit of the CESS rated power is denoted by $\overline{P}^{B}_{k}$. The state-of-energy of the CESS is governed by constraint (5.23), where $E^{B}_{i,k,s}(t)$, μ^{ch}_{k}, and μ^{dis}_{k} are the state-of-energy at time t, charging and discharging efficiencies of the CESS, respectively. The state-of-energy is limited by the CESS size, as described by (5.24). Here, $\underline{\sigma_k}$ and $\overline{\sigma_k}$ are the lower and upper percentage coefficients of the CESS size, respectively. Moreover, the continuous operation of the CESS over the next day is guaranteed by constraint (5.25), where ξ_k is a small positive number, and $t_c \in \mathcal{T}_C$ where $\mathcal{T}_C = \{1, 2, ..., |\mathcal{T}_m| /24\}$.

$$\sum_{i \in \mathcal{J}} A_{m,k,i} \leq 1 \quad \forall k \in \mathcal{K},\ m \in \mathcal{M},\ A_{m,k,i} \in \{0,1\} \tag{5.18}$$

$$A_{m,k,i} \leq A_{m+1,k,i} \quad \forall k \in \mathcal{K},\ m \in \mathcal{M},\ i \in \mathcal{J},\ A_{m,k,i} \in \{0,1\} \tag{5.19}$$

$$A_{m,k,i}\underline{E}^{B}_{k} \leq E^{B,C}_{m,k,i} \leq A_{m,k,i}\overline{E}^{B}_{k} \quad \forall k \in \mathcal{K},\ m \in \mathcal{M},\ i \in \mathcal{J},\ A_{m,k,i} \in \{0,1\} \tag{5.20}$$

$$E^{B,C}_{m,k,i} = D_k P^{B,P}_{m,k,i} \quad \forall k \in \mathcal{K},\ m \in \mathcal{M},\ i \in \mathcal{J} \tag{5.21}$$

$$0 \leq e^{B,ch}_{i,k,s}(t) \leq x_{i,k,s}(t) \tag{5.22a}$$

$$e^{B,ch}_{i,k,s}(t) \leq x_{i,k,s}(t) \leq \overline{P}^{B}_{k} \Delta t B_{i,k,s}(t) \tag{5.22b}$$

$$-\overline{P}^{B}_{k} \Delta t(1 - B_{i,k,s}(t)) \leq x_{i,k,s}(t) - P^{B,P}_{m,k,i} \Delta t \leq 0 \tag{5.22c}$$

$$0 \leq e_{i,k,s}^{B,dis}(t) \leq y_{i,k,s}(t) \tag{5.22d}$$

$$e_{i,k,s}^{B,dis}(t) \leq y_{i,k,s}(t) \leq \overline{P}_k^B \Delta t (1 - B_{i,k,s}(t)) \tag{5.22e}$$

$$\begin{gathered} -\overline{P}_k^B \Delta t B_{i,k,s}(t) \leq y_{i,k,s}(t) - P_{m,k,i}^{B,P} \Delta t \leq 0 \\ \forall k \in \mathcal{K},\ t \in \mathcal{T}_m,\ m \in \mathcal{M},\ i \in \mathcal{J},\ s \in \mathcal{S},\ B_{i,k,s}(t) \in \{0,1\} \end{gathered} \tag{5.22f}$$

$$\begin{gathered} E_{i,k,s}^B(t) = E_{i,k,s}^B(t-1) + \mu_k^{ch} e_{i,k,s}^{B,ch}(t) - \frac{1}{\mu_k^{dis}} e_{i,k,s}^{B,dis}(t) \\ \forall k \in \mathcal{K},\ t \in \mathcal{T}_m,\ m \in \mathcal{M},\ i \in \mathcal{J},\ s \in \mathcal{S} \end{gathered} \tag{5.23}$$

$$\underline{\sigma_k} E_{m,k,i}^{B,C} \leq E_{i,k,s}^B(t) \leq \overline{\sigma_k} E_{m,k,i}^{B,C} \quad \forall k \in \mathcal{K},\ t \in \mathcal{T}_m,\ m \in \mathcal{M},\ i \in \mathcal{J},\ s \in \mathcal{S} \tag{5.24}$$

$$\left| E_{i,k,s}^B(24t_c) - E_{i,k,s}^B(0) \right| \leq \xi_k \quad \forall k \in \mathcal{K},\ t_c \in \mathcal{T}_C,\ m \in \mathcal{M},\ i \in \mathcal{J},\ s \in \mathcal{S} \tag{5.25}$$

5.5 Modelling Multi-Year Uncertainties

In this section, we describe how the multi-year uncertainties of the following optimisation inputs are modelled:

- Real and reactive energy consumption of prosumers and consumers;
- PV generation of prosumers;
- Number of PV installations;
- Energy trading prices.

Our approach to model the mentioned multi-year uncertainties includes three main steps, which are described in the next three sections.

5.5.1 Step 1: Generation of a Scenario Tree

In Step 1, we generate a scenario tree for different combinations of energy trading prices and the number of PV installations. We use the scenario tree illustrated in Figure

5.3 to model the mentioned multi-year uncertainties. This tree has a root (marked in blue), nodes (marked in red), and branches (marked in green). A path from the root to a node represents a scenario that has the same probability. Each node has a unique combination of energy trading prices and PV installations, and a sample representation of such combinations is marked near each node in Figure 5.3.

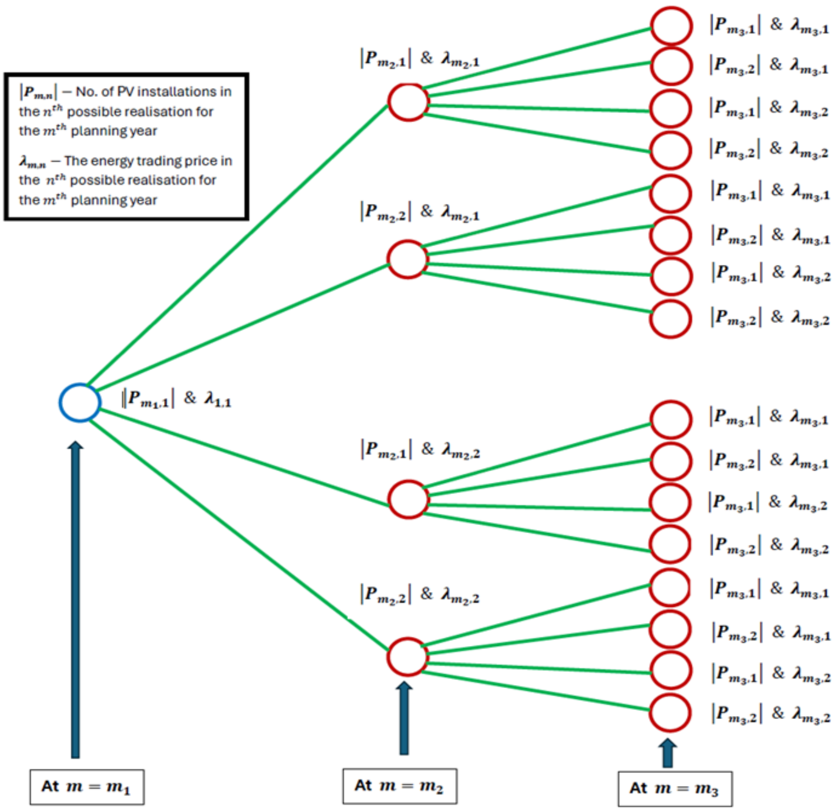

Figure 5.3: A sample scenario tree representing different combinations (marked near each node) of the number of PV installations and energy trading prices in the multi-year period. The scenario tree is drawn considering two possible realisations each for the energy trading price and the number of PV installations.

5.5.2 Step 2: Generation of Multiple Scenario Trees

In Step 2, we generate multiple scenario trees by combining the scenario tree obtained in Step 1, with independent scenarios of PV generation and real and reactive energy consumption generated by Monte Carlo simulations (MCSs) for each year of the planning horizon. We use normal distributions in our MCSs to generate the scenarios as in Chapter 4, leveraging the advantages of Monte Carlo methods such as ease of implementation and robust handling of uncertainties. We combine these generated scenarios with the ones obtained in Step 1 and calculate the probability $\Omega_{m,k,w}(t)$ of multi-year scenarios $\forall t \in \mathcal{T}_m,\ m \in \mathcal{M},\ k \in \mathcal{K},\ w \in \mathcal{W}$.

5.5.3 Step 3: Reduction of Multi-Year Scenarios

In Step 3, we use the K-Means clustering method described in [Scarlatache et al., 2012] to reduce the number of multi-year scenarios obtained from the scenario trees in Step 2 to maintain the optimisation tractable. We specifically leveraged K-Means clustering method for scenario reduction due to its scalability and ease of implementation compared to methods such as hierarchical clustering and density-based spatial clustering methods. Finally, we compute $\omega_{m,k,s}(t)$ in (5.26), which gives the overall probability for scenario s at time t in the m^{th} planning year, given the CESS provider as k.

$$\omega_{m,k,s}(t) = \frac{\Omega_{m,k,s}(t)}{\sum_{s\in\mathcal{S}} \Omega_{m,k,s}(t)} \quad \forall t \in \mathcal{T}_m,\ m \in \mathcal{M},\ k \in \mathcal{K},\ s \in \mathcal{S} \tag{5.26}$$

5.6 Simulations and Results

In this section, we first present the test data, followed by the simulation results.

5.6.1 Test data

The test data describes the data used to evaluate our multi-objective stochastic optimisation framework. We first mention the network and community data, followed by the data of the CESS providers', energy trading prices' and the generation of multi-year scenarios.

5.6.1.1 Network and Community Data

We used a 63-node radial feeder from the Australian Capital Territory in Australia as shown in Figure 5.4 for simulations. Therefore, $|\mathcal{V}| = 64$ and $|\mathcal{E}| = 63$, and we set $\mathcal{M} = \{1, 5, 10\}$. The data of the network, prosumers and consumers were sourced from [pro, 2021]. At $m = 1$, there are 12 prosumers and 27 consumers. Hence, $|\mathcal{P}| = 12$, and $|\mathcal{C}| = 27$ at $m = 1$. We took the possible CESS installation nodes as the ones that do not have prosumers, consumers and the slack node. Therefore, $\mathcal{J} = \mathcal{V} \setminus \{\mathcal{P} \cup \mathcal{C} \cup 0\}$. The locations of consumers, prosumers and possible CESS nodes in the network are reported in Table 5.1. The real energy consumption and PV generation are available in 1-hour resolution for 1 year, and hence, we set $\Delta t = 1h$. To generate energy consumption and PV generation profiles for the remaining years of the planning period, we assumed a 2% increment per year of energy consumption, and the PV generation to be the same over the planning period. Additionally, we assumed the reactive energy consumption of prosumers and consumers is correlated with their real energy consumption by a 0.9 power factor. The voltage limits of nodes are maintained as per the Australian standards AS 61000.3.100 and AS 60038 [pro, 2021]. Therefore, $\underline{V} = 0.94\,p.u.$ and $\overline{V} = 1.1\,p.u.$ with $V_0 = 1\,p.u.$.

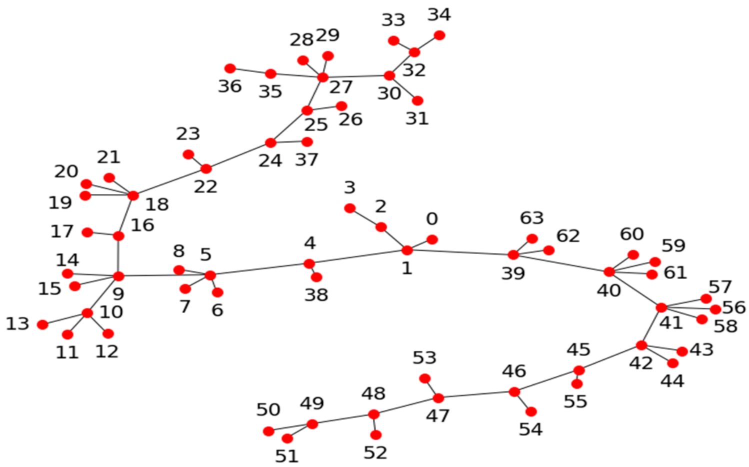

Figure 5.4: Network topology of the 63-node radial feeder.

Table 5.1: Locations of prosumers, consumers and candidate CESS locations.

	Nodes
Prosumers $\lvert\mathcal{P}\rvert = 12$ (at $m = 1$)	7, 8, 13, 14, 23, 26, 29, 31, 33, 55, 56, 63
Consumers $\lvert\mathcal{C}\rvert = 27$ (at $m = 1$)	3, 6, 11, 12, 15, 17, 19, 20, 21, 28, 34, 36, 37, 38, 43, 44, 50, 51, 52, 53, 54, 57, 58, 59, 60, 61, 62
Candidate CESS locations $\lvert\mathcal{J}\rvert = 24$	1, 2, 4, 5, 9, 10, 16, 18, 22, 24, 25, 27, 30, 32, 35, 39, 40, 41, 42, 45, 46, 47, 48, 49

5.6.1.2 CESS Providers' Data

We modelled the project offers of three CESS providers interested in installing and operating a CESS. We denote the potential CESS providers by CP_1, CP_2, and CP_3, and their project offers are succinctly given in Table 5.2 [Cole and Karmakar, 2023]. According to [Cole and Karmakar, 2023], it is expected that the investment costs $B_{m,k}$ of CESSs will reduce over the next couple of decades. Thus, we assumed $B_{m,k}$ to reduce by 2% per year as per the cost projections mentioned in [Cole and Karmakar, 2023]. Additionally, we assumed all the CESS providers use Li-ion as the CESS technology.

Table 5.2: Project offers of the competing CESS providers.

	CP_1	CP_2	CP_3
$B_{1,k}$ (AUD/kWh)	2000	1600	1400
$\underline{E}_k^B$ (kWh)	20	20	20
$\overline{E}_k^B$ (kWh)	700	700	700
$\overline{P}_k^B$ (kW)	200	200	200
D_k (h)	2	4	6
d_k	0.10	0.12	0.14
T_k (years)	10	12	14
μ_k^{ch}	0.98	0.98	0.98
μ_k^{dis}	0.98	0.98	0.98
$\underline{\sigma_k}$	0.2	0.2	0.2
$\overline{\sigma_k}$	1	1	1
ξ_k (kWh)	0.0001	0.0001	0.0001
δ_k	0.75	0.50	0.25
Technology	Li-ion	Li-ion	Li-ion

5.6.1.3 Energy Trading Prices' Data

We exploited the time-of-use tariff scheme used in previous chapters as the energy import price from the grid $\lambda^{G,Im}_{m,s}(t)$, and its per-day tariff at $m = 1$ is shown in Figure 5.5 [Origin, 2018]. Note that, the energy export price to the grid $\lambda^{G,Ex}_{m,s}(t)$ by prosumers is deduced from the relationship $\lambda^{G,Ex}_{m,s}(t) = a\lambda^{G,Im}_{m,s}(t)$ with $a = 0.3$, and the energy import/export price from/to the CESS is obtained from $\lambda^{B,Im}_{m,s}(t) = \delta_k\lambda^{G,Im}_{m,s}(t)$ and $\lambda^{B,Ex}_{m,s}(t) = \delta_k\lambda^{G,Ex}_{m,s}(t)$. Moreover, we used $\epsilon = 50\%$ in our multi-objective optimisation framework to distribute the economic benefits between all stakeholders equitably.

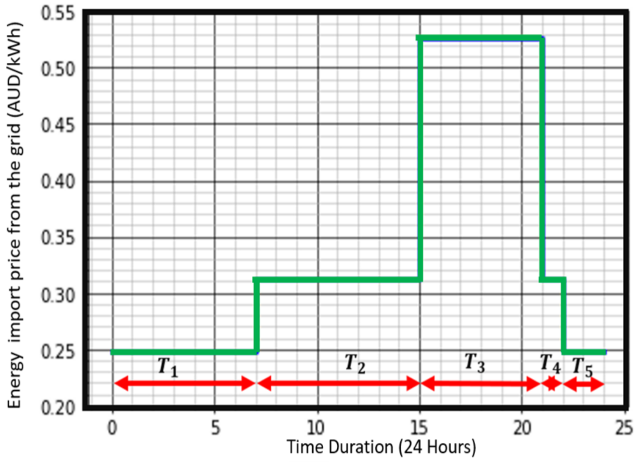

Figure 5.5: Energy import price from the grid $\lambda^{G,Im}_{m,s}(t)$ per day at $m = 1$.

5.6.1.4 Generation of Multi-Year Scenarios

We used the approach described in Section 5.5 to generate scenarios to model the multi-year uncertainties of energy trading prices, PV installations, real and reactive energy consumption, and PV generation. The approach includes 3 steps.

In Step 1, we generate a scenario tree to model combinations of realisations of energy trading prices and PV installations, as illustrated in Figure 5.6. As the realisations for energy trading prices, we considered import and export prices will reduce by either 2.5% or 5% along the years [pro, 2021]. For instance, the energy trading prices at $m = 5$ may decrease by either 2.5% or 5% at $m = 1$. The trend continues at $m = 10$, where the prices are reduced by 2.5% or 5% relative to their values at $m = 5$. To model the uncertainty of PV installations, we set the number of PV installations to increase in each planning year either by 6 or 9 and thus, there will be 60%-80% prosumers at the end of the planning period. The combinations of all these realisations produce 16 paths (i.e., 16 scenarios) as shown in Figure 5.6.

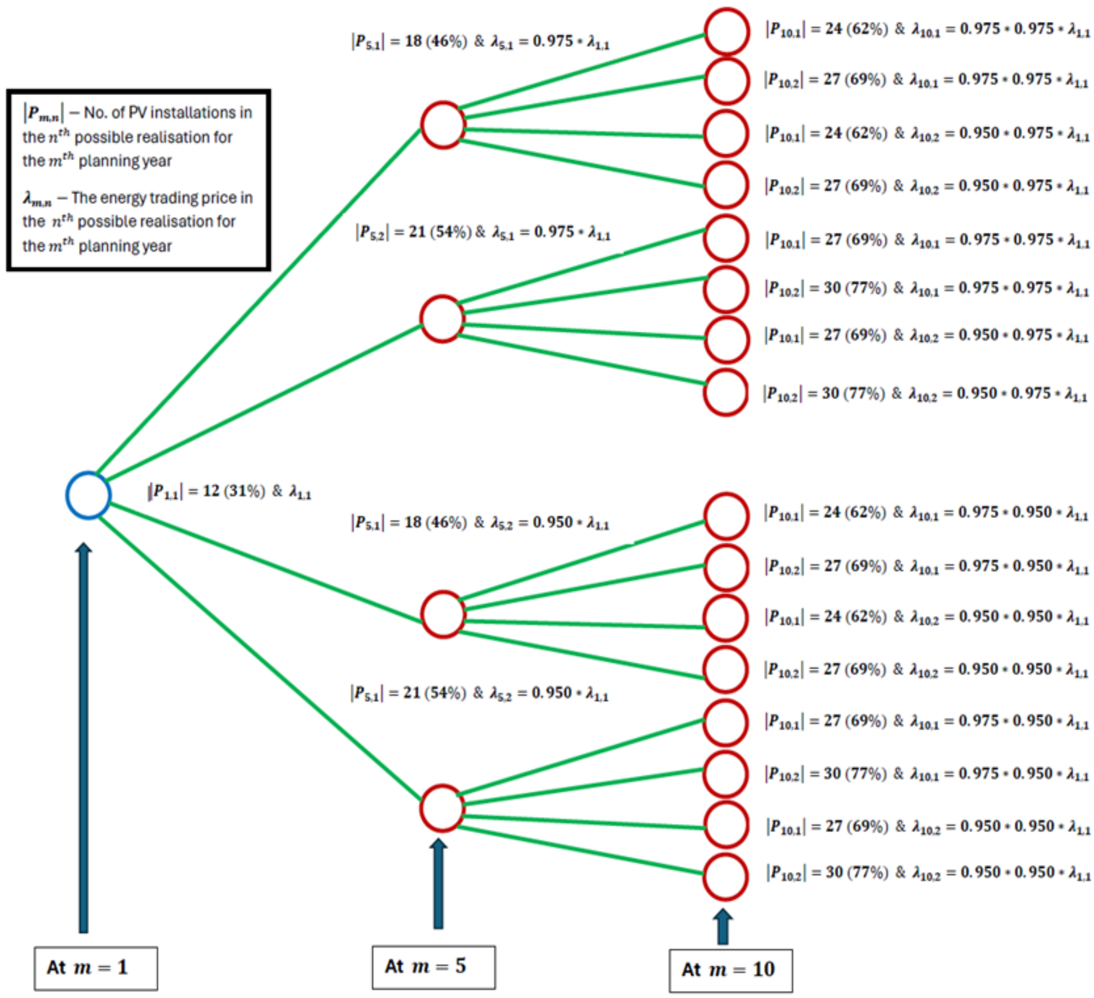

Figure 5.6: Scenario tree for the multi-year horizon. Different combinations of energy trading prices, the number of PV installations, and the percentage of prosumers in the community are marked near each node.

In Step 2, we used MCS to generate 30 independent scenarios of real and reactive energy consumption, and PV generation for each node of the scenario tree described in Figure

5.6. The combinations of these independent scenarios with the scenario tree generate multiple scenario trees with multi-year scenarios, being the total number of multi-year scenarios given by $N_w = |\mathcal{W}| = 16 \times 30 = 480$.

In Step 3, we reduced the multi-year scenarios to $N_s = |\mathcal{S}| = 50$ using the K-Means clustering method. The probabilities of those scenarios were computed from (5.26).

5.6.2 Results

This section presents the results obtained from a series of experiments. In these experiments, we first investigated how different government subsidy schemes impact the auction results, as well as the benefits for all stakeholders. We then study the effects of the uncertainties of energy trading prices and the number of PV installations in the auction results. Subsequently, we examine how different trade-off threshold percentage values impact the equitable distribution of benefits between the CESS beneficiaries in an auction setting. The experiments were conducted using the proposed optimisation framework implemented in Python and its optimisation problems were modelled in Pyomo and solved by the MILP optimiser of CPLEX.

5.6.2.1 Analysis of Different Government Subsidy Schemes

This section presents the results of the experiments conducted to evaluate the impact of three government subsidy schemes (Case I, II and III) on the auction results. In Case I, we set $S_1 = S_5 = S_{10} = 500 AUD/kWh$, so that the government support remains the same throughout the planning period. We selected 500 AUD/kWh assuming the government covers 25%-40% of the CESS investment cost. In Case II, we set S_1, S_5 and S_{10} as 500, 400, and 300 AUD/kWh, respectively. A scheme such as Case II incentivises the early installation of a CESS, as government support is reduced over the planning period. In Case III, we considered the CESS is installed without government support, and hence, $S_1 = S_5 = S_{10} = 0\ AUD/kWh$. Moreover, for Cases I-III, we took $\vartheta = 500000\ AUD$, which was the maximum contribution provided by the Australian government in 2024 auctions [Department of Climate Change and Water, 2024].

The results of the experiments for the three Cases are reported in Table 5.3. The percentages represent the increase in benefits of Cases I and II compared to Case III, that produced the least benefits for all stakeholders. The results show that provider CP_3 won the auction in all three Cases, generating a equitable distribution of economic benefits between the CESS provider, and the community. With government support, the economic gains have increased for all beneficiaries compared with the scheme with no support.

Table 5.3: Auction results for the three government subsidy schemes.

	Selected CESS Provider	CESS installation year (m)	CESS node ($A_{m,k,i}$)	CESS size ($E^{B,C}_{m,k,i}$) (kWh)	Expected annualised net revenue of the CESS provider $f^{E,B}$ (AUD)	Expected annualised net revenue of prosumers and consumers $f^{E,U}$ (AUD)
Case I ($S_1 = S_5 = S_{10}$)	CP_3	10	24	365	694975 (18%)[1]	293512 (14%)[1]
Case II ($S_1 > S_5 > S_{10}$)	CP_3	1	42	494	964774 (64%)[1]	399082 (55%)[1]
Case III ($S_1 = S_5 = S_{10} = 0$)	CP_3	10	1	205	587571	257631

[1] Percentage increase in the revenue of stakeholders compared to their lowest benefit case.

In Case III, the auction results show that the best time to install a CESS is at the end of the planning period, since it minimises the investment cost as per the cost projections [Cole and Karmakar, 2023]. A similar auction result is observed for Case I, which suggests a CESS installation at $m = 10$. However, in Case II, the auction results suggest the installation of the CESS at $m = 1$, as this case considers a government subsidy scheme that incentivises the installation of CESSs as early as possible. Due to this, the benefits are the highest in Case II with 64% and 55% increment of profits for the CESS provider, and the community of prosumers and consumers, respectively. Additionally, with this scheme, the CESS provider receives government support of AUD 78190, which is about 36% of the CESS investment cost (i.e., AUD 218931) to install a CESS of 494 kWh size. Therefore, the results show that providing incentives to install CESSs as early as possible, as in Case II, increases the benefits for all stakeholders and ensures their equitable distribution.

5.6.2.2 Analysis of the Impact of the PV Installations' Uncertainty

We conducted a series of experiments to study how the uncertainty of the number of PV installations can impact the auction results, as well as the planning of CESSs with government support. We did this analysis using the same data of Case II (including the realisations for energy trading prices shown in Figure 5.6) for two more cases as Case IV and V, but with different number of PV installations. In Case IV, we set less than 60% are prosumers, and in Case V, more than 80% are prosumers at the end of the planning period. Therefore, in Case IV and V, we took the number of PV installations increase by either 2 or 4, and 10 or 12, respectively. The scenario trees obtained from different realisations of PV installations in the multi-year horizon for Case IV and V are shown in Figure 5.7(a) and 5.7(b), respectively. A summary of auction results of Case IV and V is given in Table 5.4. and we compare them with the auction results in Case II.

Table 5.4: Auction results for three cases of scenario trees of PV installations.

	Selected CESS Provider	CESS installation year (m)	CESS node ($A_{m,k,i}$)	CESS size ($E^{B,C}_{m,k,i}$) (kWh)	Expected annualised net revenue of the CESS provider $f^{E,B}$ (AUD)	Expected annualised net revenue of prosumers and consumers $f^{E,U}$ (AUD)
Case IV	CP_3	1	2	429	704656	300418
Case II	CP_3	1	42	494	964774 (37%)[1]	399082 (33%)[1]
Case V	CP_3	1	30	577	1363030 (93%)[1]	562760 (87%)[1]

[1] Percentage increase in the revenue of stakeholders compared to their lowest benefit case.

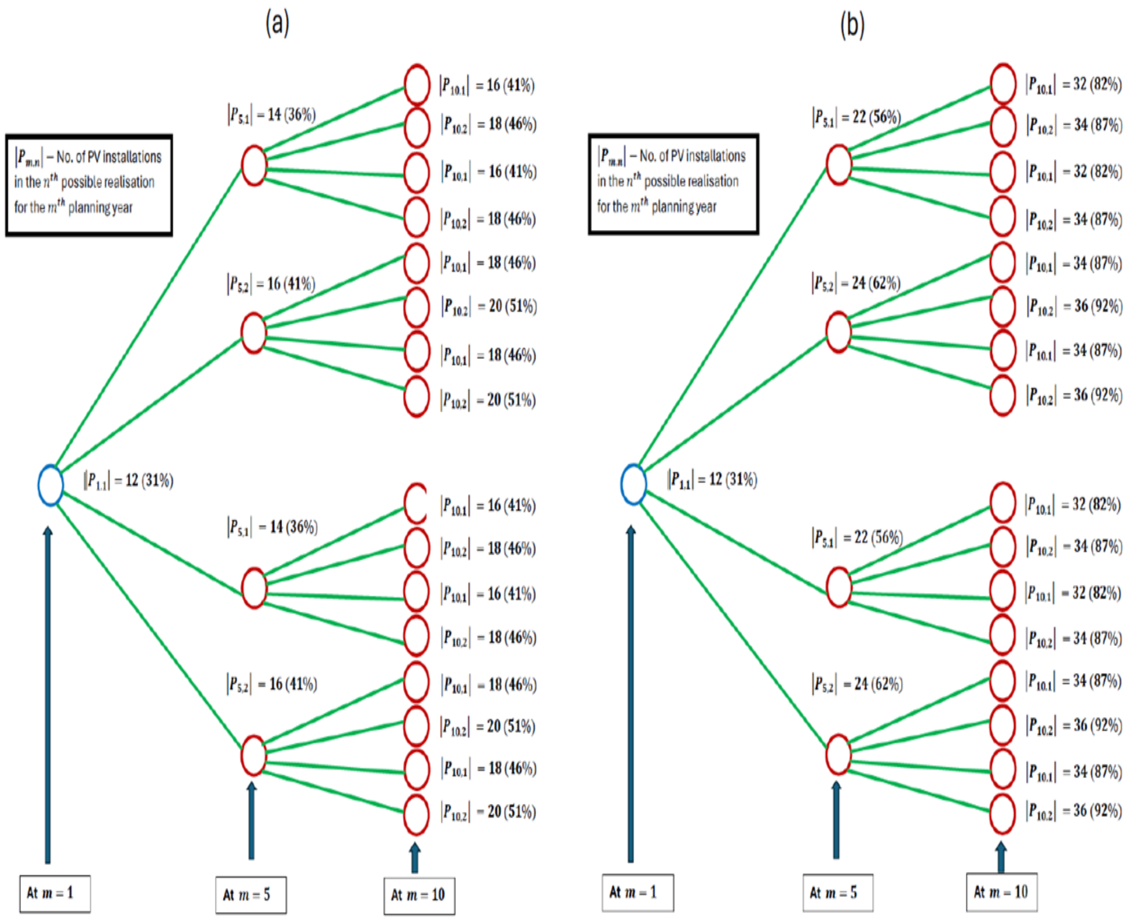

Figure 5.7: Scenario trees representing different realisations of PV installations number in the multi-year period. (a) Scenario tree in Case IV, (b) Scenario tree in Case V. Number of PV installations and prosumers' percentage in the community are marked near each node.

The auction results illustrated in Table 5.4 show that the CESS provider CP_3 won the auction in the three cases. The highest benefits for all stakeholders have been recorded in Case V, which has the highest number of PV installations (i.e., prosumers), whereas Case IV, with the lowest number of PV installations, has generated the lowest revenue for all stakeholders. Moreover, the CESS sizes in all three cases increase with the PV installation growth to accommodate the increase of PV generation in the network. Therefore, the benefits of the CESS provider, and prosumers and consumers increase with the increase in the number of PV installations.

5.6.2.3 Analysis of the Impact of Energy Trading Prices' Uncertainty

We conducted a series of experiments using different realisations of energy trading prices to investigate the impact of their uncertainty on the auction results. For this, we used the same input data of Case II (including the realisations for PV installations shown in Figure 5.8) and two more cases, Case VI and VII, with different energy trading prices. In Case VI, we assumed energy import and export prices of the CESS provider and the grid were reduced by either 7.5% or 10%, and in Case VII by either 12.5% or 15% over the planning years. Figure 5.8(a) and 5.8(b) illustrate two scenario trees built from different realisations of energy trading prices for Case VI and VII, respectively.

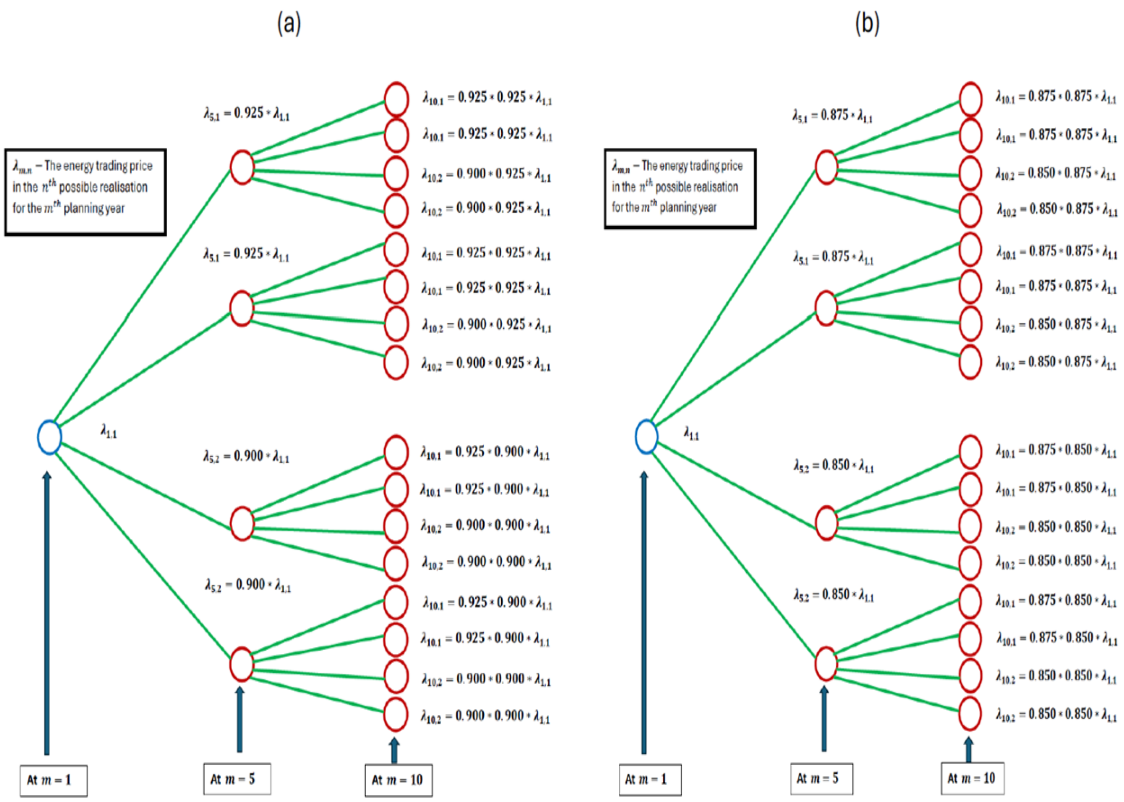

Figure 5.8: Scenario trees representing different realisations of energy trading prices in the multi-year period. (a) Scenario tree in Case VI, (b) Scenario tree in Case VII. Energy trading prices are marked near each node.

Table 5.5 summarises the auction results for each case, including the ones for Case II, initially described in Table 5.3. The auction was won by the CESS provider CP_3 and the CESS installation was suggested to $m = 1$ in all three cases, as in the previous experiments. The economic benefits of all stakeholders are reduced with the reduction of energy trading prices because both the CESS provider and the community benefit more from the export prices than time-of-use import prices in this case study. This is why reducing import and export prices by the same percentage reduces the benefits for all stakeholders.

Table 5.5: Auction results for three cases of scenario trees of energy trading prices.

	Selected CESS Provider	CESS installation year (m)	CESS node ($A_{m,k,i}$)	CESS size ($E^{B,C}_{m,k,i}$) (kWh)	Expected annualised net revenue of the CESS provider $f^{E,B}$ (AUD)	Expected annualised net revenue of prosumers and consumers $f^{E,U}$ (AUD)
Case VI	CP_3	1	40	466	877140 (11%)[1]	354548 (08%)[1]
Case II	CP_3	1	42	494	964774 (22%)[1]	399082 (21%)[1]
Case VII	CP_3	1	27	452	793491	329705

[1] Percentage increase in the revenue of stakeholders compared to their lowest benefit case.

5.6.2.4 Analysis of the Impact of Trade-off Threshold Percentages

This section presents the results used to understand how the trade-off threshold percentage (ϵ) affects the auction outcomes. To do this, we ran experiments by changing the value of ϵ to 25% (in Case VIII) and 75% (in Case IX), with the same input data as Case II. The results of these experiments are reported in Table 5.6.

The auction results regarding the CESS provider and installation year are the same as in the previous sections. The differences are in the economic benefits and CESS sizes. The CESS size is the highest in Case VIII, whereas in Case IX, the size is the lowest. The reason for this is that in Case VIII, the objective of the CESS provider is degraded least, resulting in the highest benefits for the CESS provider with the largest CESS size.

Table 5.6: Auction results for three trade-off threshold percentage values.

	Selected CESS Provider	CESS installation year (m)	CESS node ($A_{m,k,i}$)	CESS size ($E^{B,C}_{m,k,i}$) (kWh)	Expected annualised net revenue of the CESS provider $f^{E,B}$ (AUD)	Expected annualised net revenue of prosumers and consumers $f^{E,U}$ (AUD)
Case VIII ($\epsilon = 25\%$)	CP_3	1	30	571	1028274 (58%)[1]	383376 (43%)[2]
Case II ($\epsilon = 50\%$)	CP_3	1	42	494	964774 (48%)[1]	399082 (41%)[2]
Case IX ($\epsilon = 75\%$)	CP_3	1	5	312	652016	674882

[1] Revenue increase percentage considering min. revenue. [2] Revenue decrease percentage considering max. revenue.

In contrast, in Case IX, the objective of the CESS provider is traded-off most, leading to the least benefits for the CESS provider with the smallest CESS size.

In terms of economic benefits in the three cases, Case VIII has generated the highest revenue increase for the CESS provider and the lowest revenue for prosumers and consumers. Conversely, the lowest revenue for the CESS provider and highest revenue for prosumers and consumers has been obtained in Case IX. Therefore, the CESS project in Case VIII favours more the CESS provider as the objective of the CESS provider is traded off less, and prosumers and consumers are benefited more in the CESS auction in Case IX as the objective of the CESS provider is traded-off significantly. However, a value of 50% for ϵ used in the auction in Case II, trades-off the objective of the CESS provider moderately, so the benefits are spread equitably among all stakeholders.

5.7 Concluding Remarks

In this chapter, we have proposed a multi-objective stochastic optimisation framework to help governments run competitive auctions to select CESS projects to support financially. Selected CESS projects should maximise the economic benefits of CESS providers and communities and ensure a equitable distribution of benefits. In our multi-objective stochastic optimisation framework, we use the hierarchy method (ϵ-constraint method) to manage the conflicted objectives between CESS providers and communities of prosumers and consumers. We model the multi-year uncertainties of PV generation, real and reactive energy consumption, energy trading prices, and PV installations. The multi-year uncertainties are modelled using scenarios generated by scenario trees and Monte Carlo simulations. The number of scenarios is reduced by the K-Means clustering method to keep the optimisation problems tractable.

We assessed our optimisation framework's benefits through extensive experiments on a community of prosumers and consumers located on a 63-node LV radial feeder in Australia. The results showed that without government financial support, there is no economic incentive to install CESSs now. In other words, it makes economic sense to postpone the installation of CESSs based on their current prices. Nevertheless, it was observed that government financial support can be used to bring forward the installation of CESSs and improve their business case by increasing the distribution of economic benefits between CESS providers and communities and ensuring their equitable distribution.

In Chapters 3, 4, and 5, we developed CESS planning models based on an energy trading scheme that allows unrestricted energy trading among prosumers (without residential batteries), consumers, the grid, and the CESS provider. However, in the real-world, various factors such as regulatory, policy, technical, and geographical constraints may impose restrictions on energy trades between these entities, necessitating the adoption of alternative energy trading schemes. Additionally, some prosumers may already have residential batteries and still seek to benefit from a CESS. In the next chapter, we investigate how the CESS planning can benefit a community of prosumers, both with and without residential batteries, under different energy trading schemes.

Chapter 6

Evaluation of the Economic Benefits of Community Energy Storage Systems for Prosumers Under Different Energy Trading Schemes

This chapter examines how the economic merits for prosumers can be enhanced through CESS planning under different energy trading schemes (ETSs). In this context, we propose an optimisation framework to optimally plan CESSs and identify the most suitable ETS to benefit a community of prosumers, both with and without batteries.

6.1 Introduction

As discussed in Chapter 2, a CESS accommodates the surplus PV generation of prosumers and releases the energy back to them, especially, when the grid energy price is too high. Thus, a CESS can be exploited as an efficient tool to reduce prosumers' operating costs (i.e., the energy trading cost with the grid and/or the CESS). Prosumers' energy trade with both the grid and the CESS may not be possible always, particularly due to policy, infrastructure, technical, and geographical barriers. This necessitates the use of different energy trading schemes between prosumers, the grid and the CESS. Additionally, prosumers with batteries may also be interested to trade energy with a CESS and improve their benefits. In literature, there is no study that investigates to benefit a community of prosumers with and without batteries by optimising the CESS planning under different energy trading schemes.

In this chapter, we evaluate the economic benefits for prosumers gained from optimal CESS planning under four different ETSs. First, we consider an ETS where prosumers may trade energy with the grid and the CESS, second, an ETS where prosumers may trade energy only with the grid, third, an ETS where prosumers may trade energy only with the CESS, and fourth, an ETS where prosumers with batteries may trade energy only with the grid, and prosumers without batteries, may trade energy with the grid and the CESS. To size and place a CESS under the four ETSs, we formulate mixed-integer linear optimisation problems that minimise the operating costs (i.e., the cost of trading energy with the grid and/or the CESS) of prosumers. We conduct simulation experiments on the LV feeder (mentioned in Chapter 3 and 4) with 10 prosumers with batteries and 20 prosumers without batteries, to optimally plan a CESS and select the best ETS that generates the highest benefits for prosumers.

This chapter is structured as follows. Section 6.2 describes the ETSs, and the system models are detailed in Section 6.3. Section 6.4 presents the optimisation framework, the results are discussed in Section 6.5, and the conclusion of the chapter is given in Section 6.6.

6.2 Energy Trading Schemes

This section describes the four ETSs considered in this chapter to model energy trades between prosumers, the grid, and the CESS. In this chapter also, we consider a radial LV network with prosumers and a CESS. Prosumers $\mathcal{P}$ are divided into prosumers with batteries $\mathcal{P}^R$ and prosumers without batteries $\mathcal{P}^N$. In this study, it is assumed that PV units, batteries, and the CESS operate at a unity power factor. For simplicity, we do not model any uncertainty, and a third party installs and operate the CESS with no competition. Also, we do our analysis at time $t \in \mathcal{T}$, where $\mathcal{T}$ is the set of time intervals, and Δt is the difference between two adjacent time instances.

6.2.1 ETS 1: Prosumers Trade Energy With the Grid and the CESS

In ETS 1, $\forall p \in \mathcal{P}$, $t \in \mathcal{T}$, prosumers trade energy $e_p^B(t)$ with the CESS and $e_p^G(t)$ the grid, whenever there is a mismatch between their PV energy $e_p^{PV}(t)$ and real energy consumption $e_p^D(t)$. The energy transactions between the CESS, the grid, and prosumers in this ETS are shown in Figure 6.1(a), and they are mathematically described by (6.1)-(6.2).

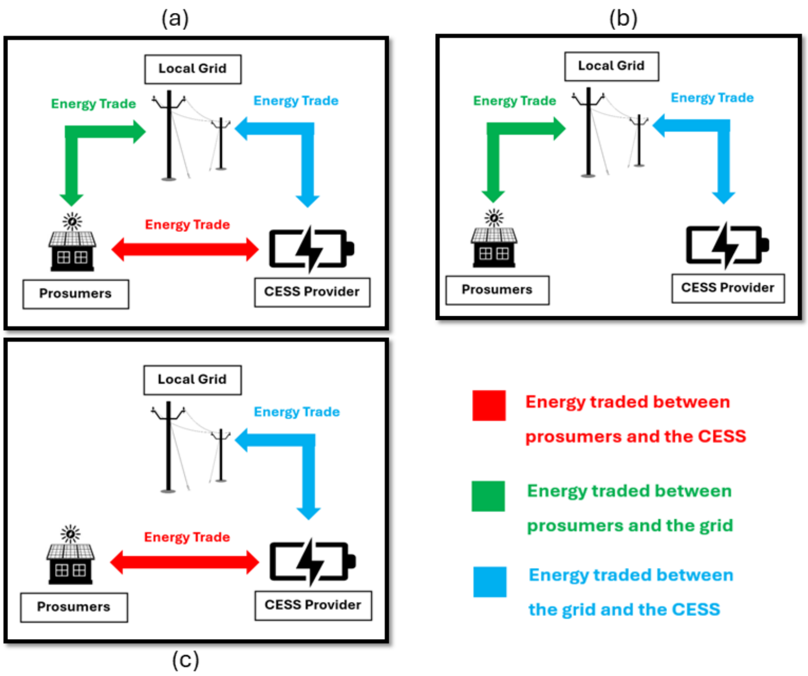

Figure 6.1: Energy transactions between prosumers, the CESS, and the grid in (a) ETS 1, (b) ETS 2, and (c) ETS 3.

$$\begin{aligned} &If\ \ e_r^{PV}(t) \geq e_r^D(t) \\ &e_r^G(t) + e_r^B(t) + e_r^{RB,ch}(t) = e_r^D(t) - e_r^{PV}(t) \leq 0 \qquad \forall\, r \in \mathcal{P}^{\mathcal{R}},\ t \in \mathcal{T} \end{aligned} \tag{6.1a}$$

$$\begin{aligned} &If\ \ e_n^{PV}(t) \geq e_n^{D}(t) \\ &\qquad e_n^{G}(t) + e_n^{B}(t) = e_n^{D}(t) - e_n^{PV}(t) \leq 0 \qquad \forall\, n \in \mathcal{P}^{\mathcal{N}},\ t \in \mathcal{T} \end{aligned} \tag{6.1b}$$

$$\begin{aligned} &If\ \ e_p^{PV}(t) \geq e_p^{D}(t) \\ &\qquad e_p^{D}(t) - e_p^{PV}(t) \leq e_p^{G}(t) \leq 0 \qquad \forall\, p \in \mathcal{P},\ t \in \mathcal{T} \end{aligned} \tag{6.1c}$$

$$e_p^{D}(t) - e_p^{PV}(t) \leq e_p^{B}(t) \leq 0 \qquad \forall\, p \in \mathcal{P},\ t \in \mathcal{T} \tag{6.1d}$$

$$\begin{aligned} &If\ \ e_r^{PV}(t) \leq e_r^{D}(t) \\ &0 \leq e_r^{D}(t) - e_r^{PV}(t) = e_r^{G}(t) + e_r^{B}(t) + e_r^{RB,dis}(t) \qquad \forall\, r \in \mathcal{P}^{\mathcal{R}},\ t \in \mathcal{T} \end{aligned} \tag{6.2a}$$

$$\begin{aligned} &If\ \ e_n^{PV}(t) \leq e_n^{D}(t) \\ &\quad 0 \leq e_n^{D}(t) - e_n^{PV}(t) = e_n^{G}(t) + e_n^{B}(t) \qquad \forall\, n \in \mathcal{P}^{\mathcal{N}},\ t \in \mathcal{T} \end{aligned} \tag{6.2b}$$

$$\begin{aligned} &If\ \ e_p^{PV}(t) \leq e_p^{D}(t) \\ &\qquad 0 \leq e_p^{G}(t) \leq e_p^{D}(t) - e_p^{PV}(t) \qquad \forall\, p \in \mathcal{P},\ t \in \mathcal{T} \end{aligned} \tag{6.2c}$$

$$0 \leq e_p^{B}(t) \leq e_p^{D}(t) - e_p^{PV}(t) \qquad \forall\, p \in \mathcal{P},\ t \in \mathcal{T} \tag{6.2d}$$

In (6.1)-(6.2), $e_r^{RB,ch}(t)$ and $e_r^{RB,dis}(t)$ are the charging and discharging energy of prosumer-owned batteries. The energy imports of prosumers from the CESS are represented by $e_p^{B}(t) > 0$, while the energy exports to the CESS are represented by $e_p^{B}(t) < 0$. The same sign convention is used for energy trade by prosumers with the grid, and energy trade by the CESS with the grid $e^{B,G}(t)$.

6.2.2 ETS 2: Prosumers Trade Energy Only With the Grid

In ETS 2, prosumers may trade energy only with the grid. A complete graphical representation of this ETS is given in Figure 6.1(b). The energy transactions of this ETS are modelled by (6.1)-(6.3).

$$e_p^B(t) = 0 \quad \forall\, p \in \mathcal{P},\ t \in \mathcal{T} \tag{6.3}$$

6.2.3 ETS 3: Prosumers Trade Energy only With the CESS

In contrast to ETS 2, prosumers may trade energy only with the CESS in ETS 3. The energy transactions under this ETS are illustrated in Figure 6.1(c), and they are mathematically described by (6.1)-(6.2), and (6.4).

$$e_p^G(t) = 0 \quad \forall\, p \in \mathcal{P},\ t \in \mathcal{T} \tag{6.4}$$

6.2.4 ETS 4: Prosumers With Batteries Trade Energy only With the Grid

In ETS 4, prosumers with batteries may trade energy only with the grid, as illustrated in Figure 6.1(b). On the other hand, prosumers without batteries can trade energy with both the grid and the CESS, as shown in Figure 6.1(a). For this ETS, (6.1)-(6.2), and (6.5) model the energy transactions between each entity.

$$e_r^B(t) = 0 \quad \forall\, r \in \mathcal{P}^{\mathcal{R}},\ t \in \mathcal{T} \tag{6.5}$$

6.3 System Models

This section presents the system models not described in Section 6.2. We begin by describing the network power flow model, which is followed by the models of prosumers' batteries and the CESS.

6.3.1 Network Power Flow Model

Consider a radial distribution network which is described by the graph $\mathcal{G} = (\mathcal{V}, \mathcal{E})$, where $\mathcal{V} = \{0, 1, ..., N\}$ is the set of all nodes, and $\mathcal{E} = \{(\alpha, \beta)\} \subset \mathcal{V} \times \mathcal{V}$ is the set of all lines.

The slack node (Node 0) represents the secondary side of the distribution transformer. The resistance and the reactance of the line (α, β) are $r_{\alpha,\beta}$ and $x_{\alpha,\beta}$, respectively. The real and reactive power flow from α to β node at time t are represented by $P_{\alpha,\beta}(t)$ and $Q_{\alpha,\beta}(t)$, respectively. Also, $\forall \alpha \in \mathcal{V} \setminus \{0\}$, $t \in \mathcal{T}$, real power absorption, reactive power absorption, and voltage magnitude are given by $p_\alpha(t)$, $q_\alpha(t)$, and $V_\alpha(t)$, respectively. In this study also, we use the linearised Distflow equations, which provide a good approximation for small radial grids [Baran and Wu, 1989]. Let $U_\alpha(t) = V_\alpha^2(t)$.

$$P_{\alpha,\beta}(t) = p_\alpha(t) + \sum_{\theta:\beta\to\theta} P_{\beta,\theta}(t) \quad \forall (\alpha,\beta) \in \mathcal{E},\ t \in \mathcal{T} \tag{6.6}$$

$$Q_{\alpha,\beta}(t) = q_\alpha(t) + \sum_{\theta:\beta\to\theta} Q_{\beta,\theta}(t) \quad \forall (\alpha,\beta) \in \mathcal{E},\ t \in \mathcal{T} \tag{6.7}$$

$$U_\beta(t) = U_\alpha(t) - 2(r_{\alpha,\beta} P_{\alpha,\beta}(t) + x_{\alpha,\beta} Q_{\alpha,\beta}(t)) \qquad \forall (\alpha,\beta) \in \mathcal{E},\ t \in \mathcal{T} \tag{6.8}$$

Assuming there are multiple prosumers at each node, real and reactive power absorption at node α at time t are written as (6.9) and (6.10), respectively. The set of prosumers with batteries at node α is denoted by $\mathcal{P}_\alpha^{\mathcal{R}} \subset \mathcal{P}^{\mathcal{R}}$, and the set of prosumers without batteries is given by $\mathcal{P}_\alpha^{\mathcal{N}} \subset \mathcal{P}^{\mathcal{N}}$. Also, the CESS charging and discharging energy are denoted by $e_\alpha^{B,ch}(t)$ and $e_\alpha^{B,dis}(t)$, and $e_r^Q(t)$ and $e_n^Q(t)$ are the reactive energy consumption per prosumer with and without batteries.

$$\begin{aligned} p_\alpha(t) = \frac{1}{\Delta t} \Bigg\{ & \sum_{r \in \mathcal{P}_\alpha^{\mathcal{R}}} e_r^D(t) + \sum_{n \in \mathcal{P}_\alpha^{\mathcal{N}}} e_n^D(t) - \sum_{r \in \mathcal{P}_\alpha^{\mathcal{R}}} e_r^{PV}(t) - \sum_{n \in \mathcal{P}_\alpha^{\mathcal{N}}} e_n^{PV}(t) \\ & + \sum_{r \in \mathcal{P}_\alpha^{\mathcal{R}}} e_r^{RB,ch}(t) - \sum_{r \in \mathcal{P}_\alpha^{\mathcal{R}}} e_r^{RB,dis}(t) + e_\alpha^{B,ch}(t) - e_\alpha^{B,dis}(t) \Bigg\} \quad \forall \alpha \in \mathcal{V} \setminus \{0\}, \quad t \in \mathcal{T} \end{aligned} \tag{6.9}$$

$$q_\alpha(t) = \frac{1}{\Delta t} \left\{ \sum_{r \in \mathcal{P}_\alpha^{\mathcal{R}}} e_r^Q(t) + \sum_{n \in \mathcal{P}_\alpha^{\mathcal{N}}} e_n^Q(t) \right\} \quad \forall \alpha \in \mathcal{V} \setminus \{0\},\ t \in \mathcal{T} \tag{6.10}$$

Inequality (6.11) makes sure the voltage magnitude at each node is within lower ($\underline{V}$) and upper ($\overline{V}$) bounds, where $\underline{U} = \underline{V}^2$ and $\overline{U} = \underline{V}^2$. Additionally, we do not explicitly model the line thermal limits in this study.

$$\underline{U} \leq U_\alpha(t) \leq \overline{U} \quad \forall \alpha \in \mathcal{V} \setminus \{0\}, \, t \in \mathcal{T} \tag{6.11}$$

6.3.2 Prosumers' Battery Model

In this work, we assume locations, capacities, and rated power of prosumer-owned batteries are known prior. For simplicity, $\forall r \in \mathcal{P}^{\mathcal{R}}$, rated battery power $P_r^{RB,P}$, charging efficiency μ_r^{ch}, discharging efficiency μ_r^{dis}, minimum battery energy level $\underline{E_r}^{RB,C}$ and maximum battery energy level/battery size $\overline{E_r}^{RB,C}$ are considered to be same. Equations (6.12a) and (6.12b) guarantee the charging and discharging energy of prosumer-owned batteries are bounded by the rated battery power. The binary variable $H_r(t)$ makes sure the charging and discharging of batteries do not occur simultaneously. The battery energy level at time t $E_r^{RB}(t)$ is described by (6.13a), and the inequality in (6.13b) maintains the battery energy level within its minimum and maximum energy limits. Also, (6.13c) facilitates the continuity of battery operation over the next day. Here, ξ is a small positive number, and $t_c \in \mathcal{T}_C$ where $\mathcal{T}_C = \{1, 2, ..., |\mathcal{T}| / 24\}$.

$$0 \leq e_r^{RB,ch}(t) \leq P_r^{RB,P} \Delta t H_r(t) \quad \forall \, r \in \mathcal{P}^{\mathcal{R}}, \; t \in \mathcal{T}, \; H_r(t) \in \{0, 1\} \tag{6.12a}$$

$$0 \leq e_r^{RB,dis}(t) \leq P_r^{RB,P} \Delta t (1 - H_r(t)) \quad \forall \, r \in \mathcal{P}^{\mathcal{R}}, \; t \in \mathcal{T}, \; H_r(t) \in \{0, 1\} \tag{6.12b}$$

$$E_r^{RB}(t) = E_r^{RB}(t-1) + \mu_r^{ch} e_r^{RB,ch}(t) - \frac{1}{\mu_r^{dis}} e_r^{RB,dis}(t) \; \forall \, r \in \mathcal{P}^{\mathcal{R}}, \; t \in \mathcal{T} \tag{6.13a}$$

$$\underline{E_r}^{RB,C} \leq E_r^{RB}(t) \leq \overline{E_r}^{RB,C} \; \forall \, r \in \mathcal{P}^{\mathcal{R}}, \; t \in \mathcal{T} \tag{6.13b}$$

$$\left|E_r^{RB}(24t_c) - E_r^{RB}(0)\right| \leq \xi \quad \forall\, r \in \mathcal{P}^{\mathcal{R}},\ t_c \in \mathcal{T}_C \tag{6.13c}$$

6.3.3 Community Energy Storage System Model

The set of equations (6.14)-(6.16) model the CESS planning aspects, namely its location α, size $E_\alpha^{B,C}$ and the rated power $P_\alpha^{B,P}$. Moreover, equations (6.17)-(6.20) model the CESS operation. The binary variable A_α in (6.14) determines the optimal CESS node. When $A_\alpha = 1$, it suggests α as the optimal CESS location. As given in (6.15) and (6.16), $\underline{E}^B$ and $\overline{E}^B$ are the minimum and maximum CESS size limits, and $\overline{P}^B$ is the maximum allowable rated CESS power. The CESS charging and discharging are described by (6.17a)-(6.17f). The inequalities in (6.17) are formulated in a way that charging and discharging of the CESS do not occur concurrently, and they do not exceed the optimal rated CESS power. For this, a binary variable $B_\alpha(t)$ and two additional variables $x(t)$, $y(t) \in \mathbb{R}^+$ are used. When the CESS charges, $B_\alpha(t) = 1$, and thus, $0 \leq e_\alpha^{B,ch}(t) \leq x(t) = P_\alpha^{B,P}\Delta t \leq \overline{P}^B \Delta t$. When the CESS discharges, $B_\alpha(t) = 0$, and hence, $0 \leq e_\alpha^{B,dis}(t) \leq y(t) = P_\alpha^{B,P}\Delta t \leq \overline{P}^B \Delta t$. The temporal variation of the CESS energy level is described by (6.18), the CESS energy level is maintained within the minimum and maximum CESS energy levels by (6.19), and the continuity of CESS operation over the next day is facilitated by (6.20). Here, $E_\alpha^B(t)$ is the CESS energy level at time t. The parameters μ^{ch}, μ^{dis} and $\underline{\sigma}, \overline{\sigma}$ are the charging and discharging efficiencies of the CESS, and the minimum and maximum percentage coefficients of the CESS size, respectively.

$$\sum_{\alpha=1}^{N} A_\alpha = 1 \quad \forall \alpha \in \mathcal{V} \setminus \{0\}, A_\alpha \in \{0,1\} \tag{6.14}$$

$$A_\alpha \underline{E}^B \leq E_\alpha^{B,C} \leq A_\alpha \overline{E}^B \quad \forall \alpha \in \mathcal{V} \setminus \{0\}, A_\alpha \in \{0,1\} \tag{6.15}$$

$$0 \leq P_\alpha^{B,P} \leq A_\alpha \overline{P}^B \quad \forall \alpha \in \mathcal{V} \setminus \{0\}, A_\alpha \in \{0,1\} \tag{6.16}$$

$$0 \leq e_\alpha^{B,ch}(t) \leq x(t) \tag{6.17a}$$

$$e_{\alpha}^{B,ch}(t) \leq x(t) \leq \overline{P}^{B} \Delta t B_{\alpha}(t) \tag{6.17b}$$

$$-\overline{P}^{B} \Delta t(1 - B_{\alpha}(t)) \leq x(t) - P_{\alpha}^{B,P} \Delta t \leq 0 \tag{6.17c}$$

$$0 \leq e_{\alpha}^{B,dis}(t) \leq y(t) \tag{6.17d}$$

$$e_{\alpha}^{B,dis}(t) \leq y(t) \leq \overline{P}^{B} \Delta t(1 - B_{\alpha}(t)) \tag{6.17e}$$

$$\begin{gathered} -\overline{P}^{B} \Delta t B_{\alpha} \leq y(t) - P_{\alpha}^{B,P} \Delta t \leq 0 \\ \forall \alpha \in \mathcal{V} \setminus \{0\}\,,\ t \in \mathcal{T},\ B_{\alpha}(t) \in \{0,1\} \end{gathered} \tag{6.17f}$$

$$E_{\alpha}^{B}(t) = E_{\alpha}^{B}(t-1) + \mu^{ch} e_{\alpha}^{B,ch}(t) - \frac{1}{\mu^{dis}} e_{\alpha}^{B,dis}(t) \quad \forall \alpha \in \mathcal{V} \setminus \{0\}\,,\ t \in \mathcal{T} \tag{6.18}$$

$$\underline{\sigma} E_{\alpha}^{B,C} \leq E_{\alpha}^{B}(t) \leq \overline{\sigma} E_{\alpha}^{B,C} \quad \forall \alpha \in \mathcal{V} \setminus \{0\}\,,\ t \in \mathcal{T} \tag{6.19}$$

$$\left| E_{\alpha}^{B}(24 t_c) - E_{\alpha}^{B}(0) \right| \leq \xi \quad \forall \alpha \in \mathcal{V} \setminus \{0\}\,,\ t_c \in \mathcal{T}_C \tag{6.20}$$

6.4 Optimisation Framework

This chapter aims to optimise the CESS planning to minimise prosumers' operating costs expressed by (6.21). The first term of (6.21) is the cost of trading energy with the grid, and the latter is the cost of trading energy with the CESS. Here, we do not consider the CESS investment cost, as we want to assess the potential benefits of installing a CESS without factoring in its capital costs. To value the energy imports and exports equally, from the CESS and the grid by prosumers, we use a one-for-one non-dispatchable energy buyback method for the grid energy price $\lambda^{G}(t)$, and the CESS energy price $\lambda^{B}(t)$ [Martin, 2012]. We also assume that there is no competition among prosumers to trade energy with the CESS.

$$\mathbf{x}^* = \underset{\mathbf{x}\in X}{argmin} \sum_{t\in\mathcal{T}} \sum_{\alpha=1}^{N} \lambda^G(t) \left(\sum_{r\in\mathcal{P}_\alpha^\mathcal{R}} e_r^G(t) + \sum_{n\in\mathcal{P}_\alpha^\mathcal{N}} e_n^G(t) \right) + \lambda^B(t) \left(\sum_{r\in\mathcal{P}_\alpha^\mathcal{R}} e_r^B(t) + \sum_{n\in\mathcal{P}_\alpha^\mathcal{N}} e_n^B(t) \right) \tag{6.21}$$

Here,

$$\mathbf{x} = (\mathbf{A}_\alpha, \mathbf{P}_\alpha^{\mathbf{B,P}}, \mathbf{E}_\alpha^{\mathbf{B,C}}, \mathbf{e}_\alpha^{\mathbf{B,ch}}, \mathbf{e}_\alpha^{\mathbf{B,dis}}, \mathbf{e}_\mathbf{r}^\mathbf{G}, \mathbf{e}_\mathbf{n}^\mathbf{G}, \mathbf{e}_\mathbf{r}^\mathbf{B}, \mathbf{e}_\mathbf{n}^\mathbf{B}) \tag{6.22}$$

Let $\mathbf{x}$ be the vector of decision variables which constitutes the vectors of optimal CESS location - $\mathbf{A}_\alpha$, CESS size - $\mathbf{E}_\alpha^{\mathbf{B,C}}$, CESS rated power - $\mathbf{P}_\alpha^{\mathbf{B,P}}$, CESS charging energy - $\mathbf{e}_\alpha^{\mathbf{B,ch}}$, CESS discharging energy - $\mathbf{e}_\alpha^{\mathbf{B,dis}}$, energy trade with the grid by prosumers with and without batteries - $\mathbf{e}_\mathbf{r}^\mathbf{G}$, $\mathbf{e}_\mathbf{n}^\mathbf{G}$, and energy trade with the CESS by prosumers with and without batteries - $\mathbf{e}_\mathbf{r}^\mathbf{B}$, $\mathbf{e}_\mathbf{n}^\mathbf{B}$. The feasibility set is denoted by X, which is constrained by (6.1)-(6.2), (6.6)-(6.20) for the ETS 1, (6.1)-(6.3), (6.6)-(6.20) for the ETS 2, (6.1)-(6.2), (6.4), (6.6)-(6.20) for the ETS 3, and (6.1)-(6.2), (6.5)-(6.20) for the ETS 4 in Section 6.2 and 6.3. The optimisation problem of each ETS is solved as a MILP.

6.5 Simulations and Results

This section presents a description of test data, followed by an analysis of results.

6.5.1 Test Data

To test our optimisation model, we considered the 7-node radial LV network used in Chapter 3 and 4, and it is shown in Figure 6.2. Its network data can be found in [Zeraati et al., 2018]. The forecasted real energy consumption and PV generation of 30 prosumers ($|\mathcal{P}| = 30$) in an Australian residential community, for a duration of 1 year, measured in 1-hour time intervals were used for simulations [sol]. We assumed that the reactive energy consumption is 0.5 times the real energy consumption considering the case of a typical Australian LV network, and in this network there are 10 prosumers with batteries ($|\mathcal{P}^{\mathcal{R}}| = 10$) and 20 prosumers without batteries ($|\mathcal{P}^{\mathcal{N}}| = 20$), who were randomly allocated to each node (see Figure 6.2). As the model parameters, we considered $V_0 = 1\,p.u.$, $\underline{V} = 0.95\,p.u.$, $\overline{V} = 1.05\,p.u.$, $\underline{E}^B = 100\,kWh$, $\overline{E}^B = 600\,kWh$, $\overline{P}^B = 400\,kW$, $\mu^{ch} = \mu^{dis} = 0.98$, $\underline{\sigma} = 0.05$, $\overline{\sigma} = 1$, $\xi = 0.0001\,kWh$ and $\Delta t = 1\,h$. Also, $P_r^{RB,P} = 4\,kW$, $\underline{E_r}^{RB,C} = 0.5\,kWh$, $\overline{E_r}^{RB,C} = 10\,kWh$, $\mu_r^{ch} = \mu_r^{dis} = 0.98\ \forall r \in \mathcal{P}^{\mathcal{R}}$. For $\lambda^G(t)$, the time-of-use tariff scheme used in Chapter 3,4 and 5 was used [Origin, 2018] , and its variation for a duration of 24 hours is shown in Figure 6.3. Due to the lack of accurate real data about the CESS energy price, we assumed $\lambda^B(t) = \frac{\sum_{t=1}^{24} \lambda^G(t)}{24}$. Hence, $\lambda^B(t) = 0.34180\,AUD/kWh$. The optimisation models were implemented in Python-Pyomo and solved using the MILP solver from CPLEX.

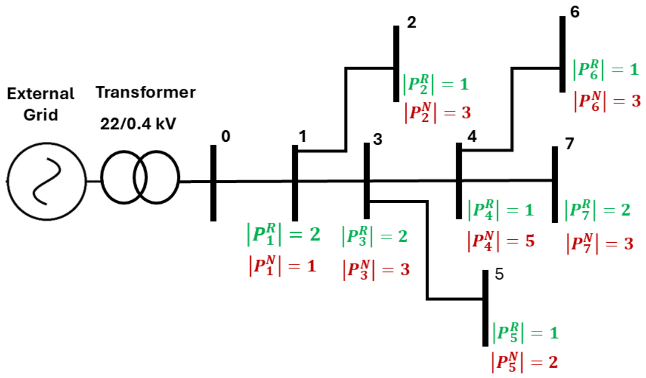

Figure 6.2: 7-Node LV radial feeder with Prosumers.

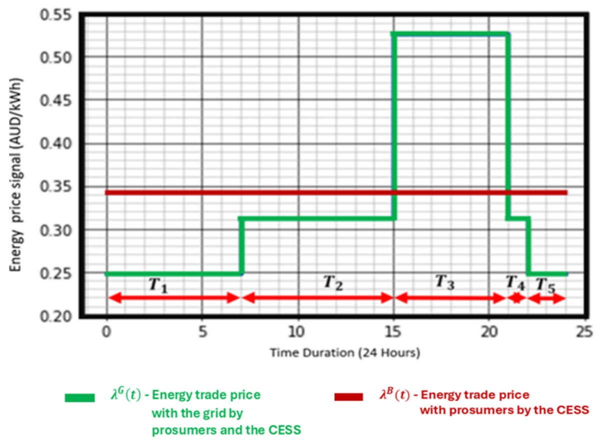

Figure 6.3: Variation of the grid energy price $\lambda^G(t)$, and the CESS energy price $\lambda^B(t)$.

6.5.2 Results

In this section, we analyse the impact of different ETSs on prosumers' benefits and the CESS planning results, followed by a discussion on energy trade between different stakeholders.

6.5.2.1 Impact of ETSs on CESS Planning and Prosumers' Costs

A summary of results obtained for the four ETSs is presented in Table 6.1. For all ETSs, the optimal CESS location is node 7. However, the optimal CESS size and its rated power are unique for each ETS, as the amount of energy traded with the CESS by prosumers varies with the ETS. In ETS 1 and 4, negative costs for trading energy with the CESS imply revenues for prosumers from the CESS.

Table 6.1: Optimal CESS planning results and prosumers' operating costs for each ETS.

	Optimal CESS node (A_α)	Optimal CESS size ($E_\alpha^{B,C}$) (kWh)	Optimal CESS rated power ($P_\alpha^{B,P}$) (kW)	Prosumers' annual energy costs with the grid (AUD)	Prosumers' annual energy costs with the CESS (AUD)	Prosumers' annual operating costs (AUD)
ETS 1	7	557	149	72024	-56160	15864 (73%)[1]
ETS 2	7	477	126	58716	N/A	58716
ETS 3	7	600	148	N/A	40824	40824 (30%)[1]
ETS 4	7	499	112	71652	-47472	24180 (59%)[1]

[1] Percentage cost reduction with respect to the highest operating costs in ETS 2.

The minimum operating costs were obtained from ETS 1. Since prosumers are enabled to trade energy with both the CESS and the grid, they have the flexibility to choose with whom they need to trade energy, to minimise operating costs. The highest operating costs were obtained from ETS 2. Here, prosumers do not trade energy with the CESS.

This impacts prosumers' operating costs in two ways. First, prosumers earn a lesser revenue for their exported energy to the grid as $\lambda^G(t) < \lambda^B(t)$ during T_2. Second, prosumers have to import high-priced energy from the grid as $\lambda^G(t) > \lambda^B(t)$ during T_3. Also, as T_2 and T_3 occupy a substantial time duration during a day, the impact of receiving a lower revenue from the grid, and requiring to pay more to the grid for the imported energy will be significant. This results in escalating the operating costs of prosumers in ETS 2. In ETS 3, the operating costs have increased compared to ETS 1. Here, as prosumers are unable to trade energy with the grid, they have to incur a higher cost for importing energy from the CESS, particularly during T_1, T_4, and T_5. The second minimum operating costs were obtained from the ETS 4. Since prosumers with batteries cannot trade energy with the CESS, they receive a lower revenue from the grid for their exported energy as $\lambda^G(t) < \lambda^B(t)$ during T_2, increasing the costs compared to ETS 1. As a whole, ETS 1 generates the minimum annual operating costs, which is approximately a 73% reduction compared to the ETS which generates the least economic benefits for prosumers.

6.5.2.2 Energy Transactions of Different Entities

Here, we analyse how prosumers, the CESS, and the grid do energy transactions in the four ETSs. For this, we randomly selected a day that was used for simulations. Figure 6.4 and 6.5 show how prosumers trade energy with the grid and the CESS in the four ETSs.

In ETS 1, prosumers import the low-priced energy from the grid during T_1, T_4, and T_5. As seen in Figure 6.5, during T_3, prosumers import energy from the CESS so they have to pay less. During T_2, they export the excess PV generation to the CESS, as they can earn a higher revenue (see Figure 6.4 and 6.5). In ETS 2, prosumers import energy only from the grid during T_1, T_3, T_4 and T_5, while they export energy to the grid during T_2 (see Figure 6.4). Similarly, in ETS 3, as prosumers are not allowed to trade energy with the grid, they export energy only to the CESS during T_2, and import energy from the CESS during T_1, T_3, T_4 and T_5. Hence, in ETS 2 and 3, prosumers cannot choose with whom that they need to trade energy to minimise their operating

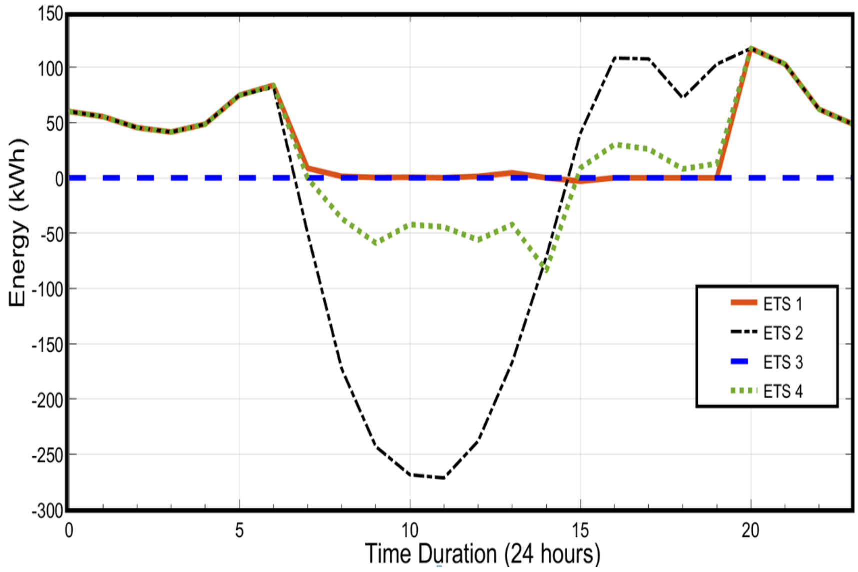

Figure 6.4: Variation of the total energy trade with the grid by prosumers in each ETS.

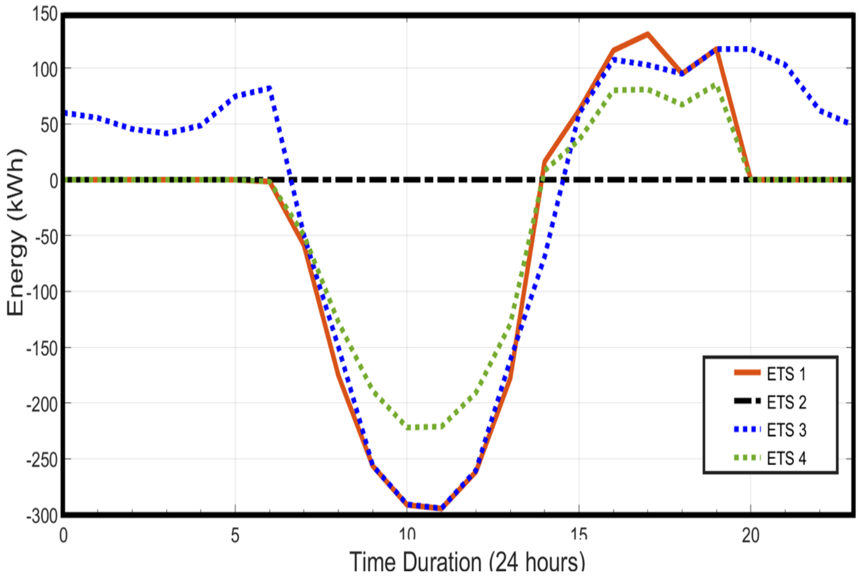

Figure 6.5: Variation of the total energy trade with the CESS by prosumers in each ETS.

costs, resulting in higher costs for them. In ETS 4, during T_1, T_4 and T_5, prosumers with and without batteries import the low-priced energy from the grid, similar to as in ETS

1. But, during T_2, prosumers with batteries export their excess PV generation to the grid, while prosumers without batteries export to the CESS. During T_3, prosumers with batteries import energy from the grid, while the others import energy from the CESS. Hence, prosumers with batteries earn lesser revenue and incur higher costs, resulting in increased operating costs compared to that in ETS 1.

Figure 6.6 shows the energy level variation of the CESS and batteries. They charge during T_2 using the surplus PV generation, and discharge during T_3 - T_5 when the PV generation is low. In ETS 1 and 3, prosumers increase the energy exchange with the CESS to increase their revenue, using a certain amount of energy that was exchanged with their batteries in ETS 2 and 4. This is seen as a reduction of the energy level of batteries in ETS 1 and 3, compared to ETS 2 and 4.

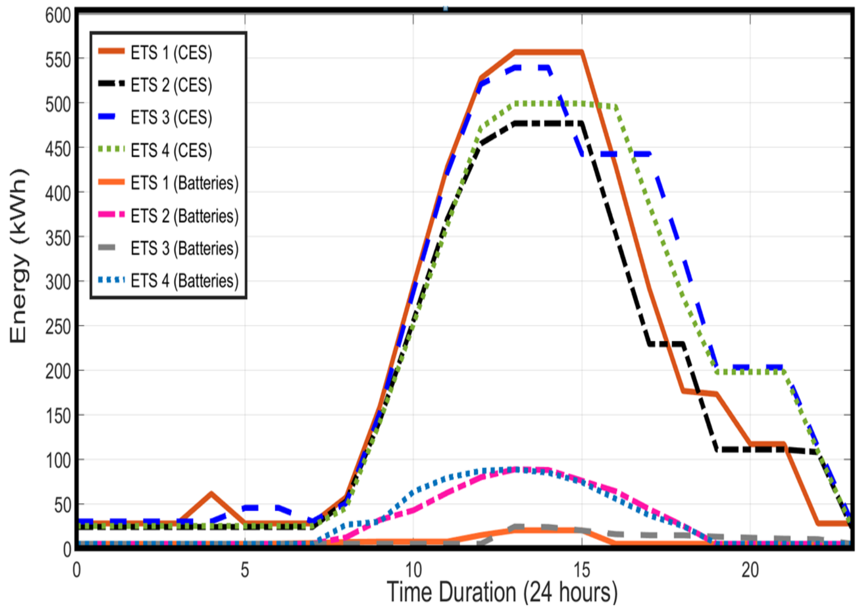

Figure 6.6: Variation of the CESS and the cumulative energy level of batteries in each ETS.

6.6 Concluding Remarks

In this chapter, we have investigated how the optimal planning of a CESS can economically benefit LV prosumers with and without batteries. For this, we have formulated mixed-integer linear optimisation models to compare four types of ETSs based on the energy trading capability between prosumers, the CESS, and the grid, and thereby, identify the ETS which minimises prosumers' operating costs. The results showed that ETS 1, the scheme where prosumers trade energy with the grid and the CESS, outperforms the other three ETSs, delivering a significant cost reduction compared to the ETS with the highest cost.

Chapter 7

Conclusions and Future Directions

In this chapter, we summarise our research works discussed in the previous chapters, including their main contributions and key findings. We also discuss the potential future extensions of our thesis.

7.1 Conclusions

In this thesis, we developed optimal community energy storage system (CESS) planning frameworks to benefit multiple stakeholders, namely prosumers, consumers, the CESS provider, and the network. The following conclusions are drawn from this thesis.

- As the first research problem, we explored how to generate techno-economic benefits for multiple stakeholders from a CESS planning framework. To address this problem, we developed a multi-objective CESS planning model that can generate technical benefits for the network, and economic benefits for prosumers and the CESS provider. The multi-objective function was built using the weighted-sum method and the analytic hierarchy process to weigh each objective fairly. Then, the multi-objective optimisation framework was solved as a mixed-integer quadratic program to minimise the network real energy loss, energy trading costs of prosumers and the CESS provider with the grid, and the CESS investment cost. We tested our model on a low-voltage (LV) radial feeder, and the results demonstrated that it yields improved techno-economic benefits compared to models that do not utilise a CESS and the ones that optimise only the CESS operation.

- In our first research work, we did not value the energy trade through a CESS, so the economic benefits for the CESS provider and prosumers may not be fully revealed. Additionally, we assumed that photovoltaic (PV) generation and real energy consumption of prosumers are known ahead of their forecasts. Typically, these parameters are subjected to high levels of uncertainty that need to be accounted for suitably. Also, it is important to distribute the benefits of a CESS in balance among all its beneficiaries.

  In our second piece of work, we addressed the above-mentioned limitations and also investigated how to benefit multiple stakeholders in balance by optimally planning a CESS under uncertainty and valuing the CESS energy trade suitably. For this, we proposed a multi-objective stochastic optimisation framework to select the best CESS solution (i.e., the optimal CESS planning aspects, and the energy pricing scheme (EPS) of the CESS provider) that delivers the most equitable outcome to the competing economic objectives of the CESS provider and prosumers. The presented optimisation framework minimises the investment and expected operating cost of the CESS provider and the expected operating costs of prosumers. We exploited the hierarchical (ϵ- constraint) method to rank the objectives of the CESS provider and prosumers based on their importance for decision-makers under three EPSs. Also, we modelled the uncertainties of PV generation, and real and reactive energy consumption using stochastic scenarios generated initially by a roulette wheel mechanism and then aggregated by the K-Means clustering algorithm to reduce the computational complexity of our optimisation problems. Simulation results indicated that optimal equity in benefits for both the CESS provider and prosumers is achieved when energy trading occurs at the average grid energy price in our case study. In this scenario, a moderate trade-off ($\epsilon = 50\%$) of the planning and operating objectives of the CESS provider enhanced the economic benefits for prosumers, resulting in the most equitable outcome for both stakeholders.

- Given the wide range of benefits from PV systems and their increased uptake, there is a growing demand for CESSs. This enhances the interest among CESS providers in installing and operating CESSs. However, the CESS installation should be managed properly to ensure the CESS benefits are distributed in balance. Also, CESSs are installed to harness their benefits for many years. Parameters such as PV generation, real and reactive energy consumption, energy prices, and the number of PV installations that impact CESS planning, are subject to multi-year uncertainties.

  Our third research work accounted for the aforementioned considerations and also explored how to manage CESS installations in an auction setting to select the best CESS project that can economically benefit multiple stakeholders in balance. To do this, we proposed a multi-objective stochastic optimisation framework to help governments run competitive auctions to select CESS projects to support financially. Selected CESS projects should maximise the economic benefits of CESS providers and communities and ensure an equitable distribution of benefits. In this study also, we used the hierarchy method to manage the conflicted objectives between CESS providers and communities of prosumers and consumers. We modelled the multi-year uncertainties of PV generation, real and reactive energy consumption, energy trading prices, and PV installations. The multi-year uncertainties were modelled using scenarios generated by scenario trees and Monte Carlo simulations. The number of scenarios was reduced by the K-Means clustering method to keep the optimisation problems tractable.

  We evaluated the benefits of our optimisation framework through a series of analyses using simulation experiments on an Australian community of prosumers and consumers within a 63-node LV network. We first analysed how different government subsidy schemes impacted the auction results. The results showed that without government financial support, there is no economic incentive to install CESSs now. In other words, it makes economic sense to postpone the installation of CESSs based on their current prices. On the other hand, with government financial support, the installation of CESSs can be brought forward. In addition, CESS projects supported by government subsidies produced higher and more equitable benefits to CESS providers and communities compared to CESS projects without government support. In our experiments, a subsidy scheme that incentivises the early installation of CESSs in the planning period generated the highest benefits by significantly increasing the profits of the CESS provider, and the community of prosumers and consumers compared to the benefits generated by a CESS project without government support. Therefore, government financial support can be used to bring forward the installation of CESSs and improve their business viability by increasing economic benefits for CESS providers and communities and ensuring their balanced distribution.

We conducted further experiments to understand the impact of the uncertainty of PV installations and energy trading prices on the auction results. For this, we used the same input data of the best government subsidy scheme described above and exploited different combinations of energy trading prices and the number of PV installations. The energy trading price results showed the revenue of all stakeholders was the highest in the case with the smallest decrease in import and export prices, as both CESS providers and communities benefit more from the export prices than time-of-use import prices in our case study. The PV installation results showed that the best outcomes for CESS providers and communities are obtained when the number of PV installations is the highest.

In this study, we used the hierarchy method and ranked the objective of the CESS provider as more important than the community objective. We then allowed the optimisation to degrade the objective of the CESS provider by a trade-off threshold

ϵ to improve the objective of the community of prosumers and consumers. To understand how the trade-off threshold margin ϵ impacts the auction results and equitable distribution of benefits, we conducted experiments for different ϵ values using the same input data of the best government subsidy scheme described earlier. The results showed that a relatively high ϵ value degrades the benefits of the CESS provider more, whereas a relatively low ϵ value reduces the benefits of the community of prosumers and consumers. However, a moderate ϵ value, such as 50%, generated the most equitable distribution of benefits for all stakeholders. Therefore, benefits among all stakeholders can be equitably distributed using a moderate ϵ value.

- In the aforementioned studies, we considered an energy trading scheme (ETS) with no restrictions for energy trade between prosumers, the grid, and the CESS provider. However, in the real-world, there may be policy constraints, network infrastructure challenges, and geographical limitations, that might restrict the energy trade between different entities. Additionally, prosumers with residential batteries may also be interested in benefiting from a CESS.

  Our fourth piece of work accounted for the above-mentioned considerations and evaluated how the economic benefits for prosumers with and without residential batteries, are impacted by planning CESSs under different ETSs. For this, we formulated mixed-integer linear programs under four types of ETSs. First, we considered an ETS where prosumers may trade energy with the grid and the CESS, second, an ETS where prosumers may trade energy only with the grid, third, an ETS where prosumers may trade energy only with the CESS, and fourth, an ETS where prosumers with batteries may trade energy only with the grid, and prosumers without batteries, may trade energy with the grid and the CESS. We then solved them one by one as mixed-integer linear problems to select the best ETS that minimises the energy trading cost with the grid and the CESS by prosumers with and without batteries.

We conducted experiments on a LV feeder using energy consumption and PV generation date of an Australian residential community. The results showed that the ETS, enabling prosumers to trade energy with the grid and the CESS, outperformed the other three ETSs, and delivered a significant cost reduction. As prosumers can trade energy with both the CESS and the grid, they have the flexibility to select which entity they should trade energy with to reduce their operating costs.

7.2 Future Directions

This section presents potential future extensions of this thesis that need further investigation.

7.2.1 Competition Among Prosumers and Consumers to Access the CESS

As CESSs are integrated more and more into local energy networks, competition emerges at multiple levels. For instance, prosumers as well as consumers may compete to access the CESS energy for maximising their economic benefits. This competition arises mainly due to CESS size limitations. At times, the CESS size may be insufficient to serve all prosumers and consumers in the network. In addition to prosumers' and consumers' competition, multiple CESS providers may also compete to install and operate these systems as discussed in Chapter 5.

Future research could explore how these dual layers of competition among prosumers and consumers for CESS energy access, and among providers to install and operate, can be managed to improve economic outcomes for all beneficiaries in balance. Further investigation lies in the areas of developing equitable access policies, designing robust CESS auction mechanisms, and evaluating how this competition impacts energy pricing, load balancing, and overall grid stability and reliability.

7.2.2 Planning of CESSs in the Presence of Electric Vehicles and Peer-to-Peer Energy Trading

The increase in the adoption of electric vehicles (EVs) and research on peer-to-peer (P2P) energy trading in modern power systems, are driven by their significant merits in a wide range of areas. EVs can act as mobile and flexible sources of energy storage that can support grid stability if managed properly. By enabling bidirectional energy flow, EVs can not only draw power from the grid but also inject energy back into the system during peak demand periods, helping to balance supply and demand. Also, P2P energy trading enables prosumers to trade surplus energy directly with one another, reducing reliance on conventional utilities and enabling a decentralised electricity market. A combination of EVs and P2P energy trading, promises enhanced flexibility and resilience in CESS-integrated LV networks. However, it also introduces new challenges in managing energy trades. The charging and discharging schedule of EVs can be highly unpredictable, creating demand surges. Additionally, P2P energy trading increases the complexity of managing the energy trade as it involves a decentralised energy trading mechanism. In this evolving energy landscape, CESSs need to be planned properly to maximise their benefits.

Future studies could focus on optimising the CESS planning under the combined uncertainties of EV mobility and P2P energy trading. An interesting area for exploration is the mitigation of voltage fluctuations and demand surges caused by unpredictable EV charging, alongside balancing energy flows during periods of high P2P energy trading activity through effective CESS energy management. This could involve optimally planning CESSs to store surplus energy during low-demand periods and release it during peak EV charging or P2P energy trading, thereby enhancing the grid stability. Additionally, it is worth to explore how the CESS planning under different energy pricing schemes could maximise benefits for all stakeholders, facilitating cost-effective EV charging, improving energy trading efficiency of prosumers, and increasing economic returns for both CESS providers and prosumers, while ensuring reliable network operation.

7.2.3 Planning of Hybrid CESSs

Hybrid CESSs integrate multiple storage technologies to optimise energy management and meet various energy requirements efficiently. By combining different technologies, such as batteries and hydrogen storage, hybrid CESSs can handle both short-term and long-term energy needs effectively. An emerging development within this framework is the incorporation of hydrogen storage as a clean energy solution. Hydrogen can be produced from excess renewable energy through electrolysis and stored to be used later. The integration of hydrogen storage enhances a system's long-term storage capabilities and supports decarbonisation efforts across many areas.

Planning hybrid CESSs that incorporate both battery and hydrogen technologies presents a promising avenue for future research. Studies could focus on developing hybrid CESS planning frameworks that determine the ideal mix of battery and hydrogen storage capacities to address both short-term and long-term energy needs efficiently. Additionally, this includes optimising the hybrid CESS operation to manage daily energy fluctuations with batteries while reserving hydrogen storage for seasonal or prolonged energy demands. Moreover, research could explore the economic feasibility of hybrid systems, assessing cost-benefit trade-offs, including infrastructure investments and operational costs. Another critical area is the investigation of environmental impacts, particularly how hybrid CESSs contribute to decarbonisation goals by integrating with renewable energy sources. Also, multi-stakeholder models could be developed to evaluate how such hybrid CESSs can equitably benefit communities, grid operators, and energy providers, ensuring widespread adoption and sustainability.

7.2.4 Social and Behavioural Impacts of Community on CESS Planning

In the planning of CESSs, understanding the social and behavioural impacts of community members is essential for better energy management. The CESS ownership models significantly impact how stakeholders engage with and utilise CESSs. For instance, community ownership can create a high level of responsibility and investment, leading to higher participation rates. This strengthens social ties within the community, creating a supportive environment for sustainable energy practices, such as minimising energy consumption. Also, increased community engagement can lead to better CESS energy management, thereby lowering their energy costs. Economic incentives also play an important role in encouraging community engagement with CESSs. Financial rewards, subsidies, and educational initiatives can motivate comminutes to invest in and actively participate in energy management. Additionally, considering social aspects such as trust and collective decision-making supports better CESS energy management.

A potential avenue for future work is investigating how social factors such as trust, community cohesion, and collective decision-making can be integrated into CESS planning to enhance energy management. Research could investigate the role of social capital in enhancing participation rates, particularly in different ownership models, and how these social dynamics can be leveraged to optimise the CESS planning and its energy usage. Additionally, studies could examine the design of incentive structures that align financial rewards with social engagement, ensuring that economic benefits of CESSs are shared equitably among community members. Understanding how to foster a sense of ownership and responsibility in communities could lead to more sustainable and efficient CESS energy management, contributing to long-term success and widespread adoption. Moreover, exploring how community-led governance models can be integrated into CESS planning could offer valuable insights into improving transparency, trust, and collaborative decision-making processes.

Bibliography

Solar home electricity data. Online. https://www.ausgrid.com.au/Industry/Our-Research/Data-to-share/Solar-home-electricity-data/. [Cited on pages 50, 71, and 117.]

2021. Project converge - act distributed energy resources demonstration pilot. https://arena.gov.au/projects/act-distributed-energy-resources-demonstration-pilot-project-converge/. [Cited on pages 96 and 98.]

ABB, 2023. Bess case note: Gvea fairbanks. https://library.e.abb.com/public/3c4e15816e4a7bf1c12578d100500565/Case_Note_BESS_GVEA_Fairbanks-web.pdf. [Cited on page 14.]

Abraham, S.; Mishra, Y.; and Cholette, M., 2022. Optimal utilization of community battery energy storage with differential battery tariffs. In *2022 IEEE Power & Energy Society General Meeting (PESGM)*, 01–05. IEEE, Denver, CO, USA. [Cited on page 30.]

Agency, A. R. E., 2023. Community batteries funding round 1. https://arena.gov.au/funding/community-batteries-round-1/. [Cited on page 83.]

Aghaei, J.; Karami, M.; Muttaqi, K. M.; Shayanfar, A.; and Ahmadi, H. A., 2015. Mip-based stochastic security-constrained daily hydrothermal generation scheduling. *IEEE Systems Journal*, 9, 2 (2015), 615–628. [Cited on pages 65 and 67.]

Akram, U.; Nadarajah, M.; Shah, R.; and Milano, F., 2020. A review on rapid responsive energy storage technologies for frequency regulation in modern power systems. *Renewable and Sustainable Energy Reviews*, 120 (2020), 109626. [Cited on page 12.]

Alam, M. J. E.; Muttaqi, K. M.; and Sutanto, D., 2015. Community energy storage for neutral voltage rise mitigation in four-wire multigrounded lv feeders with unbalanced solar pv allocation. *IEEE Transactions on Smart Grid*, 6, 6 (November 2015), 2845–2855. [Cited on page 28.]

Alam, M. M. and Jang, Y. M., 2023. Deep learning based optimal energy management framework for community energy storage system. *ICT Express*, 9, 3 (2023), 333–340. [Cited on pages 16, 29, and 34.]

Alrashidi, M., 2022. Community battery storage systems planning for voltage regulation in low voltage distribution systems. *Applied Sciences*, 12, 18 (2022), 9083. [Cited on page 32.]

Amjady, N.; Aghaei, J.; and Shayanfar, H. A., 2009. Stochastic multiobjective market clearing of joint energy and reserves auctions ensuring power system security. *IEEE Transactions on Power Systems*, 24, 4 (2009), 1841–1854. [Cited on page 65.]

Arani, A. K.; Gharehpetian, G.; and Abedi, M., 2019. Review on energy storage systems control methods in microgrids. *International Journal of Electrical Power & Energy Systems*, 107 (2019), 745–757. [Cited on pages xviii and 11.]

Arghandeh, R.; Woyak, J.; Onen, A.; Jung, J.; and Broadwater, R. P., 2014. Economic optimal operation of community energy storage systems in competitive energy markets. *Applied Energy*, 134 (2014), 65–75. [Cited on page 24.]

Asri, R.; Aki, H.; and Kodaira, D., 2023. Optimal operation of shared energy storage on islanded microgrid for remote communities. *Sustainable Energy, Grids and Networks*, 35 (2023), 101104. [Cited on page 30.]

BARAN, M. AND WU, F., 1989. Optimal sizing of capacitors placed on a radial distribution system. *IEEE Transactions on Power Delivery*, 4, 1 (1989), 735–743. [Cited on pages 43, 44, 47, 61, and 113.]

BAZARAA, M. S.; SHERALI, H. D.; AND SHETTY, C. M., 2006. *Nonlinear Programming: Theory and Algorithms*. John Wiley & Sons. [Cited on page 23.]

BEN-TAL, A.; NEMIROVSKI, A.; AND EL GHAOUI, L., 2009. *Robust Optimization*. Princeton University Press. [Cited on page 26.]

BERTSEKAS, D. P., 1999. *Nonlinear Programming*. Athena Scientific. [Cited on page 24.]

BIRGE, J. R. AND LOUVEAUX, F., 2011. *Introduction to Stochastic Programming*. Springer Science and Business Media. [Cited on pages 24 and 26.]

BOYD, S. AND VANDENBERGHE, L., 2004. *Convex Optimization*. Cambridge University Press. [Cited on pages 23 and 26.]

BROUWER, R., 2018. Aggregated flexibility to support congestion management: A case study at eneco crowdnett. (2018). [Cited on page 21.]

BÖHRINGER, M.; CHOUDHURY, S.; WECK, S.; AND HANSON, J., 2021. Sizing and placement of community energy storage systems using multi-period optimal power flow. In *2021 IEEE Madrid PowerTech*, 1–6. IEEE, Madrid, Spain. [Cited on pages 32 and 36.]

CHANG, H.-C.; GHADDAR, B.; AND NATHWANI, J., 2022. Shared community energy storage allocation and optimization. *Applied Energy*, 305 (2022), 117944. [Cited on page 28.]

CHATZIGEORGIOU, N. G.; THEOCHARIDES, S.; MAKRIDES, G.; AND GEORGHIOU, G. E., 2024. A review on battery energy storage systems: Applications, developments, and research trends of hybrid installations in the end-user sector. *Journal of Energy Storage*, 861 (2024). [Cited on pages xviii and 22.]

Chen, X.; Dong, W.; and Yang, Q., 2022. Robust optimal capacity planning of grid-connected microgrid considering energy management under multidimensional uncertainties. *Applied Energy*, 323 (2022), 119642. [Cited on page 35.]

Choudhury, S., 2022. Review of energy storage system technologies integration to microgrid: Types, control strategies, issues, and future prospects. *Journal of Energy Storage*, 48 (2022), 103966. [Cited on page 20.]

Chreim, B.; Esseghir, M.; and Merghem-Boulahia, L., 2024. Recent sizing, placement, and management techniques for individual and shared battery energy storage systems in residential areas: A review. *Energy Reports*, 11 (2024), 250–260. [Cited on page 16.]

Coddington, M.; Sciano, D.; and Fuller, J., 2017. Change in brooklyn and queens: How new york? s reforming the energy vision program and con edison are reshaping electric distribution planning. *IEEE Power and Energy Magazine*, 15, 2 (2017), 40–47. [Cited on page 21.]

Cole, W. and Karmakar, A., 2023. Cost projections for utility-scale battery storage: 2023 update. Technical report, National Renewable Energy Laboratory. [Cited on pages 86, 97, and 101.]

Csereklyei, Z.; Dwyer, S.; Kallies, A.; and Economou, D., 2024. The role of community-scale batteries in the energy transition: Case studies from australia's national electricity market. *Journal of Energy Storage*, 93 (2024), 112277. [Cited on page 2.]

Dai, R.; Esmaeilbeigi, R.; and Charkhgard, H., 2021. The utilization of shared energy storage in energy systems: A comprehensive review. *IEEE Transactions on Smart Grid*, 12, 4 (2021), 3163–3174. [Cited on page 2.]

Das, C. K.; Mahmoud, T. S.; Bass, O.; Muyeen, S.; Kothapalli, G.; Baniasadi, A.; and Mousavi, N., 2020. Optimal sizing of a utility-scale energy storage system in transmission networks to improve frequency response. *Journal of Energy Storage*, 29 (2020), 101315. [Cited on page 12.]

Data Center Dynamics, 2024. Japan's space agency deploys battery storage system at ground station in nagano. https://www.datacenterdynamics.com/en/news/japans-space-agency-deploys-battery-storage-system-at-ground-station-in-nagano/. [Cited on page 14.]

Department of Climate Change, t. E., Energy and Water, 2024. Community batteries for household solar program. https://www.dcceew.gov.au/energy/renewable/community-batteries. [Cited on pages 82 and 101.]

DICP, 2022. Dicp achievements in catalytic chemistry and energy conversion. http://english.dicp.cas.cn/news/headline/202210/t20221010_321218.html. [Cited on page 14.]

Divshali, P. H. and Söder, L., 2019. Improving hosting capacity of rooftop pvs by quadratic control of an lv-central bss. *IEEE Transactions on Smart Grid*, 10, 1 (2019), 919–927. [Cited on page 32.]

Dong, S.; Kremers, E.; Brucoli, M.; Rothman, R.; and Brown, S., 2021. Techno-enviro-economic assessment of household and community energy storage in the uk. *Renewable and Sustainable Energy Reviews*, 135 (2021), 110195. [Cited on page 25.]

Dorahaki, S.; Rashidinejad, M.; MollahassaniPour, M.; Kasmaei, M. P.; and Afzali, P., 2023a. A sharing economy model for a sustainable community energy storage considering end-user comfort. *Sustainable Cities and Society*, 92 (2023), 104786. [Cited on page 27.]

Dorahaki, S.; Rashidinejad, M.; MollahassaniPour, M.; Kasmaei, M. P.; and Afzali, P., 2023b. A sharing economy model for a sustainable community energy storage considering end-user comfort. *Sustainable Cities and Society*, 97 (2023), 104786. [Cited on page 30.]

Duque, E. M. S.; Giraldo, J. S.; Vergara, P. P.; Nguyen, P.; van der Molen, A.; and Slootweg, H., 2022. Community energy storage operation via reinforcement learning with eligibility traces. *Electric Power Systems Research*, 212 (November 2022), 108515. [Cited on page 30.]

El-Batawy, S. A. and Morsi, W. G., 2018. Optimal design of community battery energy storage systems with prosumers owning electric vehicles. *IEEE Transactions on Industrial Informatics*, 14, 5 (2018), 1920–1931. [Cited on page 29.]

Elio, J.; Phelan, P.; Villalobos, R.; and Milcarek, R. J., 2021. A review of energy storage technologies for demand-side management in industrial facilities. *Journal of Cleaner Production*, 307 (2021), 127322. [Cited on page 16.]

Fatima, S.; Püvi, V.; and Lehtonen, M., 2020. Review on the pv hosting capacity in distribution networks. *Energies*, 13, 18 (2020), 4756. [Cited on page 16.]

Garg, A. and Niazi, K. R., 2022. Energy storage system in micro-grids: Types, issues and challenges. In *2022 2nd International Conference on Innovative Sustainable Computational Technologies (CISCT)* (Dehradun, India, 2022), 1–6. IEEE. [Cited on page 16.]

Gerdroodbari, Y. Z.; Khorasany, M.; Razzaghi, R.; and Heidari, R., 2023. Management of prosumers using dynamic export limits and shared community energy storage. *Applied Energy*, 338 (2023), 122222. [Cited on page 30.]

Ghaffari, A.; Askarzadeh, A.; and Fadaeinedjad, R., 2022. Optimal allocation of energy storage systems, wind turbines and photovoltaic systems in distribution network considering flicker mitigation. *Applied Energy*, 319 (2022), 119253. [Cited on page 36.]

Giraldo, J. S.; Salazar, M.; Vergara, P. P.; Tsaousoglou, G.; Slootweg, J. G.; and Paterakis, N. G., 2021. Optimal operation of community energy storage using stochastic gradient boosting trees. In *2021 IEEE Madrid PowerTech*, 1–6. IEEE, Madrid, Spain. [Cited on page 27.]

Glücker, P.; Pesch, T.; and Benigni, A., 2024. Optimal sizing of battery energy storage system for local multi-energy systems: The impact of the thermal vector. *Applied Energy*, 372 (2024), Article 123732. [Cited on page 34.]

Gokcek, T.; Sengor, I.; Hayes, B. P.; and Erdinc, O., 2022. A hierarchical approach for p2p energy trading considering community energy storage and pv-enriched system operator. *IET Generation, Transmission & Distribution*, (2022). [Cited on page 29.]

GOV.UK, 2023. London pioneers first 'virtual power station'. https://www.gov.uk/government/news/london-pioneers-first-virtual-power-station. [Cited on page 21.]

Grodzevich, O. and Romanko, O., 2006. Normalization and other topics in multi-objective optimization. In *Fields MITACS Industrial Problems Workshop*. [Cited on pages 28, 48, 69, 70, 79, and 87.]

Group, C. E., 2023. Stafford hill solar farm. https://www.cleanegroup.org/initiatives/technical-assistance-fund/featured-installations/stafford-hill. [Cited on page 18.]

Gu, Y.; Wang, J.; Zheng, K.; Chen, Q.; Tang, W.; and Liu, J., 2023. Cost sharing mechanism for reactive power management amidst p2p energy sharing. In *2023 IEEE International Conference on Power System Technology (POWERCON)*. IEEE. [Cited on pages 25 and 26.]

Hafiz, F.; de Queiroz, A. R.; Fajri, P.; and Husain, I., 2019. Energy management and optimal storage sizing for a shared community: A multi-stage stochastic programming approach. *Applied Energy*, 236 (February 2019), 42–54. [Cited on pages 32 and 34.]

Hameer, S. and van Niekerk, J. L., 2015. A review of large-scale electrical energy storage. *International journal of energy research*, 39, 9 (2015), 1179–1195. [Cited on pages xviii, 12, and 22.]

Hannan, M.; Wali, S.; Ker, P.; Rahman, M. A.; Mansor, M.; Ramachandaramurthy, V.; Muttaqi, K.; Mahlia, T.; and Dong, Z., 2021. Battery energy-storage system: A review of technologies, optimization objectives, constraints, approaches, and outstanding issues. *Journal of Energy Storage*, 42 (2021), 103023. [Cited on pages xviii and 11.]

Hillier, F. S. and Lieberman, G. J., 2014. *Introduction to Operations Research*. McGraw-Hill. [Cited on pages 24 and 26.]

Ho, W. S.; Macchietto, S.; Lim, J. S.; Hashim, H.; Muis, Z. A.; and Liu, W. H., 2016. Optimal scheduling of energy storage for renewable energy distributed energy generation system. *Renewable and Sustainable Energy Reviews*, 58 (2016), 1100–1107. [Cited on page 31.]

Hossain, M. A.; Chakrabortty, R. K.; Ryan, M. J.; and Pota, H. R., 2020. Energy management of community energy storage in grid-connected microgrid under uncertain real-time prices. *Sustainable Cities and Society*, 64 (2020), 102658. [Cited on page 33.]

Hosseini, S. A.; Toulabi, M.; Ashouri-Zadeh, A.; and Ranjbar, A. M., 2022. Battery energy storage systems and demand response applied to power system frequency control. *International Journal of Electrical Power & Energy Systems*, 136 (2022), 107680. [Cited on page 12.]

Hou, L.; Tong, X.; Chen, H.; Fan, L.; Liu, T.; Liu, W.; and Liu, T., 2024a. Optimized scheduling of smart community energy systems considering demand response and shared energy storage. *Energy*, 295 (2024), 131066. [Cited on page 25.]

Hou, L.; Tong, X.; Chen, H.; Fan, L.; Liu, T.; Liu, W.; and Liu, T., 2024b. Optimized scheduling of smart community energy systems considering demand response and shared energy storage. *Energy*, 266 (2024), 131066. [Cited on pages 29 and 30.]

Houwing, M.; Dukovska, I.; and Paterakis, N. G., 2023. A reputation management system for the fair utilization of community energy storage systems. *IEEE Transactions on Smart Grid*, 14, 1 (Jan 2023), 582–592. [Cited on page 29.]

Hung, D. Q. and Mithulananthan, N., 2011. Community energy storage and capacitor allocation in distribution systems. In *Proceedings of the Australian University Power Engineering Conference*, 1–6. IEEE. [Cited on page 32.]

ICT, F., 2024. Fraunhofer institute for chemical technology. https://www.ict.fraunhofer.de/en/comp/ae/rw.html. [Cited on page 14.]

Iria, J.; Heleno, M.; and Cardoso, G., 2019. Optimal sizing and placement of energy storage systems and on-load tap changer transformers in distribution networks. *Applied Energy*, 250 (2019), 1147–1157. [Cited on page 13.]

Iria, J.; Scott, P.; Attarha, A.; Gordon, D.; and Franklin, E., 2021. Mv-lv network-secure bidding optimisation of an aggregator of prosumers in real-time energy and reserve markets. *Energy*, 230 (2021), 122962. [Cited on pages 20 and 21.]

Iria, J.; Scott, P.; Attarha, A.; and Soares, F., 2023. Comparison of network-(in)secure bidding strategies to coordinate distributed energy resources in distribution networks. *Sustainable Energy, Grids and Networks*, 36 (2023), 101209. [Cited on pages 20 and 21.]

Iria, J. and Soares, F., 2023. An energy-as-a-service business model for aggregators of prosumers. *Applied Energy*, 343 (2023), 121487. [Cited on page 21.]

Jo, J. and Park, J., 2020. Demand-side management with shared energy storage system in smart grid. *IEEE Transactions on Smart Grid*, 11, 5 (September 2020), 4466–4476. [Cited on page 29.]

Jokar, H.; Bahmani-Firouzi, B.; and Simab, M., 2022. Bilevel model for security-constrained and reliability transmission and distribution substation energy management considering large-scale energy storage and demand side management. *Energy Reports*, 8 (2022), 2617–2629. [Cited on page 13.]

KANG, H.; JUNG, S.; KIM, H.; HONG, J.; JEOUNG, J.; AND HONG, T., 2023. Multi-objective sizing and real-time scheduling of battery energy storage in energy-sharing community based on reinforcement learning. *Renewable and Sustainable Energy Reviews*, 185 (2023), 113655. [Cited on page 35.]

KHAN, T.; ULLAH, Z.; AGYEKUM, E. B.; HASANIEN, H. M.; AND YU, M., 2024. Multi-objective optimization of combined heat and power system integrated with multi-energy storage systems for rural communities. *Journal of Energy Storage*, 99 (2024), 113433. [Cited on page 35.]

KHEZRI, R.; MAHMOUDI, A.; AND AKI, H., 2022. Optimal planning of solar photovoltaic and battery storage systems for grid-connected residential sector: Review, challenges and new perspectives. *Renewable and Sustainable Energy Reviews*, 153 (2022). [Cited on page 20.]

KOIRALA, B. P.; VAN OOST, E.; AND VAN DER WINDT, H., 2018. Community energy storage: A responsible innovation towards a sustainable energy system? *Applied Energy*, 231 (2018), 570–585. [Cited on page 16.]

LI, L.; CAO, X.; AND ZHANG, S., 2022a. Shared energy storage system for prosumers in a community: Investment decision, economic operation, and benefits allocation under a cost-effective way. *Journal of Energy Storage*, 41 (2022), 104710. [Cited on pages xviii, 22, and 26.]

LI, L.; CAO, X.; AND ZHANG, S., 2022b. Shared energy storage system for prosumers in a community: Investment decision, economic operation, and benefits allocation under a cost-effective way. *Journal of Energy Storage*, 50 (2022). [Cited on page 16.]

LI, L.; PENG, K.; YANG, X.; AND LIU, K., 2023. Coordinated design of multi-stakeholder community energy systems and shared energy storage under uncertain supply and demand: A game theoretical approach. *Sustainable Cities and Society*, 84 (2023), 105028. [Cited on page 36.]

Lin, W. and Bitar, E., 2018. Decentralized stochastic control of distributed energy resources. *IEEE Transactions on Power Systems*, 33, 1 (2018), 888–900. [Cited on pages 43, 44, and 47.]

Liu, J.; Chen, X.; Xiang, Y.; Huo, D.; and Liu, J., 2021. Optimal planning and investment benefit analysis of shared energy storage for electricity retailers. *International Journal of Electrical Power & Energy Systems*, 126 (2021), 106561. [Cited on page 33.]

Liu, J.; Nie, J.; Cui, X.; Liu, P.; Tong, P.; and Liu, X., 2024. Optimal energy configuration of integrated energy community considering carbon emission. *Sustainability (Switzerland)*, 16, 2 (2024). [Cited on page 34.]

Liu, X.; Ji, Z.; Sun, W.; and He, Q., 2023. Robust game-theoretic optimization for energy management in community-based energy system. *Electric Power Systems Research*, 214 (2023), 108939. [Cited on pages 33 and 36.]

Lu, Q.; Zhang, Z.; and Lü, S., 2020. Home energy management in smart households: Optimal appliance scheduling model with photovoltaic energy storage system. *Energy Reports*, 6 (2020), 2450–2462. [Cited on page 20.]

Luo, L.; Abdulkareem, S. S.; Rezvani, A.; Miveh, M. R.; Samad, S.; Aljojo, N.; and Pazhoohesh, M., 2020. Optimal scheduling of a renewable based microgrid considering photovoltaic system and battery energy storage under uncertainty. *Journal of Energy Storage*, 28 (April 2020), 101306. [Cited on page 28.]

Ma, Y.; Abad, M. S. S.; Azuatalam, D.; Verbič, G.; and Chapman, A., 2017. Impacts of community and distributed energy storage systems on unbalanced low voltage networks. In *2017 Australasian Universities Power Engineering Conference (AUPEC)*, 1–6. IEEE, Melbourne, VIC, Australia. [Cited on page 34.]

Ma, Y.; Hu, Z.; and Song, Y., 2022. Hour-ahead optimization strategy for shared energy storage of renewable energy power stations to provide frequency regulation service. *IEEE Transactions on Sustainable Energy*, 13, 4 (2022), 1963–1974. [Cited on pages 28 and 34.]

Mahani, K.; Farzan, F.; and Jafari, M. A., 2017. Network-aware approach for energy storage planning and control in the network with high penetration of renewables. *Applied Energy*, 195 (2017), 974–990. [Cited on page 36.]

Mahmoodi, M.; Shaw, M.; and Blackhall, L., 2020. Voltage behaviour and distribution network performance with community energy storage systems and high pv uptake. In *e-Energy '20: Proceedings of the Eleventh ACM International Conference on Future Energy Systems*, 388–390. ACM. [Cited on pages 29 and 33.]

Martin, 2012. 1-to-1 solar buyback vs solar feed-in tariffs: The economics. https://www.solarchoice.net.au/blog/the-economics-of-a-1-to-1-solar-buyback-vs-solar-feed-in-tariffs/. [Cited on pages 48, 64, and 116.]

Mediwaththe, C. P. and Blackhall, L., 2020a. Community energy storage-based energy trading management for cost benefits and network support. In *Proc. Int. Conf. Smart Grids and Energy Syst.*, 516–521. IEEE. [Cited on pages 25 and 46.]

Mediwaththe, C. P. and Blackhall, L., 2020b. Network-aware demand-side management framework with a community energy storage system considering voltage constraints. *IEEE Transactions on Power Systems*, 36, 2 (2020), 1229–1238. [Cited on pages 2, 24, and 46.]

Mediwaththe, C. P.; Shaw, M.; Halgamuge, S.; Smith, D. B.; and Scott, P., 2019. An incentive-compatible energy trading framework for neighborhood area networks with shared energy storage. *IEEE Transactions on Sustainable Energy*, 11, 1 (2019), 467–476. [Cited on pages 2 and 16.]

Mohanty, A.; Ramasamy, A.; Verayiah, R.; and Mohanty, S., 2024. Neighborhood and community battery projects: A systematic analysis of their current state and future prospects. *Journal of Energy Storage*, 95 (2024), 112525. [Cited on page 2.]

Morcilla, R. V. and Jr., N. H. E., 2023. Sizing of community centralized battery energy storage system and aggregated residential solar pv system as virtual power plant to support electrical distribution network reliability improvement. *Renewable Energy Focus*, 46 (2023), 27–38. [Cited on page 34.]

Nazari, A.; Keypour, R.; and Amjady, N., 2021. Joint investment of community energy storage systems in distribution networks using modified nash bargaining theory. *Applied Energy*, 290 (2021), 117475. [Cited on pages 31, 32, and 35.]

Nguyen, T. A.; Byrne, R. H.; and Trevizan, R. D., 2020. Utilization of existing generation fleets using large-scale energy storage systems. In *2020 IEEE Power & Energy Society General Meeting (PESGM)* (Montreal, QC, Canada, 2020), 1–5. IEEE. [Cited on page 12.]

Nick, M.; Cherkaoui, R.; and Paolone, M., 2014. Optimal allocation of dispersed energy storage systems in active distribution networks for energy balance and grid support. *IEEE Transactions on Power Systems*, 29, 5 (2014), 2300–2310. [Cited on page 25.]

NL4WorldBank, 2017. The neighborhood battery system: Conserving energy and reducing emissions in the netherlands. https://nl4worldbank.org/2017/10/02/the-neighborhood-battery-system-conserving-energy-and-reducing-emissions-in-the-netherlands/. [Cited on page 18.]

Oh, E. and Son, S.-Y., 2019. Shared electrical energy storage service model and strategy for apartment-type factory buildings. *IEEE Access*, 7 (2019), 130340–130351. [Cited on page 24.]

Origin, 2018. VIC residential energy price fact sheet. https://shorturl.at/gkmV5. [Cited on pages 51, 71, 98, and 118.]

Oskouei, M. Z. and Gharehpetian, G. B., 2024. Flexibility enhancement of multi-district discos considering a trade-off between congestion and extractable reserve capacity from virtual energy storage systems. *Applied Energy*, 353 (2024), 122181. [Cited on page 13.]

Pamshetti, V. and Singh, S., 2022. Coordinated allocation of bess and sop in high pv penetrated distribution network incorporating dr and cvr schemes. *IEEE Systems Journal*, 16, 1 (2022), 420–430. [Cited on page 33.]

Pantoš, M., 2020. Market-based congestion management in electric power systems with exploitation of aggregators. *International Journal of Electrical Power & Energy Systems*, 121 (2020). [Cited on page 13.]

Parra, D.; Norman, S. A.; Walker, G. S.; and Gillott, M., 2020. Optimum community energy storage system for demand load shifting. *Energy*, 211 (2020), 118733. [Cited on page 25.]

Parra, D.; Norman, S. A.; Walker, G. S.; and Gillott, M., 2021. Optimum community energy storage for renewable energy and demand load management. *Applied Energy*, 285 (2021), 116426. [Cited on page 25.]

Pezeshki, H.; Wolfs, P.; and Ledwich, G., 2014. A model predictive approach for community battery energy storage system optimization. In *2014 IEEE PES General Meeting — Conference & Exposition* (National Harbor, MD, USA, 2014), 1–5. IEEE. [Cited on page 27.]

Power, G. M., 2023a. Gmp pioneers patent-pending system using energy storage to make meters obsolete. https://greenmountainpower.com/gmp-pioneers-patent-pending-system/. [Cited on page 21.]

Power, W., 2023b. Powerbank community battery storage. https://www.westernpower.com.au/resources-education/network-improvements/network-upgrade-projects/powerbank-community-battery-storage/. [Cited on page 18.]

Power, W., 2024. Powerbank community battery storage. https://westernpower.c om.au/energy-solutions/projects-and-trials/powerbank-community-battery-storage/. [Cited on page 82.]

Rahman, M. M.; Oni, A. O.; Gemechu, E.; and Kumar, A., 2020. Assessment of energy storage technologies: A review. *Energy Conversion and Management*, 223 (2020), 113295. [Cited on pages xviii and 11.]

Rajan, R.; Fernandez, F. M.; and Yang, Y., 2021. Primary frequency control techniques for large-scale pv-integrated power systems: A review. *Renewable and Sustainable Energy Reviews*, 144 (2021), 110998. [Cited on page 13.]

RAO, Y.; GAO, Z.; YANG, S.; WANG, L.; LI, X.; and ZHANG, J., 2020. Operational benefit evaluation for frequency regulation application of large-scale battery energy storage. *Energy Storage Science and Technology*, 9, 6 (2020), 1828. [Cited on page 12.]

Reddy, G. K. and Padhy, N. P., 2024. Decentralised control strategy for effective utilisation of distributed community energy storage in pv-rich lv distribution network. *Electric Power Systems Research*, 234 (2024), 110536. [Cited on page 30.]

Reserve, H. P., 2023. Hornsdale power reserve. https://hornsdalepowerreserve.com.au/. [Cited on page 14.]

Roald, L. A. and et al., 2023. Power systems optimization under uncertainty: A review of methods and applications. *Electric Power Systems Research*, 214 (2023), 108725. [Cited on pages 77 and 78.]

Rodrigues, D. L.; Ye, X.; Xia, X.; and Zhu, B., 2020. Battery energy storage sizing optimisation for different ownership structures in a peer-to-peer energy sharing community. *Applied Energy*, 262 (2020), 114498. [Cited on page 35.]

Saaty, T. L., 2004. Decision making — the analytic hierarchy and network processes (ahp/anp). *Journal of Systems Science and Systems Engineering*, 13, 1 (2004), 1–35. [Cited on page 50.]

SAFARAZI, S.; DEISSENROTH-UHRIG, M.; AND BERTSCH, V., 2020. Assessing the impacts of community energy storage systems on the german electricity market: An agent-based analysis. In *2020 17th International Conference on the European Energy Market (EEM)* (Stockholm, Sweden, 2020), 1–6. IEEE. [Cited on page 29.]

SAINI, V. K.; KUMAR, R.; AL-SUMAITI, A. S.; AND PANIGRAHI, B. K., 2023. Uncertainty aware optimal battery sizing for cloud energy storage in community microgrid. *Electric Power Systems Research*, 222 (2023), 109482. [Cited on page 36.]

SARDI, J.; MITHULANANTHAN, N.; AND HUNG, D. Q., 2016. A comprehensive community energy storage planning strategy based on a cost-benefit analysis. In *2016 Australasian Universities Power Engineering Conference (AUPEC)* (Brisbane, QLD, Australia, 2016), 1–6. IEEE. [Cited on page 36.]

SARDI, J.; MITHULANANTHAN, N.; AND HUNG, D. Q., 2017. Strategic allocation of community energy storage in a residential system with rooftop pv units. *Applied Energy*, 206 (2017), 195–206. [Cited on page 34.]

SCARLATACHE, F.; GRIGORAŞ, G.; CHICCO, G.; AND CÂRŢINĂ, G., 2012. Using k-means clustering method in determination of the optimal placement of distributed generation sources in electrical distribution systems. In *2012 IEEE International Conference on Optimization of Electrical and Electronics Equipment, OPTIM*, 953–958. IEEE. [Cited on pages 33, 68, and 95.]

SCHELLER, F.; BURKHARDT, R.; SCHWARZEIT, R.; MCKENNA, R.; AND BRUCKNER, T., 2020. Competition between simultaneous demand-side flexibility options: the case of community electricity storage systems. *Applied Energy*, 269 (2020), 114969. [Cited on page 15.]

SCHRAM, W. L.; ALSKAIF, T.; LAMPROPOULOS, I.; HENEIN, S.; AND VAN SARK, W. G., 2020. On the trade-off between environmental and economic objectives in community energy storage operational optimization. *IEEE Transactions on Sustainable Energy*, 11, 4 (2020), 2653–2661. [Cited on page 29.]

Shang, Y.; Sang, S.; Tiwari, A. K.; Khan, S.; and Zhao, X., 2024. Impacts of renewable energy on climate risk: A global perspective for energy transition in a climate adaptation framework. *Renewable and Sustainable Energy Reviews*, (2024). [Cited on page 1.]

Shapiro, A.; Dentcheva, D.; and Ruszczyński, A., 2009. *Lectures on Stochastic Programming: Modeling and Theory*. SIAM. [Cited on pages 24 and 26.]

Shaqsi, A. Z. A.; Sopian, K.; and Al-Hinai, A., 2020. Review of energy storage services, applications, limitations, and benefits. *Energy reports*, 6 (2020), 288–306. [Cited on page 20.]

Shaw, M.; Sturmberg, B.; Mediwaththe, C.; Ransan-Cooper, H.; Taylor, D.; and Blackhall, L., 2020. Operating a community-scale battery: electricity tariffs to maximise customer and network benefits. [Cited on pages xviii, 2, 14, 16, and 22.]

Singh, S.; Veda, S.; Singh, S. P.; and Baggu, M., 2018. Maximizing the benefits of volt/var optimization in the presence of community energy storage. In *2018 IEEE International Conference on Power Electronics, Drives and Energy Systems (PEDES)*, 1–6. IEEE, Chennai, India. [Cited on page 25.]

SolarQuarter, 2024. Bondi unveils community battery to enhance renewable energy storage. (2024). https://solarquarter.com/2024/08/21/bondi-unveils-community-battery-to-enhance-renewable-energy-storage/. [Cited on pages xv and 17.]

SSE Renewables, 2024. Sse renewables' first battery storage project at salisbury now fully operational. https://www.sse.com/news-and-views/2024/04/sse-renewables-first-battery-storage-project-at-salisbury-now-fully-operational/. [Cited on page 14.]

Strategies, C., 2023. Coned brooklyn-queens non-wire alternative project installs first microgrid. https://cahillstrategies.com/coned-brooklyn-queens-non-wire-alternative-project-installs-first-microgrid/. [Cited on page 17.]

Synergy, 2024. Alkimos beach energy trial. https://www.synergy.net.au/Our-energy/Future-energy/Alkimos-Beach-Energy-Storage-Trial. [Cited on page 82.]

Tan, K. M.; Babu, T. S.; Ramachandaramurthy, V. K.; Kasinathan, P.; Solanki, S. G.; and Raveendran, S. K., 2021. Empowering smart grid: A comprehensive review of energy storage technology and application with renewable energy integration. *Journal of Energy Storage*, 39 (2021), 102591. [Cited on page 20.]

Tarashandeh, N. and Karimi, A., 2021. Utilization of energy storage systems in congestion management of transmission networks with incentive-based approach for investors. *Journal of Energy Storage*, 33 (2021), 102034. [Cited on page 13.]

Terlouw, T.; AlSkaif, T.; Bauer, C.; and van Sark, W., 2019. Multi-objective optimization of energy arbitrage in community energy storage systems using different battery technologies. *Applied Energy*, 255 (2019), 113796. [Cited on page 34.]

Tesla, 2023. Moss landing megapack. https://www.teslarati.com/tesla-moss-landing-megapack-battery-latest-updates-incidents/. [Cited on page 14.]

Thomas, D. et al., 2020. A local market mechanism for physical storage rights. *IEEE Transactions on Power Systems*, 35 (2020), 3087–3099. [Cited on page 36.]

To, T.; Heleno, H.; and Valenzuela, A., 2022. Risk-constrained multi-period investment model for distributed energy resources considering technology costs and regulatory uncertainties. *Applied Energy*, 319 (2022), 119210. [Cited on pages 36 and 91.]

Tucker, N. and Alizadeh, M., 2022. An online scheduling algorithm for a community energy storage system. *IEEE Transactions on Smart Grid*, 13, 6 (Nov 2022), 4651–4664. [Cited on pages 27 and 28.]

Tushar, W. et al., 2016. Energy storage sharing in smart grid: A modified auction-based approach. *IEEE Transactions on Smart Grid*, 7, 3 (May 2016), 1462–1475. [Cited on page 37.]

van der Stelt, S.; AlSkaif, T.; and van Sark, W., 2020. Techno-economic analysis of household and community energy storage for residential prosumers with smart appliances. *Energy*, 207 (2020), 118276. [Cited on pages 25 and 35.]

van Westering, W. and Hellendoorn, H., 2020. Low voltage power grid congestion reduction using a community battery: Design principles, control and experimental validation. *International Journal of Electrical Power & Energy Systems*, 114 (2020), 105349. [Cited on page 28.]

Virah-Sawmy, D. and Sturmberg, B., 2024. Socio-economic and environmental impacts of renewable energy deployments: A review. *Renewable and Sustainable Energy Reviews*, (2024). doi:10.1016/j.rser.2024.114956. Under a Creative Commons license. [Cited on page 1.]

Walker, A. and Kwon, S., 2021a. Analysis on impact of shared energy storage in residential community: Individual versus shared energy storage. *Applied Energy*, 282 (2021), 116172. [Cited on pages 2 and 15.]

Walker, A. and Kwon, S., 2021b. Design of structured control policy for shared energy storage in residential community: A stochastic optimization approach. *Applied Energy*, 298 (2021), 117182. [Cited on page 26.]

Wang, L.; Hou, C.; Ye, B.; Wang, X.; Yin, C.; and Cong, H., 2021a. Optimal operation analysis of integrated community energy system considering the uncertainty of demand response. *IEEE Transactions on Power Systems*, 36, 4 (July 2021), 3681–3691. [Cited on page 30.]

Wang, Q.; Zhang, X.; Yi, C.; Li, Z.; and Xu, D., 2022. A novel shared energy storage planning method considering the correlation of renewable uncertainties on the supply side. *IEEE Transactions on Sustainable Energy*, 13, 1 (2022), 229–239. [Cited on page 32.]

Wang, W.; Liang, H.; and Chen, J., 2016. Stochastic modelling of community energy storage system based on diffusion approximation. In *2016 IEEE Power and Energy Society General Meeting (PESGM)*, 1–5. IEEE, Boston, MA. [Cited on page 27.]

WANG, Z.; CHEN, A.; WANG, N.; AND LIU, T., 2023. Multi-objective operation optimization strategy for integrated community energy systems considering demand side management. *IEEE Transactions on Industry Applications*, 60, 1 (2023), 1332–1344. [Cited on page 29.]

WANG, Z.; GU, C.; AND LI, F., 2018. Flexible operation of shared energy storage at households to facilitate pv penetration. *Renewable energy*, 116 (2018), 438–446. [Cited on page 24.]

WANG, Z. ET AL., 2021b. Peer-to-peer energy trading strategy for energy balance service provider (ebsp) considering market elasticity in community microgrid. *Applied Energy*, 303 (2021), 117596. [Cited on page 37.]

WU, C.; ZHOU, D.; LIN, X.; WEI, F.; CHEN, C.; MA, Y.; HUANG, Y.; LI, Z.; AND DAWOUD, S. M., 2021. A novel energy cooperation framework for community energy storage systems and prosumers. *International Journal of Electrical Power & Energy Systems*, 133 (2021), 107428. [Cited on page 34.]

XIE, K.; ZHONG, W.; LI, W.; AND ZHU, Y., 2019. Distributed capacity allocation of shared energy storage using online convex optimization. *Energies*, 12, 9 (2019), 1642. [Cited on page 32.]

XIE, Y.; YAO, Y.; WANG, Y.; CHA, W.; ZHOU, S.; WU, Y.; AND HUANG, C., 2022. A cooperative game-based sizing and configuration of community-shared energy storage. *Energies*, 15, 22 (November 2022), 8626. [Cited on page 36.]

YACK, T. R., 2023. Yack01 community battery. `https://totallyrenewableyack.org.au/watts-happening/yack01-community-battery/`. [Cited on page 17.]

YANG, D.; HE, Z.; SUN, Y.; LI, B.; LI, D.; LIU, X.; AND JIANG, C., 2024a. Optimised operation of integrated community energy system considering integrated energy pricing strategy: A two-layer stackelberg game approach. *Journal of Energy Storage*, 87 (2024), 111383. [Cited on page 30.]

Yang, J.; Saha, T. K.; Alam, M. R.; and Tushar, W., 2020. Transactive control of community batteries for voltage regulation in distribution systems. *Energy Reports*, 6 (2020), 1385–1395. [Cited on page 25.]

Yang, J.; Saha, T. K.; Alam, M. R.; and Tushar, W., 2024b. Transactive control of community batteries for voltage regulation in distribution systems. *Journal of Energy Storage*, 90 (2024), 111798. [Cited on page 2.]

Yang, Y.; Hu, G.; and Spanos, C. J., 2021. *IEEE Transactions on Smart Grid*, 12, 5 (Sept 2021), 4185–4194. [Cited on pages 31 and 32.]

Yu, H. J. J., 2021. System contributions of residential battery systems: New perspectives on pv self-consumption. *Energy Economics*, 96 (2021), 105151. [Cited on page 20.]

Zaidi, B.; Bhatti, D.; and Ullah, I., 2018. Combinatorial auctions for energy storage sharing amongst the households. *Journal of Energy Storage*, 19 (2018), 291–301. [Cited on page 37.]

Zakeri, B. and Syri, S., 2015. Electrical energy storage systems: A comparative life cycle cost analysis. *Renewable and Sustainable Energy Reviews*, 42 (2015), 569–596. [Cited on page 71.]

Zeraati, M.; Hamedani Golshan, M.; and Guerrero, J., 2018. Distributed control of battery energy storage systems for voltage regulation in distribution networks with high pv penetration. *IEEE Transactions on Smart Grid*, 9, 4 (2018), 3582–3593. [Cited on pages 50, 71, and 117.]

Zhang, C.; Cheng, H.; Liu, L.; Zhang, H.; Zhang, X.; and Li, G., 2020. Coordination planning of wind farm, energy storage and transmission network with high-penetration renewable energy. *International Journal of Electrical Power & Energy Systems*, 120 (2020), 105944. [Cited on page 13.]

Zhang, Y.; Liu, Y.; Huang, Z.; and Chen, H., 2023. Strategic active and reactive power scheduling of integrated community energy systems in day-ahead distribution electricity market. *Applied Energy*, 321 (2023), 119433. [Cited on page 24.]

Zhang, Y.; Ma, T.; and Yang, H., 2022. Grid-connected photovoltaic battery systems: A comprehensive review and perspectives. *Applied Energy*, 328 (2022), 120182. [Cited on page 15.]

Zhang, Z.; Ding, T.; Zhou, Q.; Sun, Y.; Qu, M.; Zeng, Z.; Ju, Y.; Li, L.; Wang, K.; and Chi, F., 2021. A review of technologies and applications on versatile energy storage systems. *Renewable and Sustainable Energy Reviews*, 148 (2021), 111263. [Cited on pages xviii and 11.]

Zhao, C.; Andersen, P. B.; Træholt, C.; and Hashemi, S., 2023. Grid-connected battery energy storage system: a review on application and integration. *Renewable and Sustainable Energy Reviews*, 182 (2023). [Cited on page 16.]

Zheng, Y.; Song, Y.; Huang, A.; and Hill, D. J., 2020. Hierarchical optimal allocation of battery energy storage systems for multiple services in distribution systems. *IEEE Transactions on Sustainable Energy*, 11, 3 (2020), 1911–1921. [Cited on pages 48 and 50.]

Zhou, A.; Qu, B.-Y.; Li, H.; Zhao, S.-Z.; Suganthan, P. N.; and Zhang, Q., 2011. Multiobjective evolutionary algorithms: A survey of the state of the art. *Swarm and Evolutionary Computation*, 1, 1 (2011), 32–49. [Cited on pages 28 and 29.]

Zhu, H.; Ouahada, K.; and Abu-Mahfouz, A., 2022. Peer-to-peer energy trading in smart energy communities: A lyapunov-based energy control and trading system. *IEEE Access*, 35 (2022), 42916–42932. [Cited on page 36.]